

**MICROALGAE CULTIVATION AND PRODUCTION OF BIO-OIL FROM
MICROALGAE BIOMASS**

PhD THESIS

Masoud DERAKHSHANDEH

**Environmental Engineering
Supervisor: Prof. Dr. Ümran TEZCAN ÜN**

Eskişehir

Anadolu University

Graduate School of Sciences

June 2018

FINAL THESIS APPROVAL PAGE



ABSTRACT

MICROALGAE CULTIVATION AND PRODUCTION OF BIO-OIL FROM MICROALGAE BIOMASS

Masoud DERAKHSHANDEH

Environmental Engineering Department
Anadolu University, Graduate School of Sciences, June 2018

Supervisor: Prof. Dr. Ümran TEZCAN ÜN

In this research, production of bio-Oil as a renewable biofuel from microalgae biomass was studied. The work was divided into four main steps. Firstly, wild-type microalgae species from local habitat were isolated, identified and characterized based on their potential for biofuel production and/or carbon dioxide fixation capacity. The highest measured lipid content was 47.32 % for *Scenedesmus quadricauda* (I). The attempt for improving lipid extraction efficiency from microalgae cell was the subject of second step. The effect of adding microparticles of glass as a cell disruption enhancer to maximize the extracted lipid from microalgae was investigated. With the addition of 40 µm particles in 2.25 mass proportion of particle to dried biomass, lipid extraction from *Chlorella* sp. enhanced by 46.60 %. In the third step, the aim was to maximize the growth rate of the selected microalgae *Scenedesmus* sp. in the first step which was the most proper one for bio-oil production. With the optimized values of 6.3 % CO₂, 1.03 vvm flow rate, 1.47 mm diffuser diameter and 0.230 g/l initial inoculation, the maximum growth rate of 0.513 g/l.d was estimated. At the forth step, biomasses of microalgae *Scenedesmus* and *Synechosystis* species were thermochemically converted to biofuel in a fast pyrolysis process. The best pyrolysis temperature for *Scenedesmus* and *Synechosystis* biomass was respectively 500 °C and 600 °C resulted in higher biooil yield of 80.0 and 71.0 wt %.

Keywords: Microalgae, Biofuel, Growth optimization, Lipid extraction, Pyrolysis.

ÖZET

MİKROALG YETİŞTİRME VE MİKROALG BİYOKÜTLESİNDEN BİYO-YAĞ ÜRETİMİ

Masoud DERAKHSHANDEH

Çevre Mühendisliği

Anadolu Üniversitesi, Fen Bilimleri Enstitüsü, Haziran 2018

Danışman: Prof. Dr. Ümran Tezcan ÜN

Bu araştırmada, mikroalg biyokütlesinden yenilenebilir biyoyakıt olarak biyo-yağ üretimi incelenmiştir. Çalışma dört aşamadan oluşmaktadır. Birinci aşama, yerel habitattan elde edilen yabani tip mikroalg türleri izole edilmiş, tanımlanmış ve biyoyakıt üretimi ve/veya karbondioksit fiksasyon kapasitesi açısından potansiyellerine göre karakterize edilmiştir. Değerlendirilen türler içinde lipid içeriği en yüksek çıkan, % 47,32 ile *Scenedesmus quadricauda* (I) türüdür. İkinci aşamada Mikroalg hücrelerinden lipid ekstraksiyon veriminin artırılması çalışılmıştır. Mikroalgardan ekstrakt edilen lipitin maksimize edilmesi için bir hücre parçalama arttırıcı olarak cam mikropartiküllerinin eklenmesi araştırılmıştır. 40 µm'lik partikülün, kurutulmuş biyokütle miktarına 2,25 kütle oranında eklenmesiyle *Chlorella* türü için lipid miktarı % 46,60 oranında artmıştır. Üçüncü aşamada, seçilen mikroalg *Scenedesmus* türünün büyüme oranını maksimize etmek hedeflenmiştir. İlk aşamada *Scenedesmus* türü, biyo-yağ üretimi için en uygun mikroalg olarak tespit edilmiştir. Optimize edilmiş değerler, % 6,3 CO₂, 1,03 vvm akış hızı, 1,47 mm difüzör çapı ve 0,230 g/l başlangıç inokülasyonu ile birlikte maksimum 0,513 g/l.d büyüme oranı tahmin edilmiştir. Dördüncü aşamada, mikroalg *Scenedesmus* ve *Synechosystis* türlerinin biyokütleleri, hızlı piroliz işleminde termokimyasal yöntemiyle biyoyakıtta dönüştürülmüştür. *Scenedesmus* ve *Synechosystis* biyokütleleri için en iyi piroliz sıcaklığı sırasıyla 500 °C ve 600 °C'de en yüksek biyo-oil verimi % 80,0 ve % 71,0 olmuştur.

Anahtar Sözcükler: Mikroalg, Biyoyakıt, Büyüme optimizasyonu, Lipid ekstraksiyonu, Piroliz.

AKNOWLEDGMENT

I thank Allah for all the great gifts he gave me.

I thank Turkey for giving me the opportunity to complete my PhD degree in Anadolu University.

I thank my great supervisor Prof. Dr. Ümran TEZCAN ÜN for all her sincere encouragement, motivation and supports.

I thank Prof. Dr. Tahir ATICI who advised my work and many things he taught me.

I thank Prof. Dr. Funda ATEŞ who advised my work and many things she taught me.

I thank dear Prof. Dr. Cengiz TÜRE and dear Prof. Dr. Neşe ÖZTÜRK, who took part as my PhD committee members for their helpful comments.

I thank Kad. Monireh, my lovely wife, for her patience and supports.

I thank all of my friends.

Masoud DERAKHSHANDEH

STATEMENT OF COMPLIANCE WITH ETHICAL PRINCIPLES AND RULES

I hereby truthfully declare that this thesis is an original work prepared by me; that I have behaved in accordance with the scientific ethical principles and rules throughout the stages of preparation, data collection, analysis and presentation of my work; that I have cited the sources of all the data and information that could be obtained within the scope of this study, and included these sources in the references section; and that this study has been scanned for plagiarism with “scientific plagiarism detection program” used by Anadolu University, and that “it does not have any plagiarism” whatsoever. I also declare that, if a case contrary to my declaration is detected in my work at any time, I hereby express my consent to all the ethical and legal consequences that are involved.

Masoud DERAKHSHANDEH

TABLE OF CONTENTS

	<u>Page</u>
TITLE PAGE	i
FINAL THESIS APPROVAL PAGE	ii
ABSTRACT	iii
ÖZET	iv
ACKNOWLEDGMENT	v
STATEMENT OF COMPLIANCE WITH ETHICAL PRINCIPLES AND RULES	vi
LIST OF FIGURES	x
LIST OF TABLES	xiii
SYMBOLS AND ABBREVIATIONS	xiv
1. INTRODUCTION	1
1.1. Microalgae, Challenges and Prospects.....	1
1.2. Need for Screening Study	2
1.3. Enhancement of Lipid Extraction	2
1.4. Maximizing Biomass Production Rate	4
1.5. Bio crude Oil.....	5
2. THE SCREENING OF MICROALGAE SPECIES ISOLATED FROM CENTRAL ANATOLIA REGION FOR LIPID, CARBOHYDRATE AND PROTEIN CONTENT	7
2.1. Materials and Method	7
2.1.1. Chemicals.....	7
2.1.2. Sampling, culture and isolation	8
2.1.3. Calibration curve.....	9
2.1.4. Lipid determination.....	11
2.1.5. Carbohydrate.....	12
2.1.6. Protein.....	12
2.2. Results and Discussions	12
2.2.1. Identification of the isolated species.....	12
2.2.2. Growth rate	16
2.2.3. Elemental analysis and the estimation of carbon fixation rate	22
2.2.4. Biochemical composition	22
2.2.4.1. <i>Lipid</i>	23

2.2.4.2. Carbohydrate	24
2.2.4.3. Protein	24
2.2.5. Microalgae Natural Settling behavior	25
3. LIPID EXTRACTION FROM MICROALGAE CHLORELLA AND SYNECHOCYSTIS SP. USING GLASS MICROPARTICLES	27
3.1. Materials and Method	27
3.1.1. Reagents	27
3.1.2. Microalgae isolation and culture	27
3.1.3. Glass particle	30
3.1.4. Lipid extraction	30
3.1.5. Experiment design	32
3.2. Results and Discussion	33
4. OPTIMIZATION OF GROWTH RATE OF MICROALGAE SCENEDESMUS SP. :CENTRAL COMPOSITE DESIGN STATISTICAL APPROACH.....	41
4.1. Materials and Method	41
4.1.1. Chemicals	41
4.1.2. Microalgae species and medium	41
4.1.3. Growth curve and linear growth rate	42
4.1.4. Photobioreactor	43
4.1.5. Experimental Design and statistical approach	43
4.2. Results and Discussions	45
4.2.1. Experimental data	45
4.2.2. Statistical analysis	45
4.2.3. Analysis of variance (ANOVA)	46
4.2.4. The effect of carbon dioxide concentration	48
4.2.5. The effect of gas flow rate	51
4.2.6. The effect of gas diffuser diameter	52
4.2.7. The effect of initial inoculum concentration	53
4.2.8. Microalgae potential as biofuel feedstock in large scale	53
5. RENEWABLE BIOFUEL FROM FAST PYROLYSIS OF SYNECHOSYSTIS AND SCENEDESMUS WILD-TYPE MICROALGAE SPECIES	56
5.1. Materials and method	56
5.1.1. Chemicals	56
5.1.2. Microalgae strain and cultivation	57
5.1.3. Biomass harvest	58

5.1.4. Analyses of biomass	59
5.1.5. Pyrolysis.....	59
5.1.6. Analyses of product	60
5.2. Results and Discussion.....	61
5.2.1. Microalgae cultivation	61
5.2.2. Biomass characteristics	62
5.2.3. Pyrolysis product yield	65
5.2.4. Bio-oil characteristics	66
5.2.5. FTIR spectroscopy	68
5.2.6. GC-MS analysis	68
5.2.7. Biochar characteristics	71
5.2.8. Large Scale Biooil production	73
6. CONCLUSION.....	75
REFERENCES.....	77
APPENDIX.....	83
CV	94

LIST OF FIGURES

	<u>Page</u>
Figure 2.1. The growth of different microorganisms in mixed culture.....	10
Figure 2.2. The cultivation of isolated microalgae for calibration curve withdrawal and elemental analysis.....	11
Figure 2.3. The microscopic view (oil immersion) of the isolated microalgae species	14
Figure 2.4. The different behaviour of long chain strand forming microalgae in liquid medium	18
Figure 2.5. The schematic view (left) and the real view of the photobioreactors	18
Figure 2.6. The Growth curve for isolated microalgae	19
Figure 2.7. Protein, carbohydrate and protein content	21
Figure 2.8. Lipid production rate of variety of isolated microalgae.....	22
Figure 2.9. Distribution of lipid, carbohydrate and protein content in Blue-Green and Green microalgae.....	26
Figure 2.10. Distribution of natural settling efficiency in approximate cell size of isolated microalgae	27
Figure 2.11. The natural settling of microalgae cells in the solution; 1: Chroococcus disperus, 2: Gleocystis ampula, 3: Synechocystis (I), 4: Scenedesmus obliquus (I), 5: Chlorella vulgaris (I), 7: Scenedesmus quadricauda (I) 8: Synechocystis (II), 10: Scenedesmus dimorphus, 11: Microcystis aeruginosa, 12: Chlorella vulgaris(II), 13: Cyanobacterium cedrorum, 14: Chroococcus sp.(I), 15: Kirchneriella lunaris, 16: Scenedesmus quadricauda (II), 17: Chlorella vulgaris (III), 18: Nannochloris sp., 19: Chroococcus sp.(II) and 20: Micrococcus sp.	27
Figure 3.1. Up: Oil immersion light microscopic view of isolated microalgae species Chlorella & Synechocystis, Down: The cell size distribution for both microalgaes	30

Figure 3.2. Particle size distribution of 10 μm particles	31
Figure 3.3. Flowchart of lipid extraction steps	32
Figure 3.4. Normal probability plot	35
Figure 3.5. The model diagnostic plots	37
Figure 3.6. Yield of lipid extraction for a) 10 μm particle size, b) 40 μm particle size	38
Figure 3.7. Microscopic view of the debris (dashed arrows show intact cells, black arrows show the collapsed cells)	39
Figure 4.1. Scenedesmus sp. Oil immersion microscopy	43
Figure 4.2. Experimental setup. 1: One out of eight cultivation cells. 2: Gas diffuser. 3: Sampling point including a three way valve and a syringe. 4: vent. 5: In-line gas filter. 6: Rotameter type gas flow meter. 7: MFC units. 8: MFC control unit. 9: Air compressor 10: CO ₂ cylinder.	44
Figure 4.3. The growth curve for fast (run 7), moderate (run 5) and slow (run 3) growth	46
Figure 4.4. The diagnostic plots of a) Normal plot of residuals, b) Residuals vs predicted, c) Externally studentized residuals for outliers, d) the Box-Cox plot.....	49
Figure 4.5. The 3D plot output of the quadratic model, a) GR vs CO ₂ C&FR at DD:2.6 mm, IC:0.280 gr/l, b) GR vs CO ₂ C&DD at FR:3.16 vvm, IC:0.280 gr/l, c) GR vs DD&FR at CO ₂ C: 26648 ppm, IC:0.280 gr/l, d) GR vs DD&FR at CO ₂ C: 75250 ppm, IC:0.280, e) GR vs CO ₂ C&IC at DD:2.6 mm, FR:3.16 gr/l.	51
Figure 4.6. The contour plot output of the software solution for the optimized values a) GR vs CO ₂ C&FR at DD:2.86 mm, IC:0.190 gr/l, b) GR vs CO ₂ C&DD at FR:2.19 vvm, IC:0.190 gr/l, c) GR vs CO ₂ C&IC at FR: 2.19 vvm, DD:2.86 mm.	52

Figure 4.7. The experimental result for growth rate vs flow rate at different DD and CO ₂ C	53
Figure 5.1. Photobioreactors setup. 1: Bubble column type. 2: Rectangular type photobioreactors. 3: CO ₂ cylinder. 4: Air compressor. 5&6&7&8: Mass flow controllers. 9: Control Unit.....	59
Figure 5.2. Oil immersion microscopy of microalgae living cells	62
Figure 5.3. Growth curve for microalgae living cells in photobioreactors	62
Figure 5.4. SEM image of SCE and SYN dried biomasses	64
Figure 5.5. The production yield of biooil, biochar and biogas for SCE and SYN biomasses at 400, 500 and 600 °C.	67
Figure 5.6. SEM image of SCE and SYN biochar at 400, 500 and 600 °C	73

LIST OF TABLES

	<u>Page</u>
Table 2.1. The linear range of OD ₆₈₀ for isolated microalgae and the conversion factors to dried biomass concentration	13
Table 2.2. Growth characteristics and biochemical compositions of isolated microalgae	20
Table 3.1. Obtained response at different runs	34
Table 3.2. ANOVA for selected factorial model	36
Table 3.3. Lipid content of <i>Chlorella vulgaris</i> in different studies	40
Table 4.1. <i>Scenedesmus</i> sp. dried biomass CHN analysis and biochemical composition	43
Table 4.2. The adjusted variables for different runs and experimental responses	45
Table 4.3. Model fit summary statistics and lack of fit test results.....	47
Table 4.4. ANOVA for Response Surface Reduced Quadratic Model	48
Table 5.1. Proximate, ultimate, elemental and biochemical analysis of microalgae biomass	65
Table 5.2. Elemental analysis and HHV values for biooils	68
Table 5.3. GC-MS analyze of biooil samples	71
Table 5.4. Elemental analyze of SYN and SCE biochars at 400, 500 and 600 °C	74

SYMBOLS AND ABBREVIATIONS

η_r	: Reactor volume per unit area
μ	: Micro
2FI	: Two factor interaction
3D	: Three dimensional
ANOVA	: Analysis of variance
BET	: Brunauer–Emmett–Teller analysis.
BG11	: Blue Green medium
bpd	: Barrels per day
CCD	: Central Composite Design
C_e	: Elemental carbon fraction
C_f	: Conversion factor
Chl	: Chlorella
CHN/S	: Carbon hydrogen nitrogen/sulfur
CHO	: Carbohydrates
$CO_2C.$: CO_2 Concentration
Conc.	: Concentration
d	: Day
daf	: Dried ash free basis
db	: Dried basis
DD	: Diffuser Diameter
DDW	: Deionized distilled water
D_{pr}	: Diesel production rate
E_f	: Carbon dioxide emission factor
FAME	: Fatty Acid Methyl Ether
FR	: Flow Rate
FTIR	: Fourier transform infrared spectroscopy
GC-MS	: Gas chromatography–mass spectrometry
gr	: Gram
GR	: Growth Rate
Ha	: Hectare
HHV	: High heating value

hrs	: Hours
IC	: Inoculum Concentration
kg	: Kilogram
k_{La}	: Volumetric liquid phase mass transfer coefficient
L	: Lipid fraction in dried biomass
l	: Liter
LED	: Light emitting diode
m	: Meter
Max	: Maximum
MFC	: Mass Flow Controller
MJ	: Mega joule
ml	: Milliliter
mol	: Mole
MWe	: Megawatt electricity
MWh	: Megawatt hour
nm	: Nanometer
N-Prot	: Nitrogen to protein factor
OD	: Optical density
P	: Power
ppm	: Part per million
PRO	: Proteins
R^2	: Ri-squared
Ref.	: Reference
rpm	: Revolution per minute
s	: Second
SCE	: Scenedesmus
SEM	: Scanning Electron Microscopy
Sp.	: Species
SYN	: Synechosistis
v/v	: Volumetric ratio
VIF	: Variance Inflation Factor
vvm	: Volume of gas per volume of liquid medium
wt	: Weight

λ : Transformation Power
 ρ_d : Density



1. INTRODUCTION

1.1. Microalgae, Challenges and Prospects

The growing demand for the energy and the increasing carbon dioxide emissions are challenging concerns of the world. Renewable energy while being carbon neutral resources have emerged as a remedy for these concerns. Biofuels as a significant group of renewables, are categorized into multiple generations based on the nature of raw material being used. Microalgae are photosynthetic microorganisms able to consume carbon in mineral forms [2]. They are carbon fixing autotroph microorganisms i.e. able to mitigate carbon dioxide directly. They have been considered as a solution to reduce the carbon dioxide content of the atmosphere [3]. They have been also studied vastly as promising species to be produced in large scale for biofuel production [4]. They grow fast and rely on sun light for their energy requirement and can uptake carbon dioxide directly. Microalgae based biofuels are amongst third generation biofuels which do not rely on edible material and arable lands [5]. Microalgae are interesting biomass producers because of their fast growing characteristics. They are also welcomed for not competing agriculture products as is unfortunately happening for crop based biofuels. Autotrophic nature of microalgae growth made them promising technology for carbon dioxide mitigation. Unlike many agriculture products which are actively being used for large scale biofuel production like wheat, corn and soybean, microalgae can be cultivated in vertical reactors or pools without occupying arable lands [6]. Despite all the significant characteristics of microalgae, there is no commercially active biofuel production plant based on microalgae biomass [7]. There are still bottle necks hindering the emergence of microalgae biofuel technology. In short, Microalgae must be cultivated, harvested and transformed to biofuels. In cultivation step, the aim is to maximize the growth rate and at the same time the highest possible biomass concentration [8]. A variety of reactors design have been tried to optimize the rate of biomass production and finally lowering the cost [8]. Harvesting is a challenging step because the method of harvest differ from one species to another one. Some microalgae species settle easily but for many of them they float freely in the solution and form a very stable broth [9]. Those species who settle naturally when mixing is stopped are welcomed because this will reduce the cost of harvesting significantly.

Depending on the nature of final aimed biofuel, downstream processes will differ substantially. For biodiesel, an oil extraction step following by a transesterification

reaction will be needed [8] whereas for bioethanol, a saccharification step i. e. the process of breaking complex carbohydrates such as starch or cellulose into its monosaccharide components, followed by a fermentation processes are required [10].

Microalgae dried mass composes of mainly lipid, carbohydrates and proteins [11]. The lipid part can be used for oil based biofuels like biodiesel while the carbohydrate are suitable for bioalcohol production. Some protein rich species of microalgae are edible for human or can be used as animal feed [12]. Their fast growing characteristics when high oil content as high as 70% of the dried mass are also achieved, the microalgae oil production rate will be 21 to 800 times more than different oil seed plants at the cultivation per hectare basis [13].

1.2. Need for Screening Study

Altogether, finding species with high growth rates and also high oil or carbohydrate content will significantly affect the total cost of final product of interest. Moreover, locally isolated strains of microalgae would have higher chance of applicability because of adaptation to those local environment [14]. It may also reduce the risk of ecosystems imbalances due to unnatural interference of human by transferring foreign strains from other habitats [15, 16].

At the present work, microalgae species were isolated from a river located in central Anatolia region (Porsuk River, Eskişehir, Turkey) and identified morphologically. They were investigated for their growth rate, carbon dioxide mitigation rate, lipid, carbohydrate and protein content. They were also studied for their settling behavior in cultivation broth. To the extent of our knowledge, there was no previous study of this kind on the microalgae strains of this region. The detail of the work is presented in chapter 2.

1.3. Enhancement of Lipid Extraction

Microalgae are considered as a promising microorganism for biofuel production which are also known as third generation biofuel with the advantage of being carbon neutral and direct energy uptake from the sun and no need for arable land [17]. There are obstacles in the use of microalgae sources for fuel production which cause their production to be economically favorable only when crude oil price goes over 100\$ per barrel [18]. One of those challenges is the extraction of the lipid from the cell as a feedstock for biodiesel which requires pretreatment steps to disrupt the cell wall [19].

Microalgae small cell size and relative thick cell wall make them formidable against any extraction methods [20]. A variety of techniques have been tested for cell disruption including physical/mechanical methods using ultrasound, microwave, high pressure steaming, bead milling and osmotic shock [21-25] and chemical methods using acids, bases, ionic liquids, ozone, hydrogen peroxide and combinations of common solvents like dimethyl carbonate, hexane, methane and chloroform [26-29]. Biological methods like enzymatic hydrolysis and degradation by algicidal bacteria or viruses (alga-lytic) have been tried as well [30, 31]. All the proposed techniques come with drawbacks so that the technology has yet to be applicable in large scale. Halim and friends [32] compared different techniques for cell disruption and concluded that the high-pressure homogenization was more effective than ultrasonication, bead beating and sulfuric acid treatment. Pragma et al. [33] concluded that the efficiency of different methods varies largely between different species so that for *C. vulgaris* and *Scenedesmus* sp. the most effective method was microwave oven while for *Botryococcus* sp. bead beating was the better choice. The mechanical approaches are more favorable because of not being algal species specific, ease of scaling up and being fast and no need for special care as is expected in biological approaches. Moreover, possible change of products characteristics as may happen with chemical treatments is avoided in mechanical methods [34, 35]. Up to date, for proposed mechanical methods the energy requirement is so high that makes them energy inefficient. Lee and friends [35] reviewed different methods while estimating least theoretical energy required for algal cell disruption and concluded that amongst sonication, high pressure homogenization, rotor-stator homogenizers, bead mills, freeze drying, microwave, autoclaving, gas decompression and hydrodynamic cavitation, the least energy consumption was recorded for hydrodynamic cavitation which was five times more than the least theoretical energy of cell disruption.

In this study we report on a novel use of glass microparticles with mixing at relatively low revolution per minute (rpm). The goal was to avoid using complex techniques which also may consume lots of energy. Moreover, the possible recovery and reuse of microparticles from even waste glass pieces makes their use economically favorable. The idea is indeed simple but to the extent of author's knowledge have not been addressed elsewhere. The assumption is that instead of applying lots of energy in various form of compression or shear to collapse the cell, glass microparticle with sharp edges can scrape and cut the cell wall with much less energy. The effect of glass particles

size and quantity for the lipid extraction of two microalgae species of *Chlorella* and *Synechocystis* have been investigated. The details of this part of study is presented in chapter 3.

1.4. Maximizing Biomass Production Rate

Microalgae are fast growing photosynthetic microorganisms capable of fixing mineral carbon. Two main families of microalgae including green and blue-green microalgae have been studied vastly as a renewable source for producing biofuels [36]. They are also economically interesting source of valuable materials including carotenoids, phenolic compounds and immune modulators [37]. A variety of studies have been done to maximize the growth rate (GR) of microalgae [38-43]. Microalgae growth is strongly influenced by feeding rate of CO₂ into cultivation broth, light quality, intensity and dark-light period, type of reactor, temperature, pH, nutritious chemicals and type of microalgae itself [38-44]. There is no consensus among literature over the best range of these factors. For carbon dioxide percent in the inflow gas streams, a wide ranges of carbon dioxide from air (~380 ppm CO₂) (v/v) to as high as 60 % CO₂ are investigated [44-46] where the optimum value varies a lot based on different microalgae species and reactor design [46-49]. Many of microalgae species do not tolerate CO₂ more than 5.0 % (v/v) [50].

The optimum gas flow rate which are usually reported as the volume of gas per volume of liquid medium per minute (vvm) were mostly in the range of 0.1-1.0 vvm [44] where 0.5 vvm was reported as the best in [49]. The working temperature was reported as low as 18 °C for *Isochrysis galbana* [51] and as high as 40 °C for strains of *Chlorella* [42] where near 30 °C favored for many species. Another sensitively effective parameter is pH where a near neutral pH was suggested by many researchers [44]. For light intensity, suggested ranges are very different ranging from 100 to 500 μmol/m².s [43, 52]. The light color (wavelength) was studied by wang et al. [43] where a red light (620-645 nm) showed the best GR while a white light (mixture of wavelength 380-760 nm) was the poorest one. Moreover, not only the light color or intensity but the period for light-dark cycles was found very important depending on the microalgae species where a 24-0 regime, 12-12 and other combinations where proposed [43, 44, 53]. A variety of microalgae species were subjected to growth optimization studies including *Neochloris oleoabundans* [53], *Chlorella* [49, 52], *Scenedesmus Sp.* [41], *Aphanothece microscopica*

Nägeli [47], *Spirulina platensis* [43], *Chlamydomonas Sp.* [54], and mixed cultures [55]. The highest obtained growth rate was in the range of 0.106- 0.900 gr/l.d [44].

The design of photobioreactors is a very important factor since the configuration will affect the availability of light inside medium and also the efficiency of mixing for both microorganism and carbon dioxide absorption into liquid medium. Almost all of the previous reports when addressing the feeding rate of carbon dioxide, ignored the effect of gas bubble size or the geometry of bubbling point (diffuser orifice). From a mass transfer point of view, a smaller sized bubbles would result in more efficient carbon dioxide absorption into liquid medium but in contrary lowers the mixing efficiency for microalgae cells. There are many reports on the effective parameters but truly optimization studies are few. The important thing which is not well addressed in the literature is the interaction of determining factors where a statistical optimization approach at multiple levels of variable must be implemented to reveal such effects.

In the present study, the growth condition of *Scenedesmus sp.* was optimized to reach the maximum possible growth rate. Totally, four important growth factors including aeration rate, carbon dioxide percentage in the gas flow, initial inoculum density and the gas diffuser pore diameter was investigated. A central composite design (CCD) approach was implemented using Design Expert software.

1.5. Bio crude Oil

Different biofuels have been produced from microalgae biomass either through thermochemical conversion methods like gasification, thermochemical liquefaction and pyrolysis to produce syngas, Bio-oil and charcoal including bioethanol, biodiesel or through biochemical conversion methods like anaerobic digestion, fermentation and photobiological hydrogen production to produce mainly methane, ethanol and hydrogen [56]. The biofuels technologies like biodiesel or bioalcohol while being interesting products suffer from need of pretreatment steps before conversion of biomass to fuel product. They can just be produced either from lipid or carbohydrate part of biomass not both or all the biomass as whole. Pyrolysis is thermal conversion through depolymerization of organic material in the absence of oxygen into bio-oil suitable to be used as fuel [1, 11, 57-60]. Pyrolysis unselectively converts the biomass to fuel. Pyrolysis products are mainly liquids and solid char, both being valuable as fuel. Generally the liquid products are more favorable for ease of transportation and application. In Fast

pyrolysis, the process parameters can be adjusted so that the liquid product will be maximized. The biochemical composition of feed biomass is also a determining factor where higher fat content improves the conversion yield and final biooil product characteristics.

Fast pyrolysis which is known by very short residence time of 1 to 3 seconds and temperature of around 500-600 °C is reported to have high bio-oil efficiency for microalgae [61, 62]. Multiple species of microalgae have been investigated like strains of chlorella [62, 63] , *Scenedesmus* [11], *Dunaliella* [64], *Nannochloropsis* [65] and *Spirulina* [66].

In the present study, the characteristics of bio-oil produced from biomass of two different strains of microalgae have been investigated. Wild-type *Scenedesmus* and *Synechosystis* microalgae were isolated from local streams and used as biomass producers. The fast pyrolysis process at different temperature was applied to obtain bio-oil. The characteristics of such products were investigated in detail. Finally, based on the observed rate of biomass production of microalgae and the obtained biooil yield, large scale application of microalgae technology was evaluated in compare to a fossil crude oil factory input capacity. The detail of this study is presented in chapter 4.

2. THE SCREENING OF MICROALGAE SPECIES ISOLATED FROM CENTRAL ANATOLIA REGION FOR LIPID, CARBOHYDRATE AND PROTEIN CONTENT

In this study, wild-type microalgae species isolated from a central Anatolia stream have been investigated and evaluated as a biofuel production feed stock and/or carbon dioxide sink. They have been morphologically identified and then screened based on their biochemical compositions. Out of 20 identified microalgae, 18 species were studied for their growth rate, CO₂ mitigation rate, lipid, carbohydrate and protein content and also their natural settling behavior. The cultivation was followed by providing a 3500 lux light intensity provided for 24 hrs continuously, 2 vvm air flow rate in bubble column photobioreactors. The microalgae *Gleocystis ampula* had the highest growth rate equal to 0.138 gr/l.d which also was observed to fix the carbon dioxide with the highest rate of 0.281 gr/l.d . The highest measured lipid content was 47.32 % for *Scenedesmus quadricauda* (I) with an estimated lipid production rate of 52 gr/l.d. The species *Kirchneriella lunaris* and *Micrococcus* sp. were screened to have the highest carbohydrate and protein proportion respectively being 72.43 and 58.11 %. It was also concluded that, the microalgae technology has a good potential to be used as raw material for biofuel production but this technology has yet to be implemented as a treatment method to sink all carbon dioxide emission of a facility like for example a power plant.

2.1. Materials and Method

2.1.1. Chemicals

The chemicals NaNO₃, K₂HPO₄, MgSO₄.7H₂O , CaCl₂.2H₂O, Citric acid, Ammonium ferric citrate, EDTANa₂, Na₂CO₃, H₃BO₃, MnCl₂.4H₂O, ZnSO₄.7H₂O, Na₂MoO₄.2H₂O, CuSO₄.5H₂O, Co(NO₃)₂.6H₂O were purchased from Sigma-Aldrich, USA. Acetone, chloroform, methanol, phenol, sulfuric acid, KCl, and propanol were provided by Tekkim, Turkey. All the chemicals were reagent grade. Nile red (9-diethylamino-5Hbenzo[a]phenoxazine-5-one) purchased from Sigma-Aldrich,USA (assay ≥98.0% (HPLC)). Reagent water was utilized in laboratory using a water purification unit (Thermo Scientific, Germany).

2.1.2. Sampling, culture and isolation

Samples were taken from two points alongside Porsuk River, Eskişehir, Turkey. One being a deep point with very slow current adjacent to Astsabay Raif Özgür Park (39.770002, 30.498488) and the other being a shallow point with higher current and turbulences in Botanic park (39.742747, 30.460088). Previously sterilized 50 ml conical falcons were filled there and immediately transferred to lab. BG11 medium according to [67] have been used throughout the study for microalgae culture. All the cell transferring tasks were done in aseptically to reduce the risk of contamination. Ten milliliters of obtained samples were transferred to 250 ml flasks containing 100 ml BG11. Triplicates of the cultures were prepared and left over a glass plate being shed with 3500 lux white light from bottom provided by 35 W fluorescent lamps for almost one month until green color was clearly observed. The light intensity was adjusted with an illuminance Meter (T-10MA Konica Minolta; Japan). Microscopic view (Olympus, Japan) of the well-grown cultures showed a mixture of multiple green and blue-green microalgae, macroalgae species, diatoms and protozoa (Figure 2.1).

For isolation and purification of the species, single cell isolation techniques was used. In this regard, a droplet of microalgae culture were put on a glass slide and looked under microscope. A glass pasture pipet tip was heated over flame and pulled immediately for elongation to form a fiber like tip. The tip was then cut and looked under microscope to verify its approximate micro scale diameter. This pipet was attached to an adjacent second microscope and adjusted so that the pipet tip could be easily moved with a good control in the solution droplet on the slide. The microalgae cell of interest was pulled into the pipet with a very gentle suction from the other end of pipet by a pipet bulb. The possibly caught cell was transferred to a 10 ml tube containing 5 ml BG11. This was then distributed to 10 subcultures to maintain dilution and increase the chance of purification. These cultures were exposed to light over above mentioned plate for 3 months until clear green color was observed in some cultures. The purification was verified using a light microscope. This attempt was repeated many times to capture cells with different morphologies, sizes or colors.

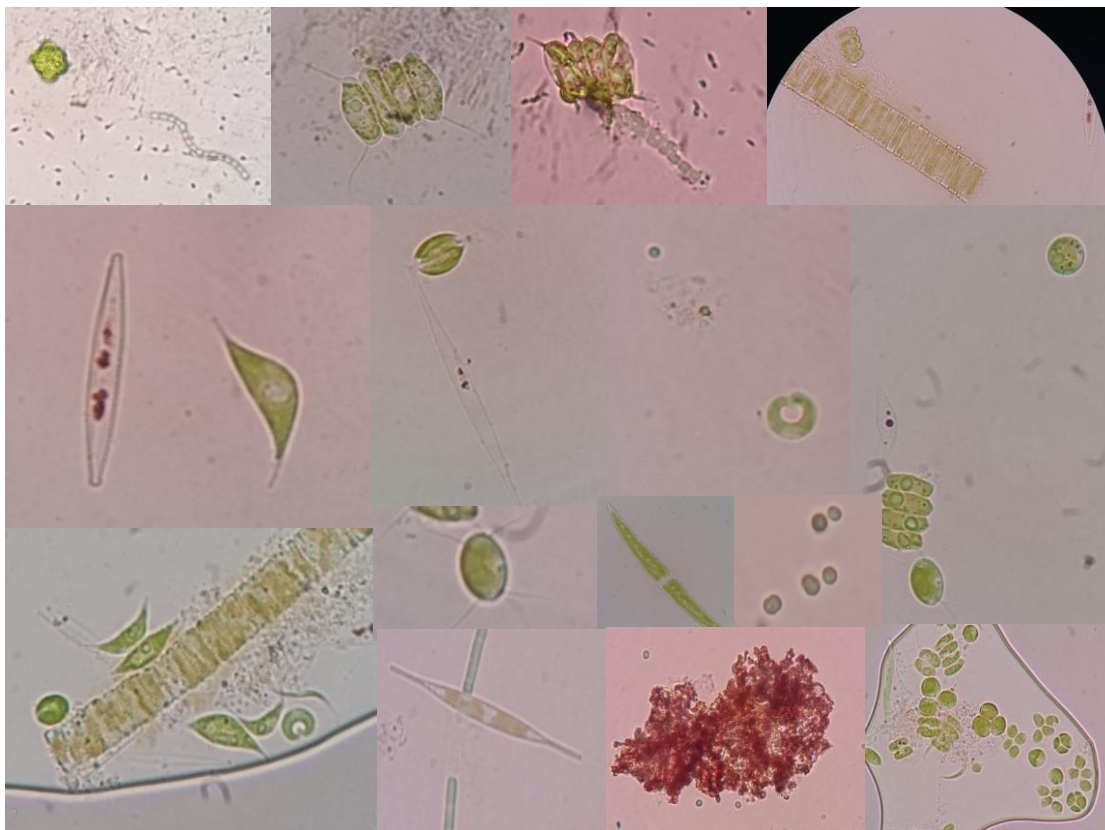


Figure 2.1. *The growth of different microorganisms in mixed culture*

2.1.3. Calibration curve

The next step in the study was to study the biochemical composition i.e., lipid, carbohydrate and protein content of the isolated microalgae. Throughout the study, a calibration curve was needed to convert optical density (OD_{680nm} , Shimadzu UV-1800 UV-Vis Spectrophotometer) to concentration in mg/l in dry basis. Cultivation of each isolated species were followed using a 1 liter flasks as photobioreactors (Figure 2.2). They were kept under sufficient light, approximately 3500 lux, and continuously aerated with approximate equal flow rates of 1 volume of gas per volume of liquid per minutes (vvm). The air flow was passed through a 0.2 μm PTFE membrane filters (Fluoropore, Merck Millipore) to maintain its sterilization. The inoculation from purified stocks were initialized at OD_{680} equal to 0.5. After 20 days cultivation the solutions were then centrifuged to have a paste like microalgae biomass then two aliquots each 5 ml were transferred to weighing dishes and dried in oven for 24 hrs at 110 $^{\circ}C$. The dishes were then cooled down in a desiccator and weighed again. In this way, dried mass in microalgae paste was calculated. In Parallel, 5 ml of paste was diluted serially and the OD_{680} was

read. In OD range were the OD vs microalgae mass concentration graph showed linear, trend line was passed through the points and the coefficient was calculated for each microalgae. The results are presented in Table 1. The OD vs concentration curves is provided as supplementary material. The observed approximate linear range for OD₆₈₀ (Table 1) showed that a range of 0.15 to 1.60 absorbance values would apply for all isolated microalgae. For the next steps of the study, the estimated coefficients were used to convert OD₆₈₀ to dried biomass concentration in gr/l according to:

$$\text{Biomass Con. (g. l}^{-1}\text{)} = C_f \times (\text{OD}_{680} - \text{OD}_b) \quad (2.1)$$

Where C_f is the conversion factor, OD_{680} is the optical density at 680 nm wavelength and OD_b is the optical density of blank.



Figure 2.2. *The cultivation of isolated microalgae for calibration curve withdrawal and elemental analysis*

Table 2.1. *The linear range of OD₆₈₀ for isolated microalgae and the conversion factors to dried biomass concentration*

Microalgae #	Apx. Linear Range OD ₆₈₀	Coefficient	R ²
1	0.3-2.50	0.153	0.994
2	0.2-2.10	0.310	0.999
3	0.17-1.85	0.154	0.998
4	0.15-2.20	0.250	0.998
5	0.15-1.88	0.194	0.998
6	----	-----	
7	0.18-2.87	0.432	0.999
8	0.44-2.12	0.171	0.997
9	----	-----	
10	0.20-2.10	0.249	0.998
11	0.2-1.90	0.087	0.999
12	0.20-1.79	0.207	0.992
13	0.18-2.24	0.133	0.990
14	0.25-2.53	0.171	0.990
15	0.23-1.96	0.151	0.997
16	0.22-1.85	0.359	0.999
17	0.20-2.65	0.249	0.993
18	0.17-2.00	0.198	0.990
19	0.25-2.40	0.162	0.990
20	0.21-2.40	0.176	0.999

2.1.4. Lipid determination

A fluorometric approach was followed for lipid determination based on the work of Elsey and friends [68] with some modifications. The samples were diluted until OD₆₈₀ fell in the range of 0.1–0.3. Per sampling, 3 mL of this algal suspension was stained with 20 µL of 7.8×10⁻⁴ M Nile Red dissolved in acetone and then excited at 486 nm before measuring the emission at 570 nm (Qubit 4 Fluorometer, Thermofisher, USA). Blanks

were also prepared by filtering (0.22 micron) microalgae solutions and the fluorescence value was subtracted from samples value. The calculated value was used for screening of the microalgae species with regard to lipid content. Higher lipid content corresponds to higher fluorescence.

For lipid content estimations, a calibration curve of fluorescence vs lipid content was prepared. Microalgae samples were centrifuged and the lipid was extracted and quantified according to the method of Bligh and Dyer [69].

2.1.5. Carbohydrate

Phenol-sulfuric acid colorimetric method was used for carbohydrate determination as was described in [70]. Dextran was used as reference sugar for standard solution preparation.

2.1.6. Protein

For estimation of protein a conversion factor of elemental nitrogen to protein (N-Prot factor) was used. Different studies reported ranges of N-Prot factor. In this study, the N-Prot factor equal to 4.78 ± 0.62 was selected based on the work of Lourenço and friends [71]. They have reported specifically on the estimation of protein content of microalgae using elemental CHN/S analysis as was used in the present work (CHN/S Elemental Analyzer, Thermoscientific, USA).

2.2. Results and Discussions

2.2.1. Identification of the isolated species

The purified cultures were morphologically identified with comparison to data available. Their microscopic view using oil immersion microscopy is provided in figure 2.3. The identified microalgae were #1: *Chroococcus disperus*, #2: *Gleocystis ampula*, #3: *Synechocystis* (I), #4: *Scenedesmus obliquus* (I), #5: *Chlorella vulgaris* (I), #6: *Phormidium uncinatum* (I), #7: *Scenedesmus quadricauda* (I) #8: *Synechocystis* (II), #9: *Phormidium uncinatum* (II), #10: *Scenedesmus dimorphus*, #11: *Microcystis aeruginosa*, #12: *Chlorella vulgaris*(II), #13: *Cyanobacterium cedrorum*, #14: *Chroococcus* sp.(I), #15: *Kirchneriella lunaris*, #16: *Scenedesmus quadricauda* (II), #17: *Chlorella vulgaris* (III), #18: *Nannochloris* sp., #19: *Chroococcus* sp.(II) and #20: *Micrococcus* sp. These species belongs to the green microalgae and cyanobacteria or blue-green microalgae

subdivisions of algae which are categorized under cyanophyta and chlorophyta phylum respectively.

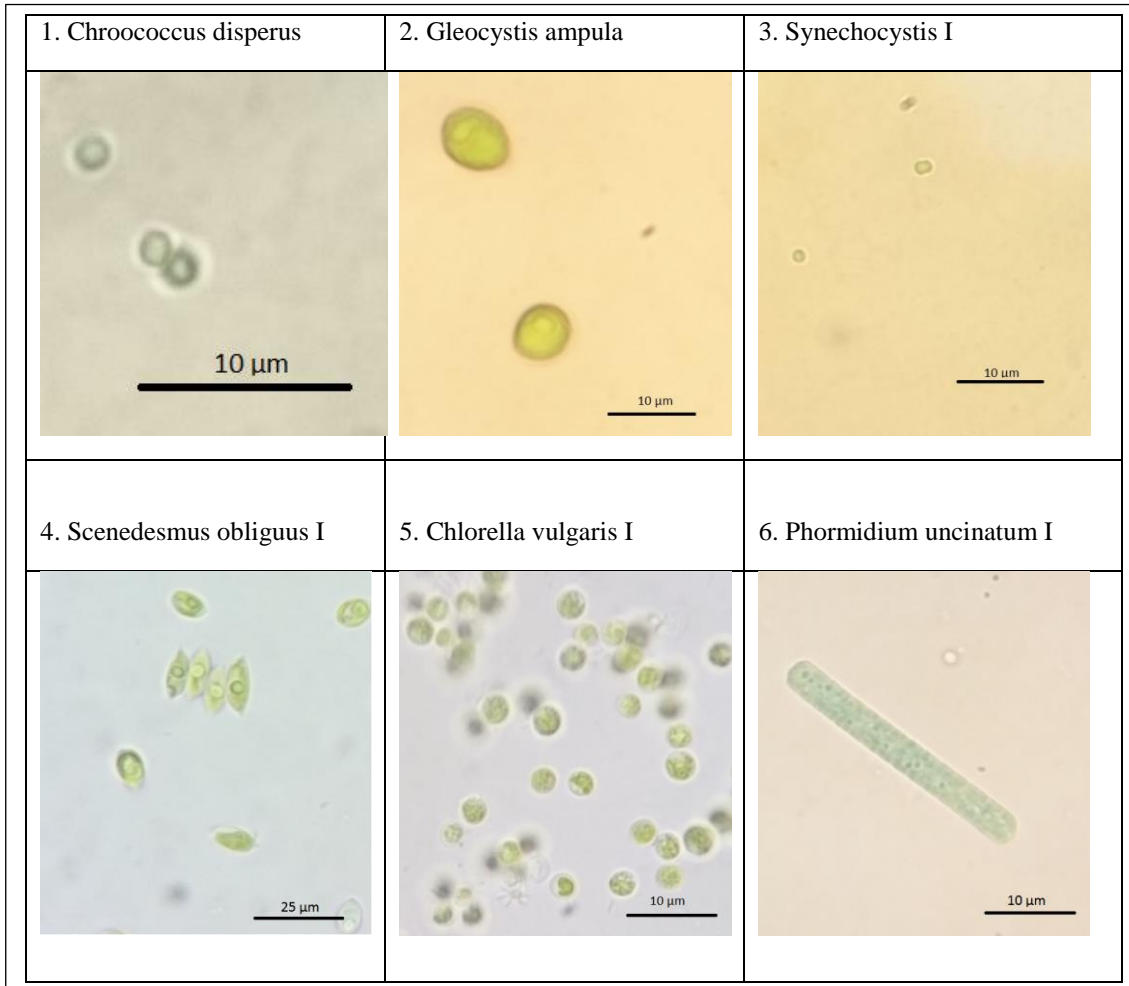


Figure 2.3. *The microscopic view (oil immersion) of the isolated microalgae species*

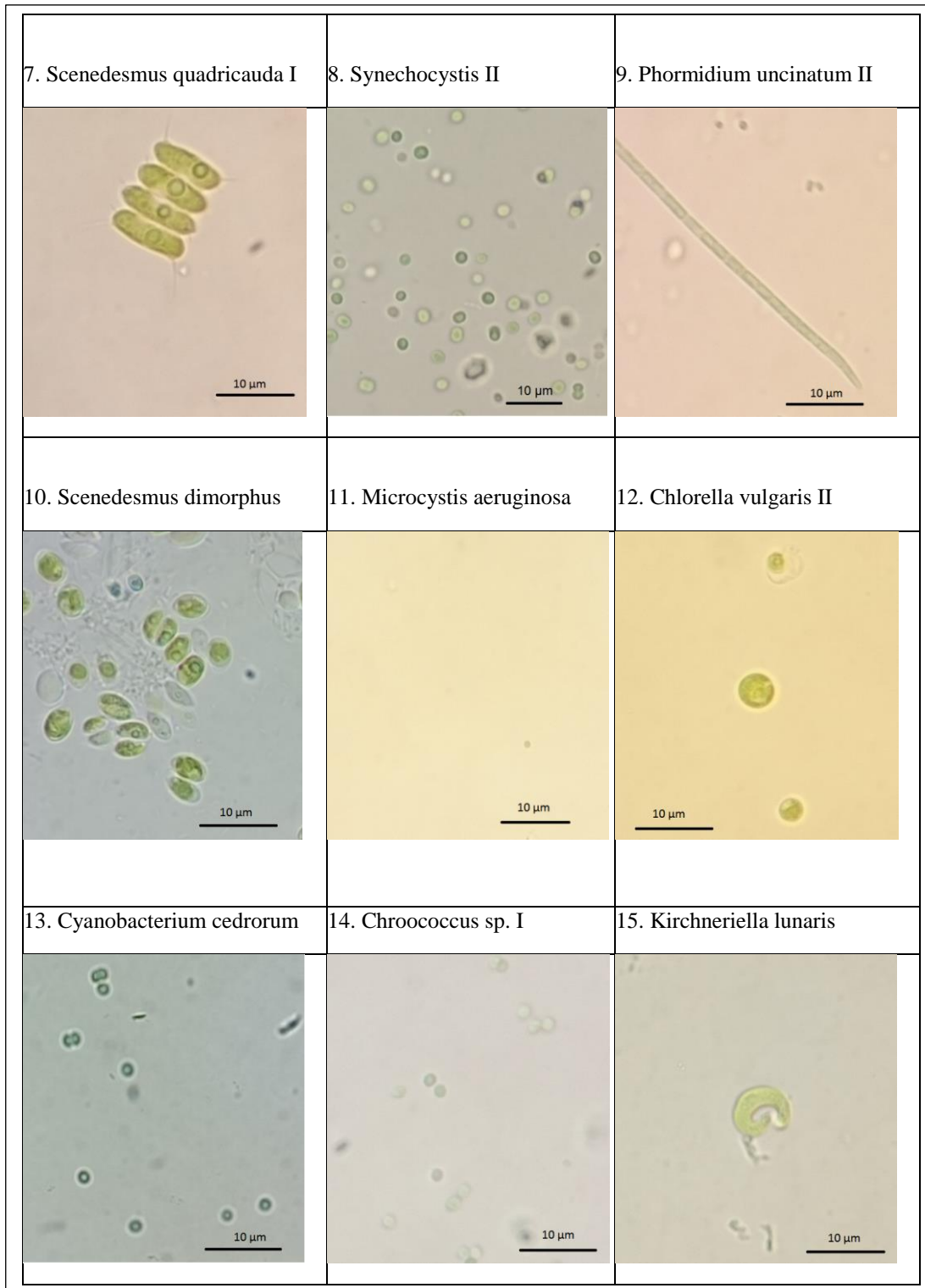


Figure 2.3. (Continued) *The microscopic view (oil immersion) of the isolated microalgae species*




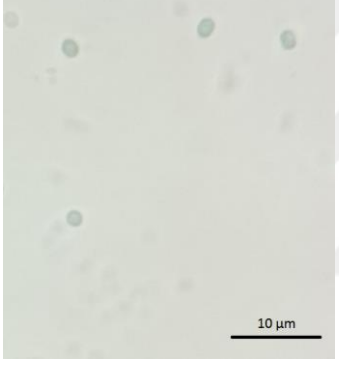
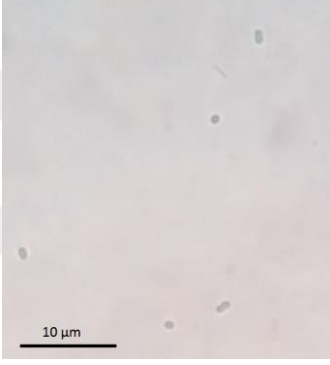
16. <i>Scenedesmus quadricauda</i> II	17. <i>Chlorella vulgaris</i> III	18. <i>Nannochloris</i> sp
		
19. <i>Chroococcus</i> sp. II	20. <i>Micrococcus</i> sp.	
		

Figure 2.3. (Continued) *The microscopic view (oil immersion) of the isolated microalgae species*

2.2.2. Growth rate

Growth rate is a very important factor to be determined for each of the isolated microalgae species because it determines the amount of obtainable biomass and equally the amount of fixed carbon. The rate of growth depends on multiple factors which also can be modified to maximize the rate and/or the final concentration of biomass in the solution. These factors mainly are light intensity and its duration, temperature, pH, gas flow rate, carbon dioxide concentration in the gas flow and nutritious composition. Totally, 18 species out of 20 identified species were studied for their growth rate because the microalgae *Phormidium uncinatum* I&II were excluded because the photobioreactor suitable for these long chain forming microalgae would be completely different in design. A preliminary cultivation in 1 litre photobioreactor with continuous bubbling for all 20 species showed that this kind of photobioreactors are not suitable for all type of microalgae. As can be seen from figure 2.4, microalgae *Phormidium uncinatum* I&II which are from Oscillatoriaceae family did not homogeneously dispersed in the liquid medium and either formed a single woven matt or attached to the surface (Figure 2.4). A sketch of the cultivation vessel with dimensions and real configuration is shown in figure 2.5. The cultivation vessels were identical. Air was charged into the cultivation vessels at 1 vvm flow rate. The light was provided at 3500 lux by 8 white fluorescent lamps. The medium was BG11 without any organic carbon. The pH was fixed at 7 while the temperature was not controlled. The ambient temperature was approximately 25 °C. Inoculation started with OD₆₈₀ equal to 0.5. For the first days of cultivation 3 ml samples were taken using sterile syringes attached to 3 way luer-lock valves without need for removing caps. For the cases where OD were out of linear range (Table 2.1), samples were diluted as much as needed. The microalgae concentration then was estimated using conversion factors (Table 2.1). The obtained growth curves are shown in figure 2.6. The slope of the linear phase of the growth was calculated as the growth rate (Table 2.2). The microalgae *Gleocystis ampula*, *Scenedesmus dimorphus* and *Chlorella vulgaris*(II) showed the highest growth rate with 0.138, 0.137 and 0.133 gr/l.d respectively. In opposite, microalgae *Kirchneriella lunaris* , *Microcystis aeruginosa* and *Chlorella vulgaris* (I) were the slowest growing species with growth rates of 0.042, 0.056 and 0.079 gr/l.d in order. The highest recorded concentration during 35 days of cultivation is also reported (Table 2.2) where microalgae *Scenedesmus quadricauda* (I), *Gleocystis ampula*

and *Scenedesmus quadricauda* (II) reached the highest concentration with 2.831, 2.625 and 2.496 gr/l in dried basis.



Figure 2.4. The different behaviour of long chain strand forming microalgae in liquid medium

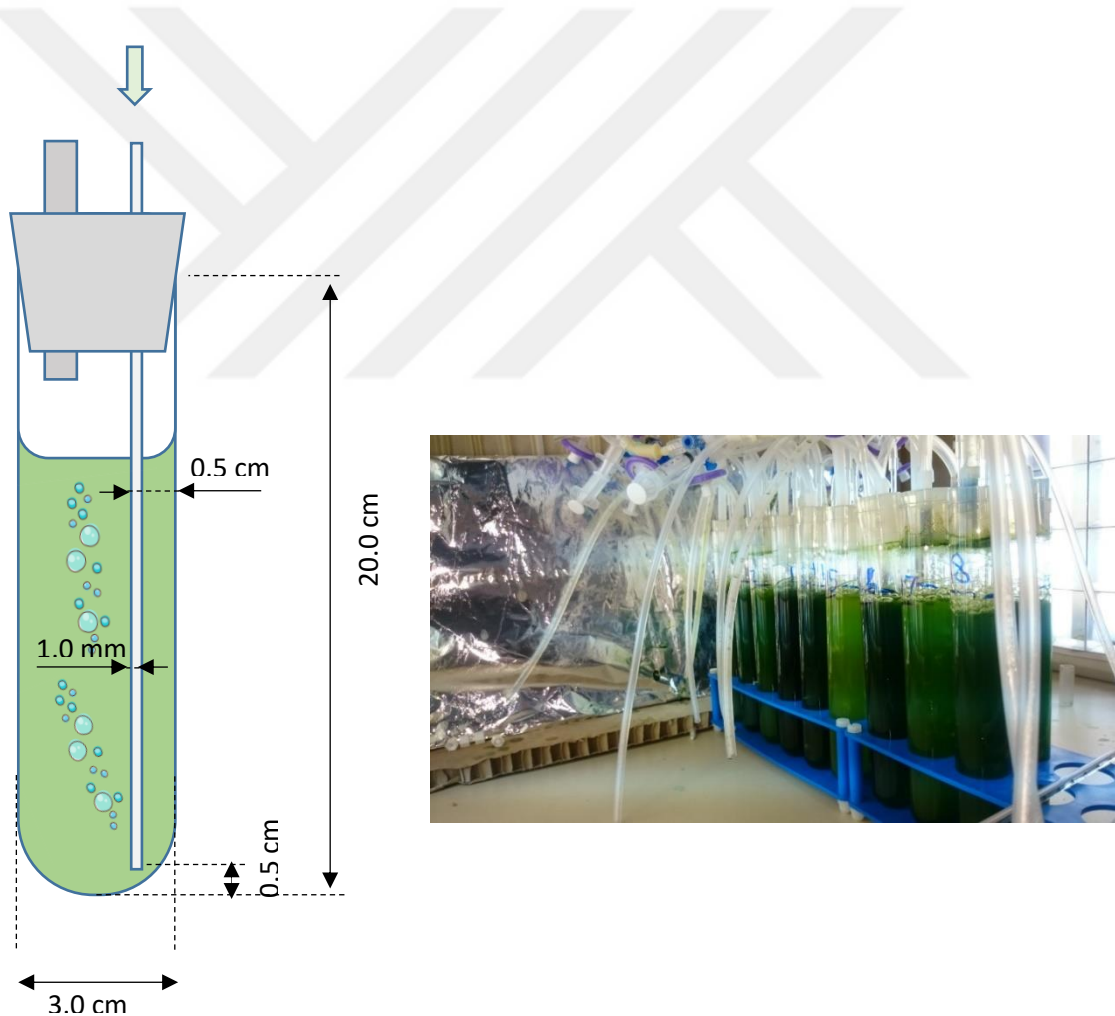


Figure 2.5. The schematic view (left) and the real view of the photobioreactors

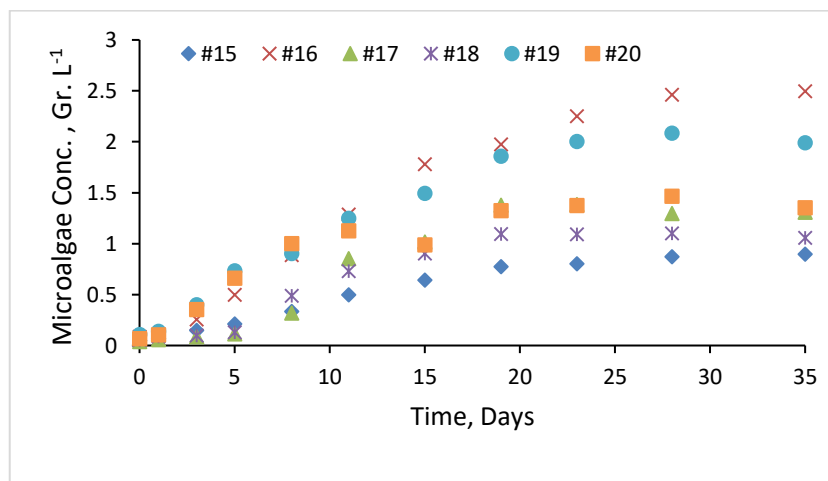
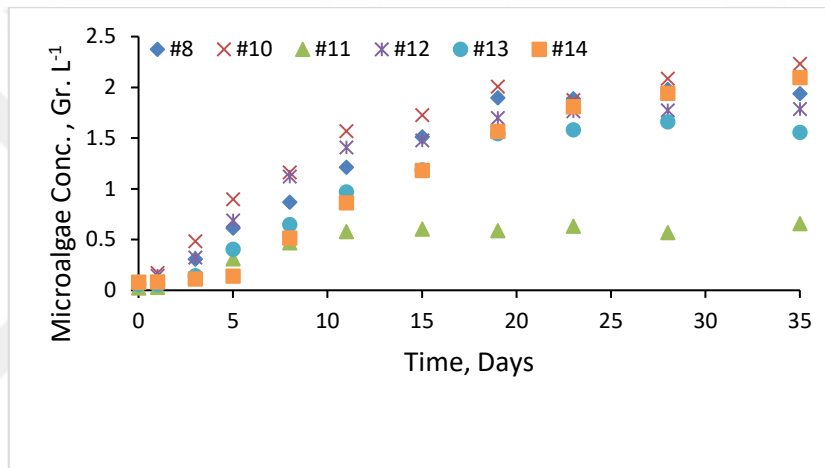
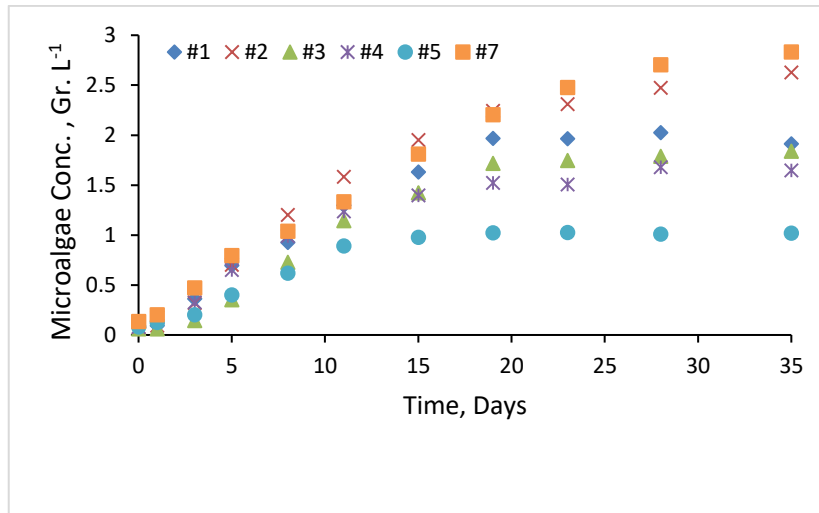


Figure 2.6. The Growth curve for isolated microalgae

Table 2.2. Growth characteristics and biochemical compositions of isolated microalgae

#	Microalgae	Family	Growth Rate	Max. Conc.	%C	%N	%H	CO ₂ fixing rate	Lipid	CHO	PRO	Lipid Prod. Rate	Settling Efficiency after 24 hr
			(g/l.d)	(g/l)	(%)	(%)	(%)	(g/l.d)	(%)	(%)	(%)	(mg/l.d)	(%)
1	Chroococcus disperus	b	0.109	2.024	56.48	10.97	7.50	0.226	6.73	19.68	52.45	7	0.35
2	Gleocystis ampula	g	0.138	2.625	55.51	7.53	7.40	0.281	21.71	31.26	35.98	30	96.04
3	Synechocystis (I)	b	0.101	1.838	53.32	11.52	7.77	0.196	4.23	26.62	55.07	4	2.53
4	Scenedesmus obliquus (I)	g	0.110	1.679	50.40	7.52	7.33	0.202	17.49	41.67	35.94	19	92.92
5	Chlorella vulgaris (I)	g	0.079	1.023	57.52	7.11	7.83	0.166	31.13	52.39	33.97	24	53.52
6	Phormidium uncinatum (I)	b	--	--	46.74	8.97	6.87	---	---	---	42.86	---	---
7	Scenedesmus quadricauda (I)	g	0.110	2.831	48.81	9.08	7.62	0.196	47.32	41.04	43.42	52	89.43
8	Synechocystis (II)	b	0.103	1.980	49.82	10.83	7.35	0.187	24.58	28.98	51.79	25	2.00
9	Phormidium uncinatum (II)	b	---	---	43.77	9.84	6.73	--	---	---	47.03	---	---
10	Scenedesmus dimorphus	g	0.137	2.232	51.45	7.21	7.58	0.259	26.97	55.02	34.46	37	92.82
11	Microcystis aeruginosa	b	0.056	0.657	51.30	11.50	7.45	0.105	39.70	17.75	54.99	22	1.19
12	Chlorella vulgaris(II)	g	0.133	1.786	56.37	7.28	7.81	0.274	30.88	55.45	34.79	41	33.54
13	Cyanobacterium cedrorum	b	0.087	1.662	52.21	10.81	7.19	0.167	16.60	32.83	51.68	14	1.76
14	Chroococcus sp.(I)	b	0.100	2.096	51.33	10.80	7.63	0.188	19.19	27.80	51.62	19	49.70
15	Kirchneriella lunaris	g	0.042	0.896	51.29	4.99	7.66	0.079	24.55	72.43	23.84	10	14.03
16	Scenedesmus quadricauda (II)	g	0.128	2.496	51.77	7.37	7.32	0.243	26.42	38.24	35.24	34	94.88
17	Chlorella vulgaris (III)	g	0.091	1.382	49.16	6.54	7.41	0.164	29.78	66.71	31.26	27	65.52
18	Nannochloris sp.	g	0.077	1.101	53.70	6.73	7.64	0.151	33.95	67.69	32.15	26	71.98
19	Chroococcus sp.(II)	b	0.096	2.084	48.32	10.49	7.13	0.170	24.30	24.99	50.12	23	0.03
20	Micrococcus sp.	b	0.106	1.465	54.96	12.16	8.05	0.213	11.56	27.19	58.11	12	2.15

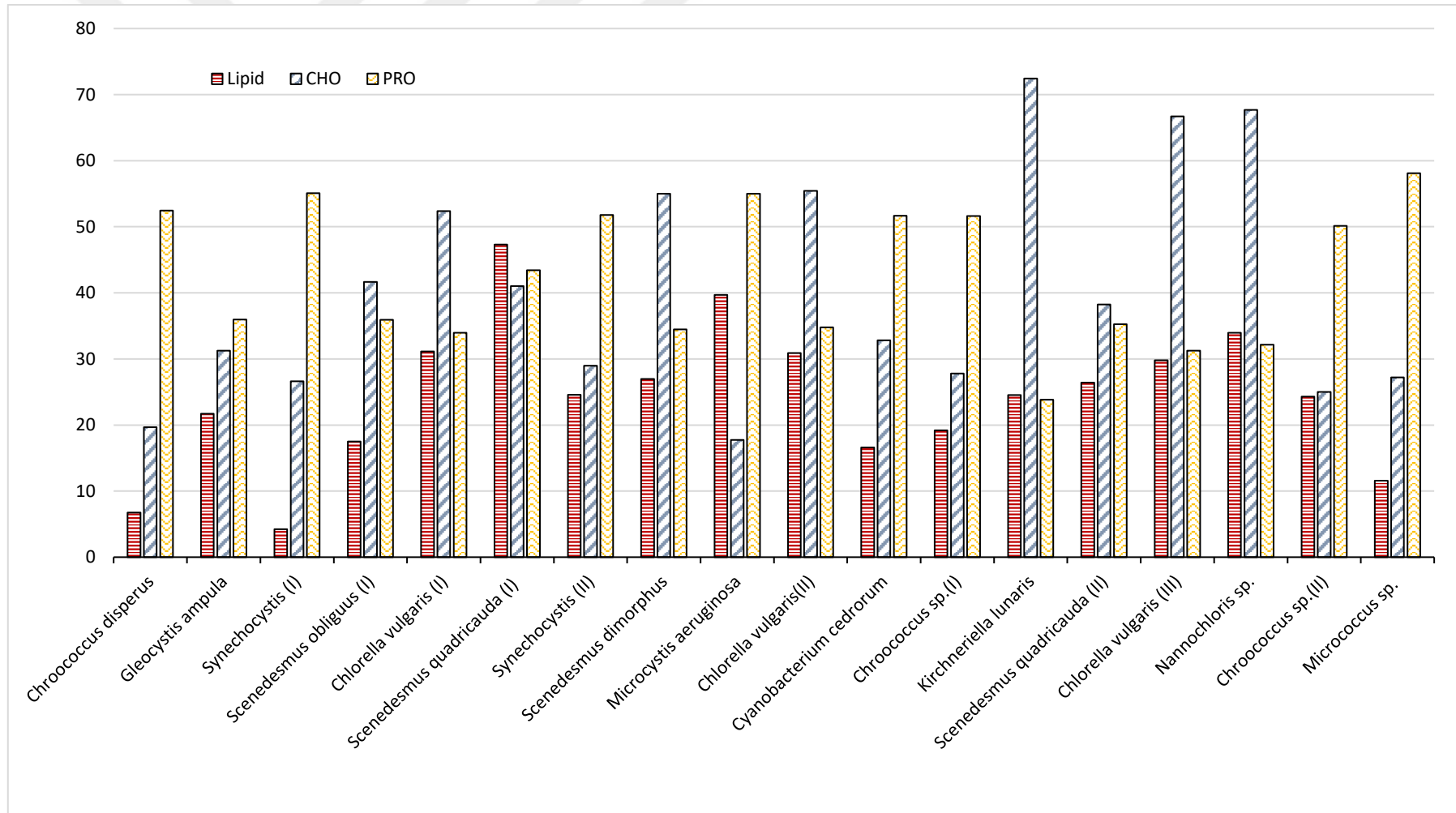


Figure 2.7. Protein, carbohydrate and protein content

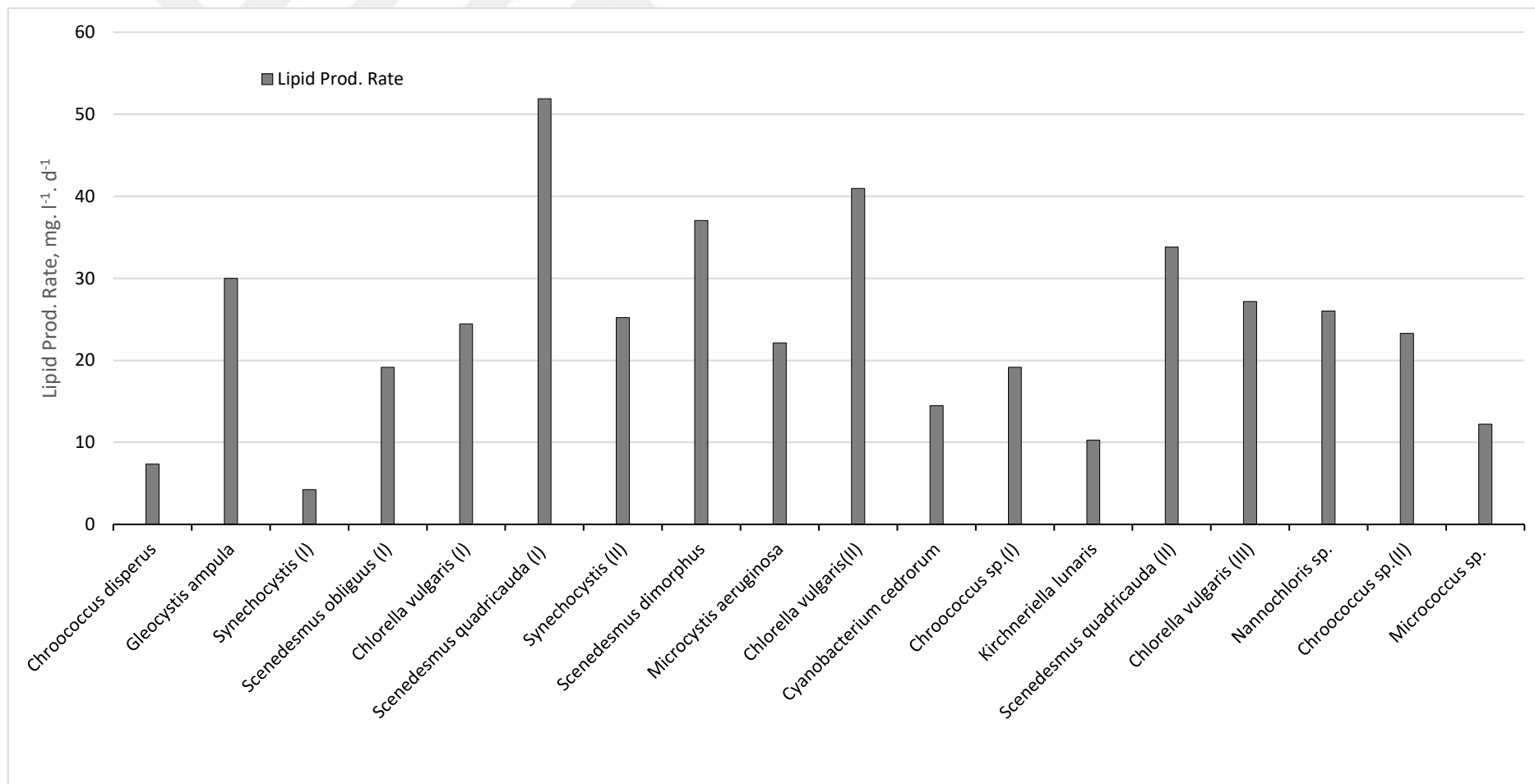


Figure 2.8. Lipid production rate of variety of isolated microalgae.

2.2.3. Elemental analysis and the estimation of carbon fixation rate

The elemental analysis for carbon, hydrogen and nitrogen is presented in Table 2.2. The carbon content of microorganism is an *important* factor since it determines the potential for carbon fixation. The microalgae *Chlorella vulgaris (I)* showed the highest elemental carbon content being 57.5%. With a lesser amount *Chroococcus disperus* and *Chlorella vulgaris (II)* respectively were composed of 56.5 and 56.4% elemental carbon. The least value was 43.8% obtained for *Phormidium uncinatum (II)*. As can be seen, there is a meaningful difference for carbon content between isolated species. From the data obtained for growth rate and the biomass elemental carbon, the rate of carbon dioxide fixation was estimated (Table 2.2). It was observed that the highest rate of carbon dioxide mitigation was 0.281 gr/1.d for *Gleocystis ampula*. If this is going to be used to capture and fix the carbon emission of a medium sized 405 MWe coal burning power plant like ICDAS Biga facility (Çanakkale, Turkey) with an approximate emission factor of 762 kg CO₂/MWh [72] which emits almost 7406640 kg CO₂ per day, a microalgal photobioreactor facility with a size of roughly 26.3 million m³ will be needed. Even though, this blind estimation ignores all the energy consumption of such microalgae plant, the result shows that the microalgae biomass technology cannot be a solution for CO₂ mitigation in large scale.

2.2.4. Biochemical composition

Lipids, carbohydrates and proteins are the main biochemical macromolecule composition of microalgae. These are important to be quantified because these are determining factors for final product of interest. The microalgae with higher lipid content is more favorable for biodiesel production while the carbohydrate rich species are suitable for bioalcohols production via fermentation. On the other hand, a protein rich species may be suitable to be used as feed ingredient for cattle or fishery industries. Although in this study, well-known procedures for determining these biochemicals have been used, the estimated results are not absolute values because for example the conversion coefficients for protein estimation is not species-specific coefficients for analyzed microalgae or the carbohydrate has been estimated using standards prepared by dextran as a reference sugar which may not be an exact indicator for isolated microalgae.

2.2.4.1. Lipid

The estimated percentage of lipid, carbohydrate and protein is presented in Table 2. A graphic presentation is also provided in figure 2.7 for ease of comparison between different species. As can be seen (Figure 2.7) *Scenedesmus quadricauda (I)*, *Microcystis aeruginosa* and *Nannochloris sp.* had the highest lipid content being 47.32, 39.7 and 33.95 % respectively. In a previous screening study for high lipid content, a *scenedesmus sp* was found to have 40.0 % lipid content [73]. Because of high lipid content of these species, they were promising candidates as biomass producers for oil based biofuels like biodiesel. From a process point of view, the rate of lipid production in a real plant may be more important than the lipid percentage in the biomass. Therefore by taking the data for growth rate in to account, the rate of lipid production for isolated species were estimated as presented in Table 2.2 and graphically shown in figure 2.8. In this case, the highest estimated lipid production rates (Figure 2.8) were 52, 41 And 37 mg/l.d respectively for *Scenedesmus quadricauda (I)*, *Chlorella vulgaris(II)* and *Scenedesmus dimorphus*. The distribution of data into two categories of blue-green and green microalgae in figure 2.9 represented a haphazard distribution of the acquired data between two groups which presented lack of correlation. Additionally, the calculated correlation factor of 0.501 revealed no relation between the microalgae type and lipid content.

To have a more sensible understanding of these results for lipid and estimated production rate, the estimated biodiesel rate with regard to the highest lipid production rate of this study was compared to the diesel production rate of Ras Tanura Refinery (Aramco, Saudi Arabiya), a petroleum refinery complex with an annual diesel production capacity of 65,893 barrel. According to a previous study [74], the microalgae oil was converted to FAME with an efficiency of almost 77 percent for some green microalgae. Assuming an average density equal to 880 kg/m³ (EN 14214) for biodiesel, the size of photobioreactor facility to produce the same amount of diesel as in Ras Tanura Refinery, would roughly be 630,000 m³. This estimation is for biomass production without any optimization on growth condition or other downstream processes. Any modification which would result in doubling the rate will reduce the size of such facility by half. A previous research [75] showed that when photobioreactor was fed with a 7% CO₂ (v/v) gas stream, the growth rate has increased by almost 148.0 % for microalgae *chlorella vulgaris*. The use of microalgae for biodiesel production is not far beyond reality and can be achieved after improving the efficiencies of different steps of the process.

2.2.4.2. Carbohydrate

The results for carbohydrate contents are presented in Table 2.2 and as bar charts in figure 2.7. The highest amount was recorded for *Kirchneriella lunaris* with 72.43% of the dried mass where Shady et al. reported 75.0 % for total carbohydrates of this microalgae [76]. At the second and third ranks were *Nannochloris* and *Chlorella vulgaris* (III) sp. respectively with 67.69 and 66.71 % carbohydrate contents. All of these three species belonged to green microalgae family. The distribution of data into two categories of blue-green and green microalgae in figure 2.9 clearly shows that the green microalgae species had obviously higher carbohydrate content. The calculated correlation factor was 0.787 which revealed the significant correlation of microalgae type and carbohydrate content. The growth rate for these species were 0.042, 0.077 and 0.091 g/l.d respectively. The growth rate could be optimized for each of the species to increase the production rate but with the same growth condition for all the species in this research, the daily carbohydrate production rate was estimated as 31, 52 and 61 mg per liter of cultivation.

2.2.4.3. Protein

As can be seen from figure 2.7 and Table 2.2, *Micrococcus*, *Synechocystis* (I) and *Microcystis aeruginosa* species had the highest protein contents which in order were 58.11, 55.07 and 54.99 % of the dried mass. Interestingly they were all cyanobacteria i. e. blue-green microalgae. The averaged data on protein content for all the isolated blue-green species was 51.57% while for green microalgae was 34.11%. The distribution of data into two categories of blue-green and green microalgae in figure 2.9 clearly shows that the blue-green microalgae species had a significantly higher protein content where the correlation factor in this case was -0.928 which showed a very strong relation between microalgae family and their protein content. The results for protein content is considerably high and can be potentially used as supplementary feed material for animals or aquaculture breeding industries [77] or even direct consumption by human [78].

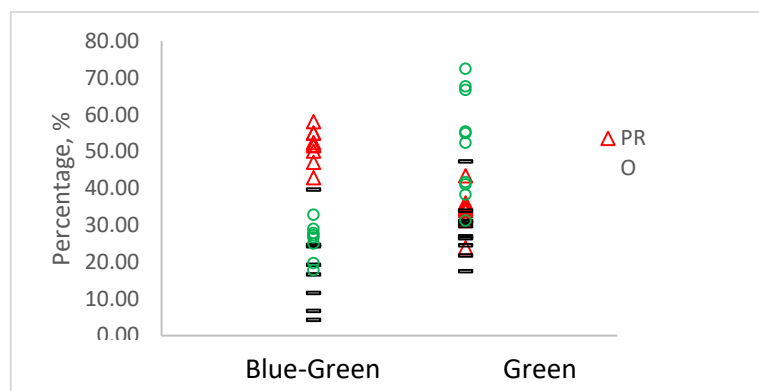


Figure 2.9. Distribution of lipid, carbohydrate and protein content in Blue-Green and Green microalgae

2.2.5. Microalgae Natural Settling behavior

Microalgae species settling behavior are different mainly because of their size, motion ability and their floating capabilities. From an application point of view this was important to be studied because the species which settle easily can be easily harvested without extra costs for processes such as centrifuge and chemical coagulation. In this regard, microalgae broth were transferred to 15 ml test tubes and left over night. The OD of the sample taken from the top layer of the broth at the start and after 24 hrs was read to measure the settling efficiency. The photograph in figure 2.11 shows that for some species the settling is almost complete like for example the microalgae *Gleocystis ampula*, *Scenedesmus quadricauda (II)* and *Scenedesmus obliquus (I)*. The settling efficiency for mentioned species were respectively 96.04, 98.88 and 92.92 %. For the Microalgae *Scenedesmus quadricauda (I)* which was the most suitable one for lipid production, the settling efficiency was 89.43 % which was very significant. Contrarily, some species formed a very stable solution with almost no settling like for instance microalgae *Chroococcus sp.(II)*, *Chroococcus disperus* and *Microcystis aeruginosa*. The analysis of correlation between estimated cell size and the settling efficiency showed a value of 0.75 which reveals a positive correlation of cell size and settling efficiency. The graph for scattered data in figure 2.10 showed that only one species i.e. *Kirchneriella lunaris* falls apart from these positive correlation. When this point was excluded, the correlation value even increased to 0.84. The calculated average of settling efficiency for blue-green and green species were 70.47 and 7.47 % respectively which showed that blue-green microalgae form much more stable solutions than green microalgae. These results showed that green microalgae can be harvested more easily and perhaps less costly.

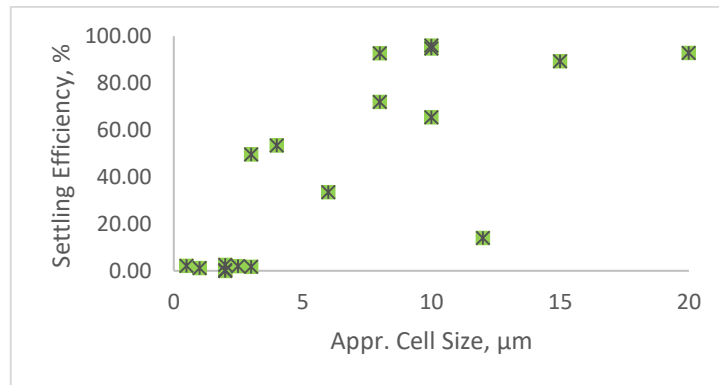


Figure 2.10. Distribution of natural settling efficiency in approximate cell size of isolated microalgae

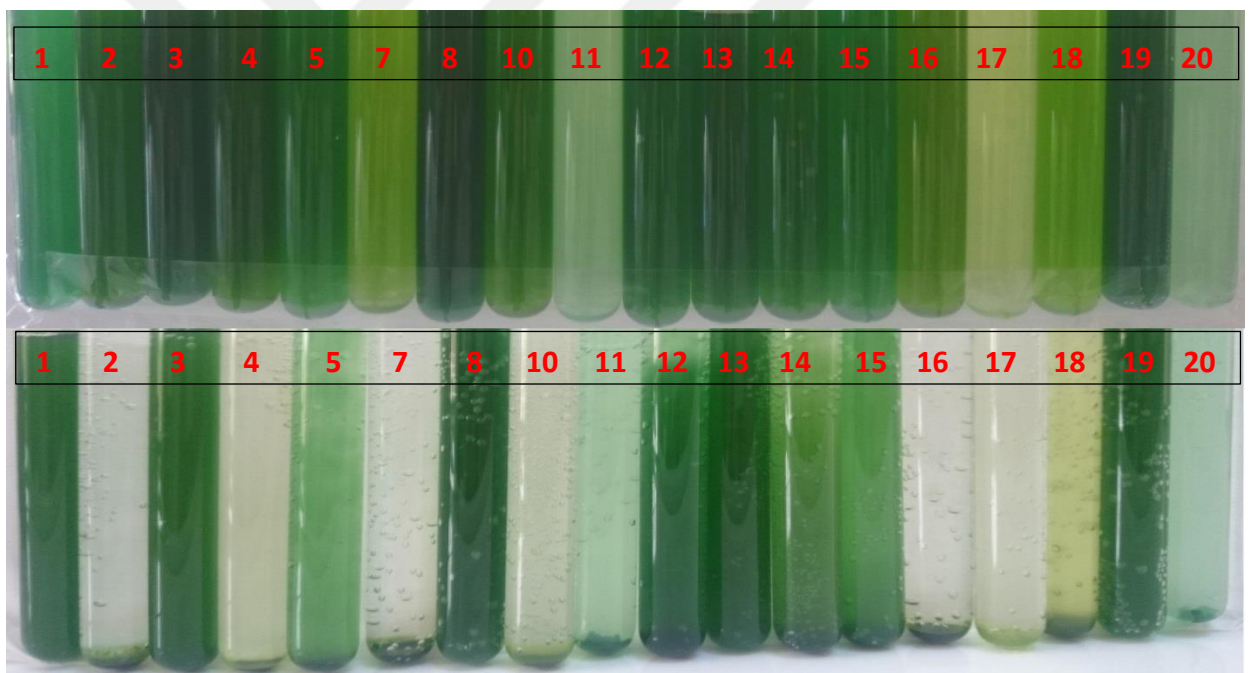


Figure 2.11. The natural settling of microalgae cells in the solution; 1: *Chroococcus disperus*, 2: *Gleocystis ampula*, 3: *Synechocystis (I)*, 4: *Scenedesmus obliquus (I)*, 5: *Chlorella vulgaris (I)*, 7: *Scenedesmus quadricauda (I)* 8: *Synechocystis (II)*, 10: *Scenedesmus dimorphus*, 11: *Microcystis aeruginosa*, 12: *Chlorella vulgaris(II)*, 13: *Cyanobacterium cedrorum*, 14: *Chroococcus sp.(I)*, 15: *Kirchneriella lunaris*, 16: *Scenedesmus quadricauda (II)*, 17: *Chlorella vulgaris (III)*, 18: *Nannochloris sp.*, 19: *Chroococcus sp.(II)* and 20: *Micrococcus sp.*

3. LIPID EXTRACTION FROM MICROALGAE CHLORELLA AND SYNECHOCYSTIS SP. USING GLASS MICROPARTICLES

In this study, the effect of adding microparticles of glass as a cell disruption enhancer to maximize the extracted lipid from wild-type microalgae *Synechocystis* and *Chlorella* sp. have been investigated. A general factorial design approach at different levels have been implemented to evaluate the effectiveness of size and quantity of glass particles for both species. The statistical analyze of variance (ANOVA) for the obtained results revealed the significance of the method and defined factors. The recorded lipid content without addition of particles were 45.02 and 23.19% for *Synechocystis* and *Chlorella* sp., respectively. With the addition of particles, the highest recorded value for lipid content of *Chlorella* was 34.01% which stands for 46.60 % enhancement of extraction efficiency. This was achieved when 40 μm particles in 2.25 mass proportion of particle to dried biomass were used. The addition of particle did not improved the lipid extraction efficiency for the *Synechocystis* sp. These findings also showed that the conventional gravimetric methods may underestimate the lipid content of microalgae species.

3.1. Materials and Method

3.1.1. Reagents

The chemicals NaNO_3 , K_2HPO_4 , $\text{MgSO}_4 \cdot 7\text{H}_2\text{O}$, $\text{CaCl}_2 \cdot 2\text{H}_2\text{O}$, Citric acid, Ammonium ferric citrate, EDTANa_2 , Na_2CO_3 , H_3BO_3 , $\text{MnCl}_2 \cdot 4\text{H}_2\text{O}$, $\text{ZnSO}_4 \cdot 7\text{H}_2\text{O}$, $\text{Na}_2\text{MoO}_4 \cdot 2\text{H}_2\text{O}$, $\text{CuSO}_4 \cdot 5\text{H}_2\text{O}$, $\text{Co}(\text{NO}_3)_2 \cdot 6\text{H}_2\text{O}$ were purchased from Sigma-Aldrich;USA. Chloroform, methanol and propanol were provided by Tekkim,Turkey. All the chemicals were reagent grade. Reagent water was provided in laboratory using a water purification unit (Thermo Scientific, Germany).

3.1.2. Microalgae isolation and culture

Samples were taken from Porsuk river in botanic park of Eskisehir province Turkey (39.742747, 30.460088), and transferred immediately to laboratory for cultivation. The cultivation was followed in a 250 mL flask with BG11 medium according to literature [67]. About 20 mL of the sample was added to the previously autoclaved 200 mL medium. After 3 weeks the green color showed sufficient growth of the mixture. The purification

was done using single cell isolation approach under microscope. The presumably pure micro-samples was transferred to 10 mL sterilized medium and then distributed to 10 test tube for higher certainty of successful purification. The tubes were kept under fluorescent lamps (3x35 W) for almost one month until green color was clearly observed. The wild type *Synechocystis* sp. and *Chlorella* sp. microalgae type was morphologically identified (Figure 3.1) and transferred gradually after apparent growth to 250 mL flask then 1 liter flask and finally 4 liter photobioreactor with the aeration rate of 0.5 vvm to obtain enough biomass for further experiments. For all the steps, cultivation medium were exposed for 24 h a day to light intensity provided with 3 fluorescent lamps (35 W TL5 Pelsan, Turkey). The growth was monitored using spectrophotometry (UV-VIS 1800 Shimadzu, Japan) at 650 nm wavelength. The approximate size distribution of both microalgae was determined by using an optical microscope (Olympus, Japan) equipped with eyepiece reticule. Harvesting was done when growth reached almost its plateau. Two liter of the solution was centrifuged and the obtained paste was kept at 4 °C for later experiments.

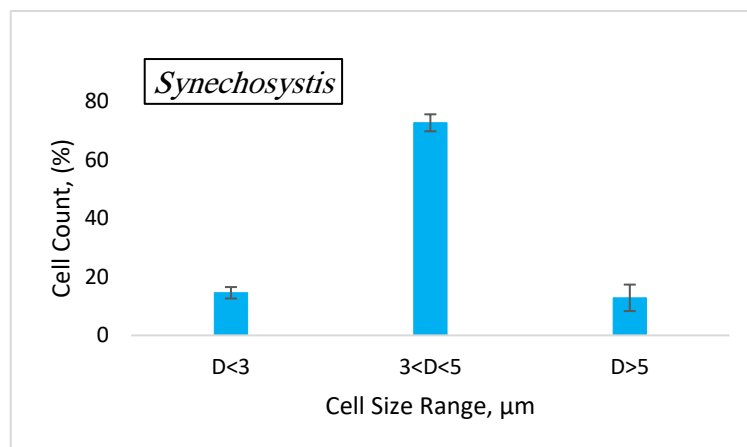
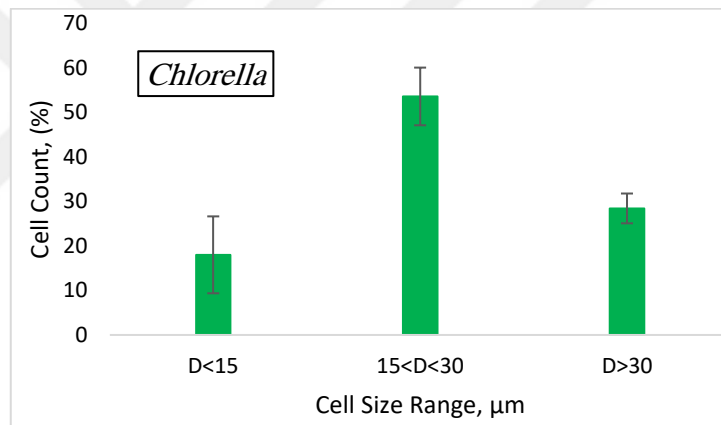
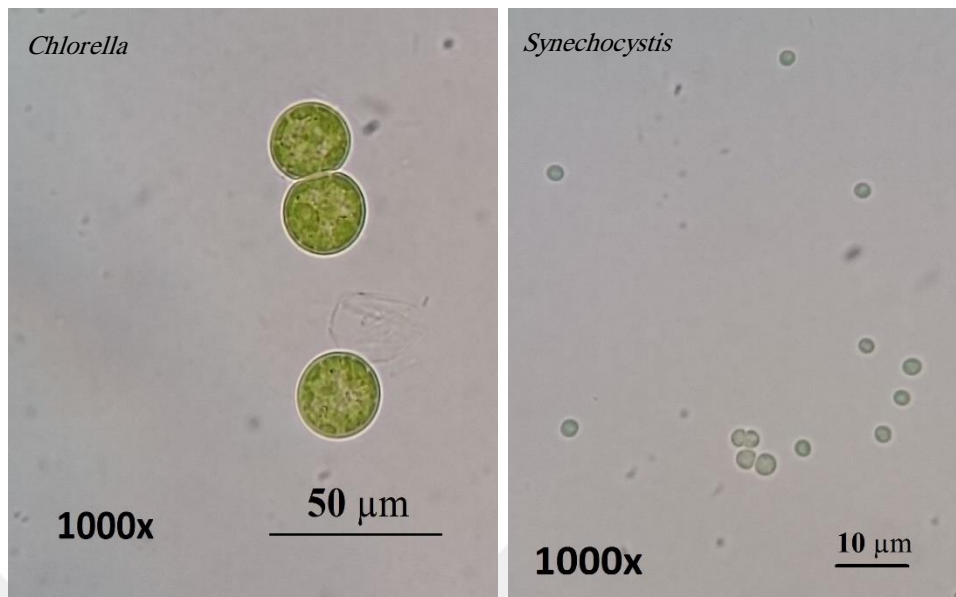


Figure 3.1. Up: Oil immersion light microscopic view of isolated microalgae species *Chlorella* & *Synechocystis*, Down: The cell size distribution for both microalgae

3.1.3. Glass particle

Pieces of colorless tea glass cup were washed and rinsed with water and propanol to remove dirt. After complete evaporation of propanol, the glass pieces grinded for 5 minute in a ring-puck pulverizer (Retsch, RS200). The product was then sieved using multi tray (125, 45 and 38 μm mesh) vibratory sieve shaker (ANALYSETTE 3 SPARTAN, Fritsch) with oscillation rate of 90 for 20 minutes. The collected powder between 45 and 38 μm sieves trays was rinsed with propanol to remove attached smaller particle and then dried and taken as nominal 40 micron size particles. The collected powder under 38 micron sieve was taken for further wet grinding using a Planetary Mono Mill (PULVERISETTE 6, Fritsch) with 4 silicon nitride balls (5 mm diameter) in a Silicon nitride bowl with propanol as dispersant liquid for 60 minutes at 300 rpm. The slurry was then dried using a rotary evaporator (G1, Heidolph). The dried product was collected using a sonication bath (Elma, TS 540). The particle size of the grinding product was determined using a laser light scattering device (Mastersizer 2000, Malvern). The result is shown in figure 3.2.

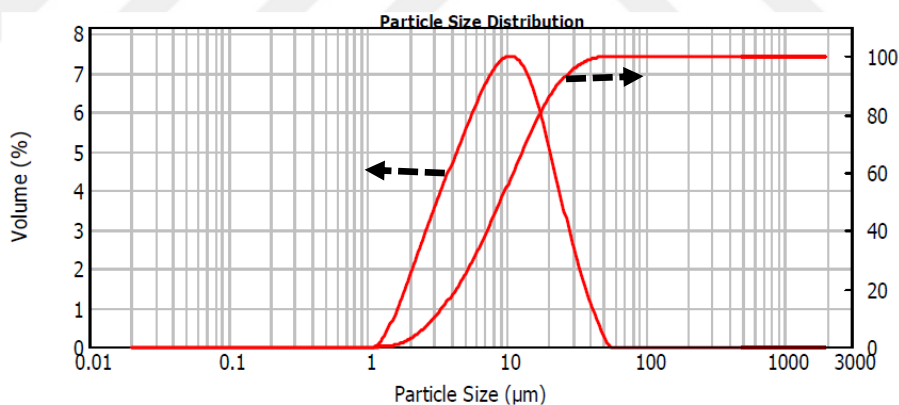


Figure 3.2. Particle size distribution of 10 μm particles

3.1.4. Lipid extraction

The basis for lipid extraction was the method of Bligh and Dyer using chloroform, ethanol and water [69]. In this method the extraction and the separation steps are basically separate stages. Preliminary tests in this study showed that extraction from a paste of microalgae gives higher lipid yield and the experiment was followed using microalgae

paste rather than a dried biomass. The disruption and extractive steps were performed simultaneously by agitating a solution where microalgae, glass particles and extracting reactants were present simultaneously. The concentration of the paste was 11.3 and 44.4 mg dried mass per mL respectively for *Synechocystis* and *Chlorella* pastes. Comparing to the method of Folch [79], the Bligh and Dyer method had the benefit of providing a homogeneous single phase at the first step of the procedure which was more favorable for an effective cell-solvent-particle contact. In the extraction step, chloroform, ethanol, water proportion was 1:2:0.8 and for the separation step the proportion was adjusted by addition of chloroform and water to 2:2:1.8 respectively. The extraction was done in 50 mL volumetric flasks on a magnet stirring plate (RT 10 IKA, Germany). The same plate was used to dry the extracts. A scale with 1 mg accuracy (SBC 31 Scaltec) was used for weighing. The detail of the procedure is schematically shown in figure 3.3.

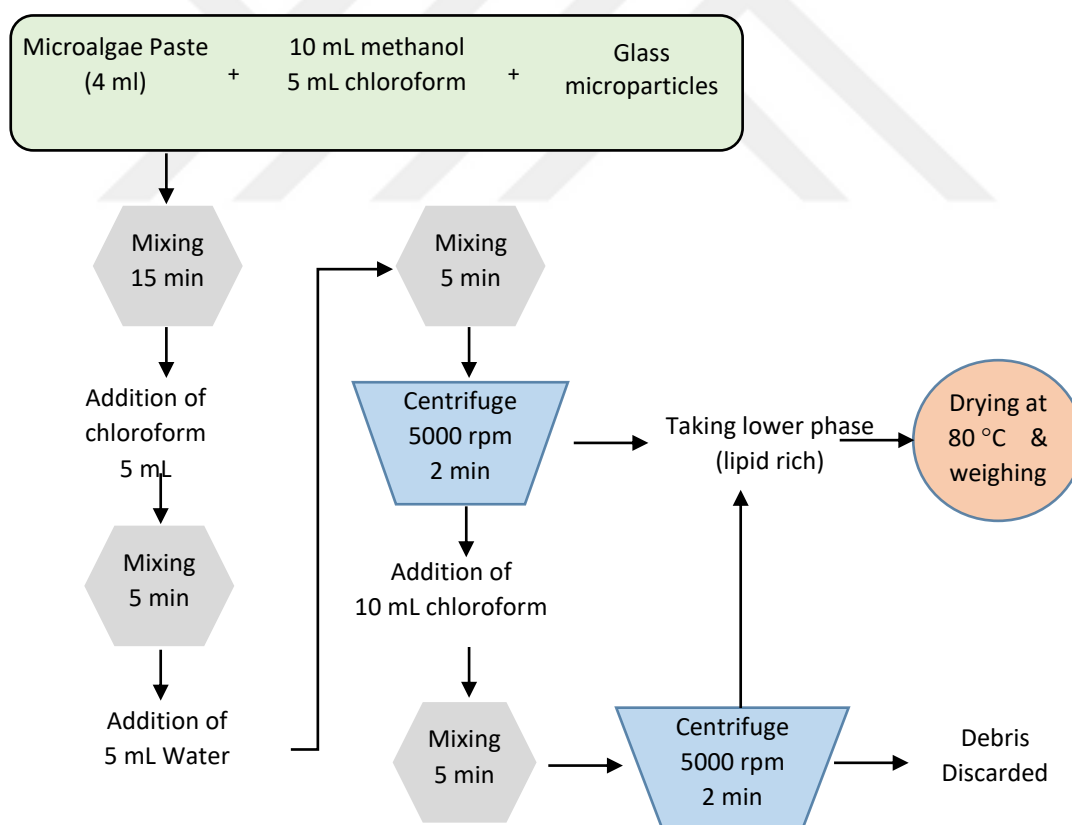


Figure 3.3. Flowchart of lipid extraction steps

3.1.5. Experiment design

The aim of this study was to investigate the effect of different factors including the size and quantity of added glass particles on the extraction yield of lipid from two microalgae species. The experiment design and further analyses were done using Design Expert software (v.7 Stat-Ease). A general factorial design approach at different levels with 2 replicates for each run was performed. A total number of 24 runs were required. After omitting the identical runs i.e. runs with zero concentration of glass particles were identical, 20 separate runs were executed. The detail of variables level for each runs are given in Table 3.1. These ranges were established after effectiveness of the method was observed following a preliminary blind run with 100 mg of 40 μm glass particles.

Table 3.1. *Obtained response at different runs*

# Run	Factor 1 A: Algae Sp.	Factor 2 B: Diameter (μm)	Factor 3 C: Particle amount (mg)	Response Lipid Content (%)
1	Syn	40	100	40.92
2	Chl	40	100	32.66
3	Syn	10	0	44.69
4	Chl	10	300	9.91
5	Chl	40	0	27.48
6	Syn	40	0	45.02
7	Chl	10	0	18.91
8	Syn	10	300	33.63
9	Syn	40	300	24.57
10	Chl	10	100	21.85
11	Chl	10	100	16.22
12	Syn	40	100	39.60
13	Chl	40	300	28.38
14	Syn	40	0	45.02
15	Chl	40	300	27.48
16	Syn	10	100	25.89
17	Chl	40	0	27.48
18	Chl	10	300	10.81
19	Syn	10	300	34.07
20	Syn	40	300	37.72
21	Syn	10	0	44.69
22	Syn	10	100	20.58
23	Chl	10	0	18.92
24	Chl	40	100	34.01

3.2. Results and Discussion

The recorded data for different runs are presented in Table 3.1. The obtained results at different runs were analyzed using Design Expert software. The statistical analysis of the results was performed to see the main and the two factor interaction effects. The

selected factors were the hypothesized three significant variables including the microalgae species, particles size and the amount of added particles. Here, the response was the mass percentage of lipid in the dried biomass. The employed code for a 2 factor interaction model (2FI) was:

$$\eta = A_0 + A_1X_1 + A_2X_2 + A_3X_3 + A_4X_1X_2 + A_5X_1X_3 + A_6X_2X_3 \quad (3.1)$$

A total number of 24 value were entered to the model as responses (Table 3.1). The Design Matrix Evaluation for Factorial 2FI Model showed no significant aliases between the estimated terms. The standard errors were approximately the same within type of coefficient. The variance inflation factor (VIF) close to 1 and the Ri-Squared terms very close to 0 indicated insignificant correlation between factors.

The analyze of factorial design using a normal probability plot (Figure 3.4) reveals that the amount of extracted lipid changes significantly with the species of microalgae, diameter of the glass particle and added amount of particle respectively. A weak interaction between two factors including microalgae species and the diameter of the added particle was also observed. As can be seen from the figure 3.4, the particle size had a positive effect but the concentration showed a negative effect in general.

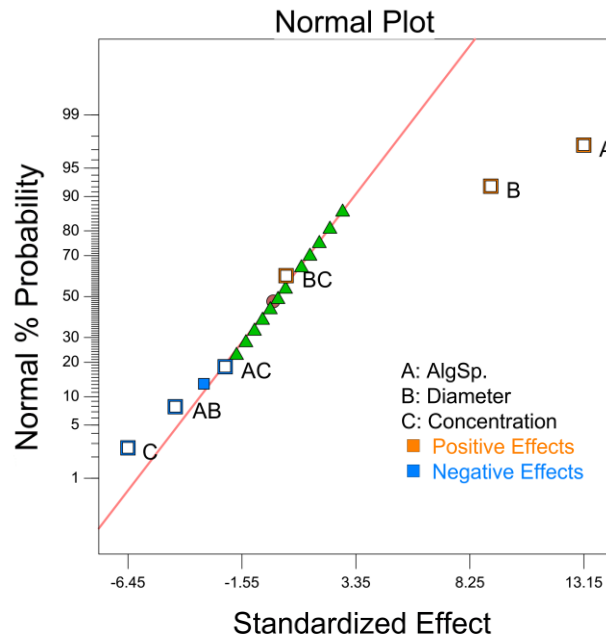


Figure 3.4. Normal probability plot

The results for analysis of variance (ANOVA) is presented in Table 3.2. The model F-value of 8.72 implies the model was significant. The probability value "Prob > F" less than 0.0500 indicated model terms were significant. This value for Model, microalgae Sp., glass microparticle diameter and glass microparticle concentration was 0.0002, 0.0001, 0.0021 and 0.0208 respectively. In this case microalgae type, particle diameter and the amount of added particle were significant as were indicated in normal probability plot. Values greater than 0.1000 indicated the insignificant model terms. Thus, indeed all the two factor interaction were not significant, a very weak interaction of factors A and B was observed as was stated before.

Table 3.2. ANOVA for selected factorial model

Analysis of variance table [Partial sum of squares - Type III]					
Source	Sum of Squares	df	Mean Square	F Value	p-value Prob > F
Model	1972.79	6	328.7984	8.717609	0.0002
A-AlgSp.	1018.75	1	1018.75	27.01067	< 0.0001
B-Diameter	493.489	1	493.489	13.08414	0.0021
C-Concentration	244.9949	1	244.9949	6.495683	0.0208
AB	114.7523	1	114.7523	3.04249	0.0992
AC	30.2803	1	30.2803	0.802838	0.3828
BC	0.731794	1	0.731794	0.019402	0.8909

The model diagnostic plots including normal probability, residual vs. predicted, residual vs. run and actual vs. predicted values are presented in figure 3.5. As can be seen, the normal probability plot didn't followed an S-shaped pattern. A random scatter of points was observed in the plot of the residuals versus the ascending predicted response values. Therefore there was no need for transformation of the response. The plot of residuals versus the experimental run with a random scatter order didn't show any lurking variables. The plot of actual response values versus the predicted response values showed that the model was able to predict the responses to a very good extent for most of the runs.

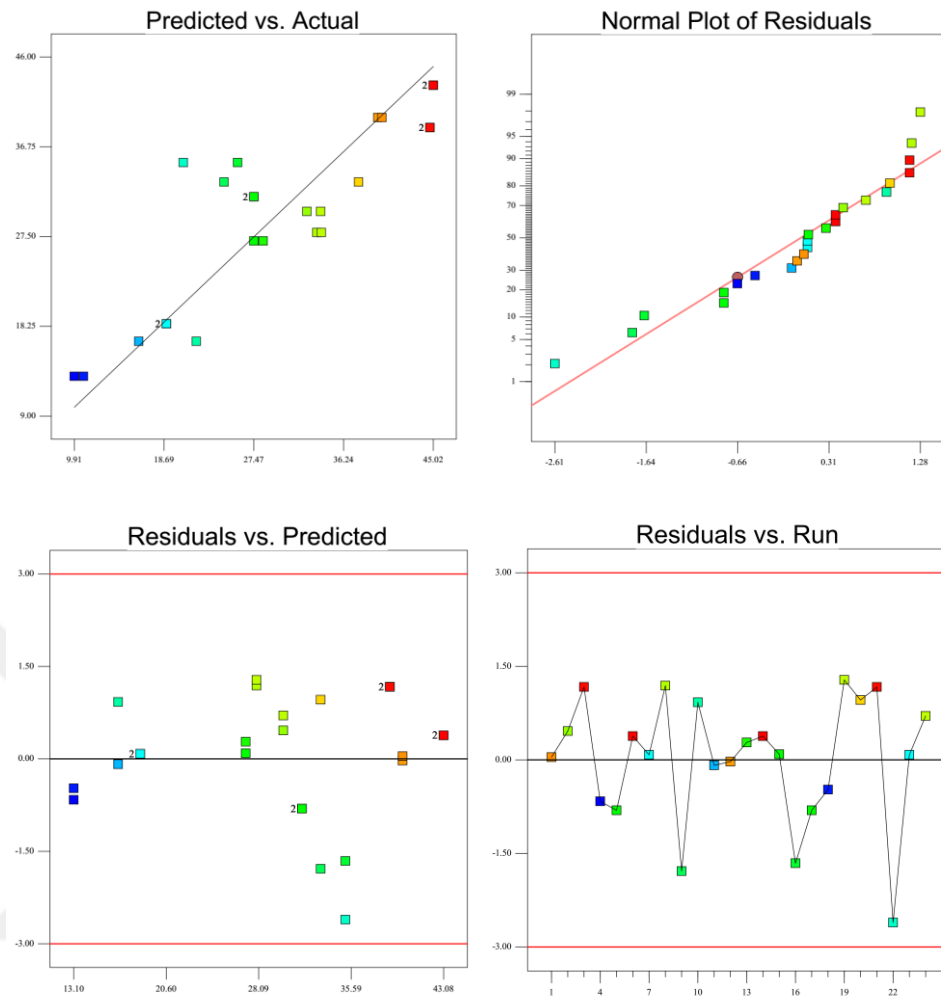


Figure 3.5. The model diagnostic plots

A minimum of 9.91% and a maximum of 45.02% were recorded for lipid percentage (Table 3.1). Summary of the results is presented in figure 3.6. For *Synechocystis*, the addition of particles was deteriorating in all cases. Generally, the results show that *Synechocystis* sp. contained higher amount of lipid comparing to the *Chlorella*. The highest recorded lipid content was 45.02% for *Synechocystis* without addition of particles whereas the least recorded lipid content was 10.36% for *Chlorella* when 300 mg of 10 micron particle was used. The best result for *Chlorella* was 34.01% when 100 mg of 40 micron particle was added while higher amounts of particle didn't help. For the 10 μ m particles the obtained lipid reduced for both species at every amounts of particles (Figure 3.6a). This could be related to the comparatively small size of the 10 μ m particles which do not maintain the required inertia to cut the cells wall. In addition,

very small size of 10 μm particles cause them to form agglomerates which would encapsulate oil droplets so that washing out by chloroform may not be possible. The results were different for 40 μm particles (Figure 3.6b) and higher lipid content were recorded for both species at every amount of particle when compared to the 10 μm particles. Larger particles move more sluggishly relative to the cells which are turning in the solution in a speed very close to the rotation speed of the bulk solution. In this case, the sharp edge of the particles would result in cutting the cell wall. It can be related to the effectiveness of relative size of particle to cell size rather than just particle size as a single factor. An approximate cell size distribution for both microalgae is presented in figure 3.1.B. For *chlorella* 53.6 % of the cell were observed to be larger than 15 μm and less than 30 μm where in total almost 82.0 % the *chlorella* cells were larger than 15 μm . In contrast, 72.6 % of *Synechocystis* cells were between 3 to 5 μm and in total 85.4 % of the cells were larger than 3 μm .

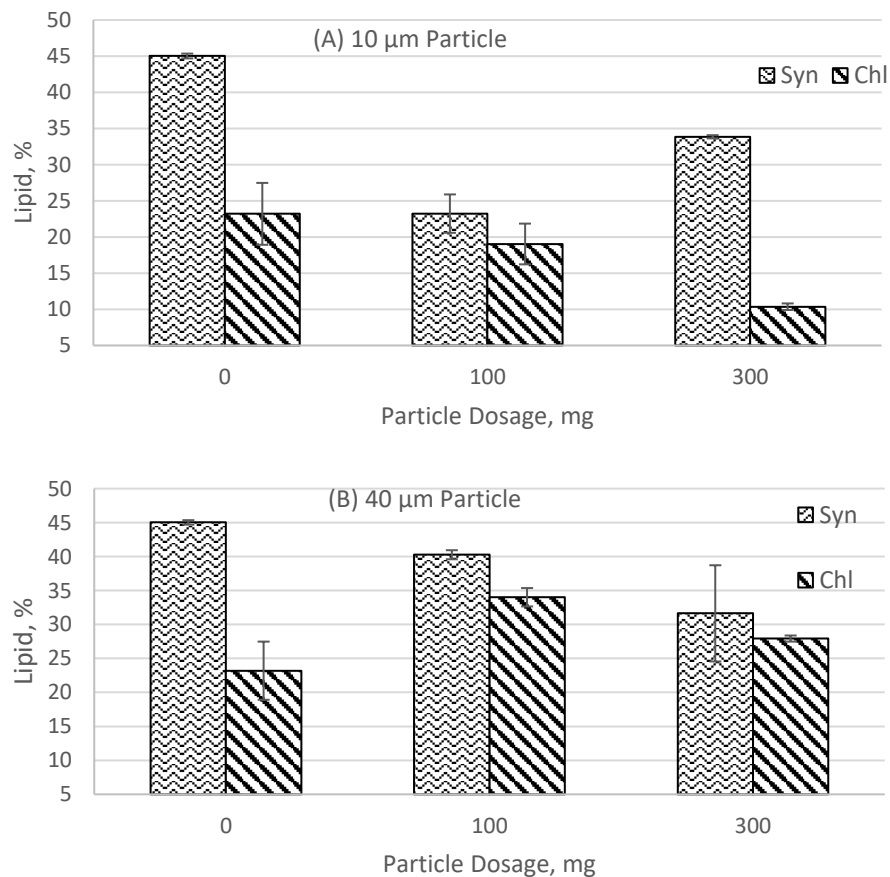


Figure 3.6. Yield of lipid extraction for a) 10 μm particle size, b) 40 μm particle size

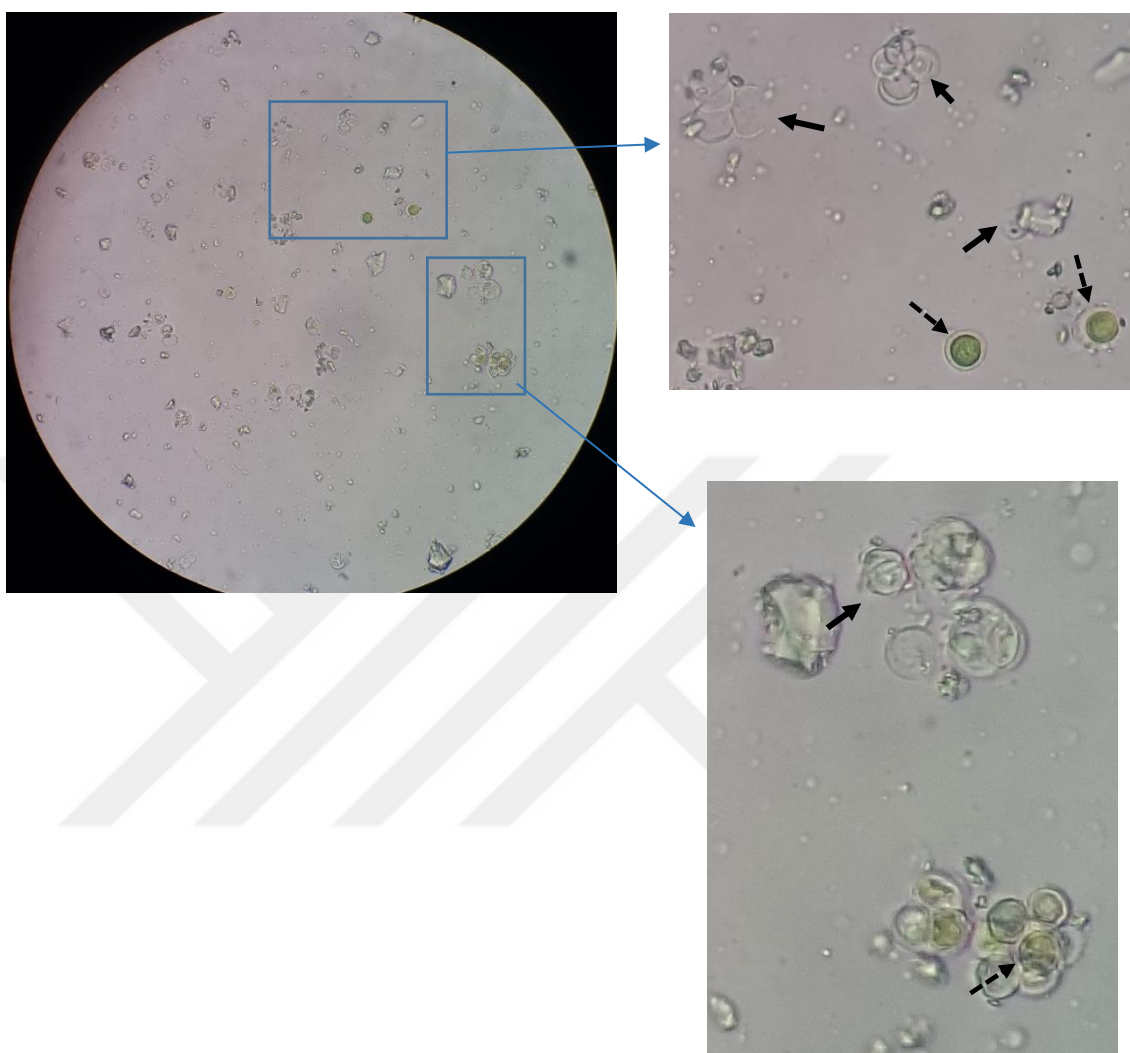


Figure 3.7. Microscopic view of the debris (*dashed* arrows show intact cells, black arrows show the collapsed cells)

The microscopic view of the cell debris after solvent treatment with particles reveals that still significant number of the cells were intact (Figure 3.7). A further treatment time or more effective mixing would result in higher extraction efficiencies. In that figure, disrupted cells are also observable. Some of them have collapsed from one point and the cytoplasm extracted out.

A summary of the previous research results for the reported lipid content of *Chlorella vulgaris* with different extraction methods and solvents is presented in Table

3.3. As can be seen from the Table 3.3, so many different values have been reported for lipid content of *Chlorella vulgaris* so that a comparative study with a reasonable judgment seems to be impossible. In many of the studies, a variety of extraction strategies have been tried including sonication, high speed homogenizers, super critical solvents, high pressure steam and bead beating devices. Although all of them enhanced the extraction efficiency, they are not applicable for a large scale application since they consume high amount of energy. Safi et al. have tried the influence of bead milling on extraction performance and reported 16 % increase in total extract yield from *Chlorella vulgaris* while concluding the high energy demand of the method [80]. Bead beating was also studied by Lee and friends [81] where they concluded on the low effectiveness of the method for *Chlorella vulgaris* and *Scenedesmus* sp.. They also argued scale up of the method. Park et al. studied the combination of homogenization at 7000 rpm with sonication again for *Chlorella* cell disruption where a significant improvement was achieved by 8.1 fold increase in the extracted lipid after 60 minutes and the final lipid in dried mass was 15.2% [82]. A good summary of the tested methods for cell disruption was reviewed by Kim and friends [20]. They have also criticized the methods for energy requirements, chemical costs, toxicity and products stability. The findings of this study showed that glass microparticles can be used effectively for some microalgae species to enhance the lipid extraction efficiency even at low mixing rates and room temperature to reduce the cost of energy. The method can be easily scaled up for any desired scale. The glass microparticles can be easily recovered and reused to avoid the cost of microparticles production.

Table 3.3. Lipid content of *Chlorella vulgaris* in different studies

Extraction method	Solvent	Lipid (%)	Ref.
Organic Solvent treatment	Hexane and Methanol	18.54	Choi et al. [28]
Organic solvent assisted by ultrasound	Chloroform- Methanol	52.20	Glacio et al. [83]
Fenton reactant treatment	H ₂ O ₂ and FeSO ₄	17.40	Concas et al. [84]
Acid-catalyzed hot-water extraction	H ₂ SO ₄ and water	33.74	Ji-Yeon et al. [85]
Ionic liquid mixture	1-ethyl-3-methyl imidazolium based ILs	20.06	Choi et al. [28]

Based on the findings of this study, researchers should be careful when they use conventional solvent extraction methods of analysis for fat determination because most of the conventional solvent treatment methods have been basically introduced for fat determination in bulk tissues and mainly animal tissues. Therefore, because of the different characteristics of microalgae cell wall and their resistance to solvents, there may be a significant underestimation of lipid content of the microalgae species.



4. OPTIMIZATION Of GROWTH RATE Of MICROALGAE *SCENEDESMUS SP.* :CENTRAL COMPOSITE DESIGN STATISTICAL APPROACH

In this research, growth rate of microalgae *Scenedesmus sp.* was modified by optimizing four effective factors. A central composite design statistical approach was implemented to evaluate the results. The examined factors were carbon dioxide concentration (0.038 (air), 2.0, 5.0, 7.0, 10.0%), aeration rate (0.2, 0.5, 1.5, 3.0, 4.0 vvm), initial inoculum concentration (0.140-0.430 g/l) and the gas diffuser diameter (0.4, 1.0, 2.6, 4.0, 5.0 mm). It was observed that this factors effect was very significant at the modeled ranges. The diffuser diameter also showed different effect when low or high carbon dioxide concentration was applied. The optimized value (6.3 % CO₂, 1.03 vvm flow rate, 1.47 mm diffuser diameter and 0.230 g/l initial inoculation) would result the maximum growth rate of 0.513 g/l.d which was very significant. It was concluded that microalgae technology is a promising solution for carbon dioxide sink in large scale and biofuel production after optimizing the biomass production rate.

4.1. Materials and Method

4.1.1. Chemicals

The chemicals NaNO₃, K₂HPO₄, MgSO₄.7H₂O , CaCl₂.2H₂O, Citric acid, Ammonium ferric citrate, EDTANa₂, Na₂CO₃, H₃BO₃, MnCl₂.4H₂O, ZnSO₄.7H₂O, Na₂MoO₄.2H₂O, CuSO₄.5H₂O, Co(NO₃)₂.6H₂O were purchased from Sigma-Aldrich, USA. Acetone, chloroform, methanol, phenol, sulfuric acid, KCl, and propanol were provided by Tekkim, Turkey. All the chemicals were of reagent grade. Reagent water was utilized in laboratory using a water purification unit (Thermo Scientific, Germany).

4.1.2. Microalgae species and medium

Scenedesmus Sp. (Figure 4.1) was isolated from Porsuk River, Eskişehir, Turkey (Botanic park 39.742747, 30.460088). The procedure was described elsewhere [86]. In this study BG11 medium was prepared according to [67] and used throughout the study for microalgae culture. The light intensity was adjusted with an illuminance Meter (T-10MA Konica Minolta; Japan). The biochemical composition and elemental analysis of well-grown *Scenedesmus Sp.* dried biomass is provided in Table 4.1.



Figure 4.1. *Scenedesmus sp.* Oil immersion microscopy

Table 4.1. *Scenedesmus sp.* dried biomass CHN analysis and biochemical composition

Elemental analyses			Biochemical composition		
%C	%N	%H	Lipid %	CHO %	PRO %
48.81	9.08	7.62	47.32	41.04	43.42

4.1.3. Growth curve and linear growth rate

The growth was monitored by daily sampling and reading optical density at 680 nm (OD_{680nm} , Shimadzu UV-1800 UV-Vis Spectrophotometer). To convert the OD_{680} to microalgae concentration in the broth in dried mass basis, a coefficient factor withdrawn and used as in Eq.1. This coefficient was obtained after centrifugation of a well-grown culture of microalgae and drying the obtained paste. An aliquot of this paste was then diluted until the OD was changing linearly with dilution. At this range the coefficient was determined and the afterward OD readings was performed at this range upon certain dilution.

$$\text{Biomass Conc. (g. l}^{-1}\text{)} = C_f \times (\text{OD}_{680} - \text{OD}_b) \quad (4.1)$$

Where, C_f is the conversion factor, OD_{680} is the optical density at 680 nm wavelength and OD_b is the optical density of blank.

4.1.4. Photobioreactor

A multicultivator (MC 100-OD, Photon Systems Instruments) with eight separate cultivation cells was used. This unit has the advantage of providing uniform light intensities up to $1000 \mu\text{mol}/\text{m}^2 \cdot \text{s}$ and precise temperature control for all cells. A schematic picture of the whole setup is shown in figure 4.2. Desired mixture of carbon dioxide and air was prepared using mass flow controller units (MKS instruments, USA) and then distributed between 8 cultivation cells with certain flow rates using pre-calibrated manometers (mzb instruments, China). A $0.2 \mu\text{m}$ PTFE membrane filters (Fluoropore, Merck Millipore) was used for each line to maintain gas stream sterilization. Daily samples were taken using luer-lock three way valves and syringes.

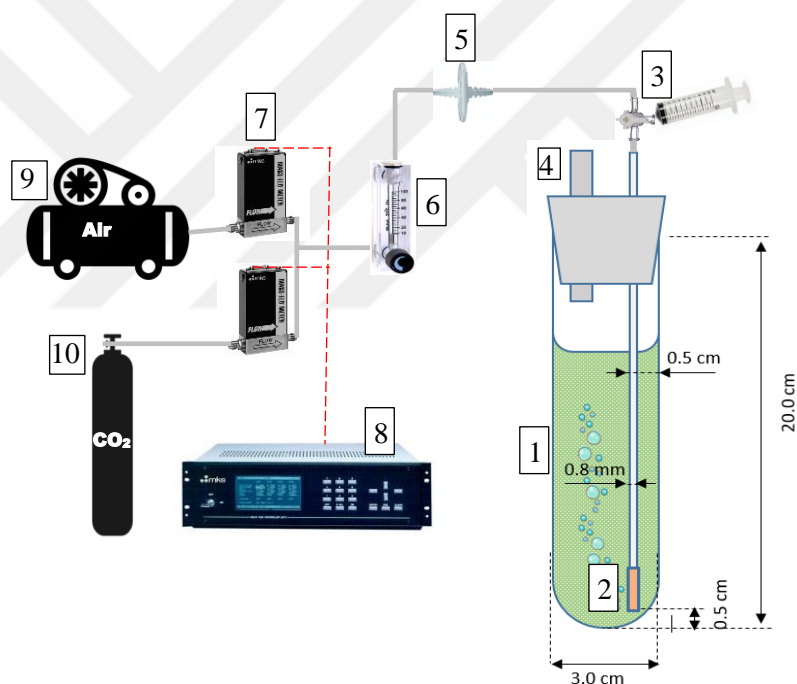


Figure 4.2. Experimental setup. 1: One out of eight cultivation cells. 2: Gas diffuser. 3: Sampling point including a three way valve and a syringe. 4: vent. 5: In-line gas filter. 6: Rotameter type gas flow meter. 7: MFC units. 8: MFC control unit. 9: Air compressor 10: CO₂ cylinder

4.1.5. Experimental Design and statistical approach

Design Expert software was used to perform statistical analysis. A central composite experimental design (CCD) was implemented. In a CCD design, each variable

is distributed in five level with five repeats at center point. With this regard, three factors including carbon dioxide concentration (0.038 (air), 2.0, 5.0, 7.0, 10.0%), flow rate (0.2, 0.5, 1.5, 3.0, 4.0 vvm) and diffuser diameter (0.4, 1.0, 2.6, 4.0, 5.0 mm) were adjusted to be optimized. The combination of these levels resulted in 18 runs. One extra repeats for the 0.038 and 10.0 % runs were added. In addition, initial inoculation concentration was adjusted in the range of 135-433 mg/l. All the twenty runs variables and the obtained experimental results for linear growth rate and the maximum concentration of microalgae in the solution as two responses are summarized in Table 4.1.

Table 4.2. *The adjusted variables for different runs and experimental responses*

Run	CO2 Concentration (ppm)	Aeration rate (vvm)	Diffuser diameter (mm)	Inoculum density (g/l)	GR (g/l.d)	Maximum Concentration (g/l)
1	50000	1.5	2.6	0.43	0.387	4.555
2	70000	3	1	0.28	0.371	3.824
3	380	1.5	2.6	0.18	0.133	3.596
4	20000	0.5	1	0.39	0.299	3.956
5	50000	1.5	0.4	0.43	0.294	4.699
6	50000	1.5	2.6	0.43	0.378	4.911
7	70000	0.5	4	0.2	0.494	4.050
8	50000	1.5	2.6	0.43	0.382	4.455
9	70000	0.5	1	0.36	0.344	3.583
10	50000	0.2	2.6	0.43	0.324	4.198
11	20000	0.5	4	0.26	0.306	3.096
12	50000	1.5	2.6	0.43	0.377	4.958
13	50000	1.5	5	0.43	0.295	4.769
14	100000	1.5	2.6	0.18	0.283	3.258
15	70000	3	4	0.14	0.385	3.859
16	50000	4	2.6	0.43	0.381	5.711
17	20000	3	4	0.25	0.272	2.695
18	20000	3	1	0.25	0.357	4.050
19	100000	1.5	2.6	0.27	0.229	3.146
20	380	1.5	2.6	0.27	0.097	2.985

4.2. Results and Discussions

4.2.1. Experimental data

For twenty runs, the cultivation were monitored for almost 30 days till the growth curve reached plateau or entered death phase. The growth curve for all runs is provided in supplementary documents 3. The results for the best, worst and a moderate performing runs are presented in figure 4.3. The highest growth rate of 0.494 g/l.d was achieved when 7.0 % CO₂ at 0.5 vvm flow rate with a 4.0 mm diameter diffuser was applied. The maximum concentration of microalgae in dried basis for this run was 4.05 g/l at day sixteen. The lowest growth rate of 0.097 g/l.d was achieved when 0.038% CO₂ (air) at 1.5 vvm flow rate with a 2.6 mm diameter diffuser was applied. The maximum concentration of microalgae in dried basis for this run was 2.98 g/l at day twenty nine. The highest microalgae concentration of 5.71 g/l was recorded for run 16 where 5.0% CO₂ (air) at 4.0 vvm flow rate with a 2.6 mm diameter diffuser was applied. Since different factors were set for each run according to the design of experiment, no judgment could be made for the optimum values without a statistical analysis. This is discussed in the following sections.

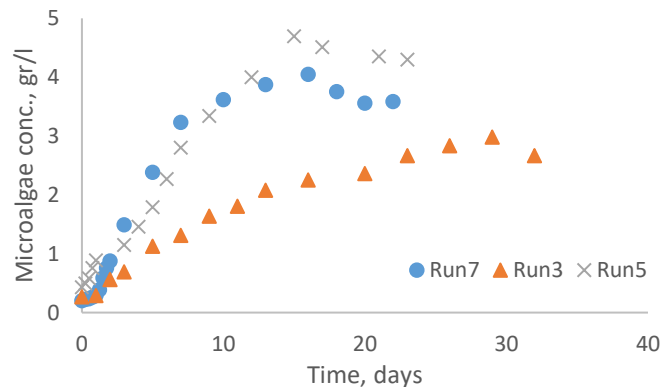


Figure 4.3. The growth curve for fast (run 7), moderate (run 5) and slow (run 3) growth

4.2.2. Statistical analysis

The obtained data for a CCD design was entered and using analysis tools of Design Expert software, these data was fitted to different models including linear, two factor interaction (2FI), quadratic and cubic models for best fit. The model summary statistics

and the lack of fit tests for the mentioned models are presented in Table 4.2. These results showed that a quadratic model was a good choice since the lack of test was insignificant (p-value 0.3299) and the adjusted R-squared and predicted R-squared values (respectively 0.995 and 0.716) were maximized and reasonably close to each other for a quadratic model. Therefore the initial quadratic model was as follows:

$$GR(gr/l.d)^\lambda = c_1A + c_2B + c_3C + c_4D + c_5AB + c_6AC + c_7AD + c_8BC + c_9BD + c_{10}CD + c_{11}A^2 + c_{12}B^2 + c_{13}C^2 + c_{14}D^2 \quad (4.2)$$

where GR is the growth rate as response, c_1 to c_{14} are the model parameters estimated coefficients, and A, B, C and D are input variables of carbon dioxide concentration (CO_2C), gas flow rate (FR), diffuser diameter (DD) and initial inoculation concentration (IC) respectively. These model was then modified to reduce the insignificant parameters. The λ is transformation value for a power function. Initially, no transformation was used, i. e. λ was one, but after diagnostic analysis of the results, λ was set to 1.83 for better fit. Therefore, the final model was a Response Surface Reduced Quadratic Model.

Table 4.3. Model fit summary statistics and lack of fit test results

Lack of Fit Tests						
Source	Sum of Squares	df	Mean Square	F Value	p-value Prob > F	
Linear	0.051	12	0.004	285.510	0.0003	
2FI	0.026	6	0.004	289.411	0.0003	
Quadratic	0.000	2	0.000	1.642	0.3299	Suggested
Cubic	0	0				Aliased
Model Summary Statistics						
Source	Std. Dev.	R-Squared	Adjusted R-Squared	Predicted R-Squared	PRESS	
Linear	0.058	0.224	0.017	-0.487	0.098	
2FI	0.054	0.606	0.169	-1.813	0.185	
Quadratic	0.004	0.999	0.995	0.716	0.019	Suggested
Cubic	0.004	0.999	0.996		+	Aliased

4.2.3. Analysis of variance (ANOVA)

The ANOVA results for the selected model after modifications and the estimated coefficients are summarized in Table 4.3. A p-value less than 0.0001 showed that the

model was significant. There was just one insignificant term (term A) and was reduced. The remaining factors were all significant. The Prob > F values less than 0.05 indicated significant model terms. The lack of fit F-value of 1.105 revealed that lack of fit was not significant comparing to the pure error. The diagnostic plots for normal probability plot of studentized residuals, studentized results vs predicted values, externally studentized residuals for outliers and the Box-Cox plot for power transformation is shown in figure 4.4. The 95% confidence interval for λ (1.57 to 2.11) did not include 1, so a transformation was appropriate. The best λ for a power transformation was 1.83. The normal plot of residuals showed approximately linear without significant outliers. The plot of residuals vs predicted values showed a random bounce around zero line with almost a horizontal band and no significant outliers. The plot of externally studentized residuals also did not show any outliers. Therefore, it was concluded that the proposed model was a very good description of experimental data.

Table 4.4. ANOVA for Response Surface Reduced Quadratic Model

Source	Sum of Squares	df	Mean Square	F Value	p-value Prob > F	Estimated Coefficient
Model	0.06567	13	0.005052	322.64	< 0.0001	
B-Flow (v/v)	0.00180	1	0.001799	114.92	< 0.0001	-0.223
C-Bubble_D	0.00013	1	0.000128	8.21	0.0286	0.015
D-Initi.Conc.	0.00141	1	0.001410	90.06	< 0.0001	0.053
AB	0.00155	1	0.001548	98.87	< 0.0001	-0.011
AC	0.00311	1	0.003105	198.33	< 0.0001	0.029
AD	0.00037	1	0.000373	23.85	0.0028	-0.014
BC	0.00028	1	0.000283	18.06	0.0054	0.022
BD	0.00431	1	0.004310	275.24	< 0.0001	0.099
CD	0.00042	1	0.000420	26.81	0.0021	0.016
A^2	0.02257	1	0.022575	1441.78	< 0.0001	-0.089
B^2	0.00117	1	0.001172	74.86	0.0001	-0.077
C^2	0.00567	1	0.005674	362.40	< 0.0001	-0.025
D^2	0.00196	1	0.001965	125.49	< 0.0001	-0.044
Intercept		1				0.130
Residual	0.00009	6	0.000016			
Lack of Fit	0.000049	3	0.000016	1.105	0.4683	
Pure Error	0.000045	3	0.000015			

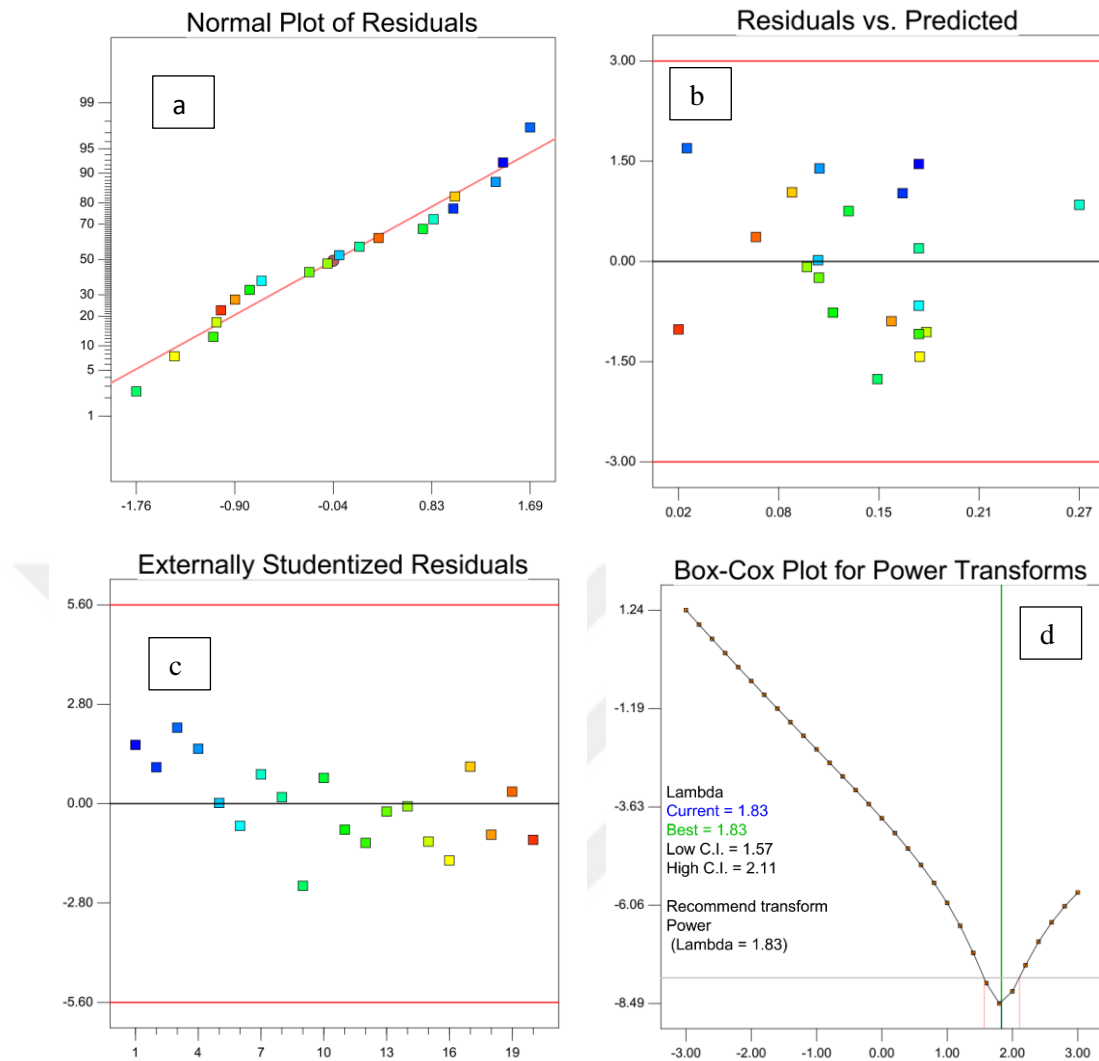


Figure 4.4. The diagnostic plots of a) Normal plot of residuals, b) Residuals vs predicted, c) Externally studentized residuals for outliers, d) the Box-Cox plot

4.2.4. The effect of carbon dioxide concentration

Microalgae are autotrophic microorganisms which means they are able to directly consume mineral carbon in the form of carbonate, bicarbonate and dissolved carbon dioxide [44]. As the carbon dioxide concentration in the gas stream increases, the dissolved carbon dioxide in the aqueous solution will increase. But on the other hand, the increased concentration of carbon dioxide in the solution will reduce the pH, something that deter the growth of microalgae. The 3D plot of the model output for the effect of carbon dioxide concentration on the GR is shown in figure 4.5a&b. As can be seen for the plotted range of 2.0% to 8.0 % CO₂ the GR formed an arc curve shape with maximum

zenith which means there is an optimum value in this range. Very high carbon dioxide concentration reduces the solution pH so that may not be tolerable for microalgae cells. Contrarily, low concentrations of CO₂ provides less available carbon source for cell growth. The experimental data when 10000 ppm CO₂ was used resulted to a GR of 0.256 g/l.d in average (Table 4.1, runs 14 and 19) where for air stream (ppm 380) was 0.115 g/l.d in average (Table 4.1, runs 3 and 20). These were comparably lower than the average GR of 0.352 g/l.d when 50000 ppm CO₂ was applied. The contour plot of the software solution for optimum range of values are shown in figure 4.6. The suggested optimum values were 63450 ppm CO₂, 1.03 vvm flow rate, 1.47 mm orifice diameter and 0.230 g/l of initial inoculation which would result in a growth rate of 0.513 g/l.d.



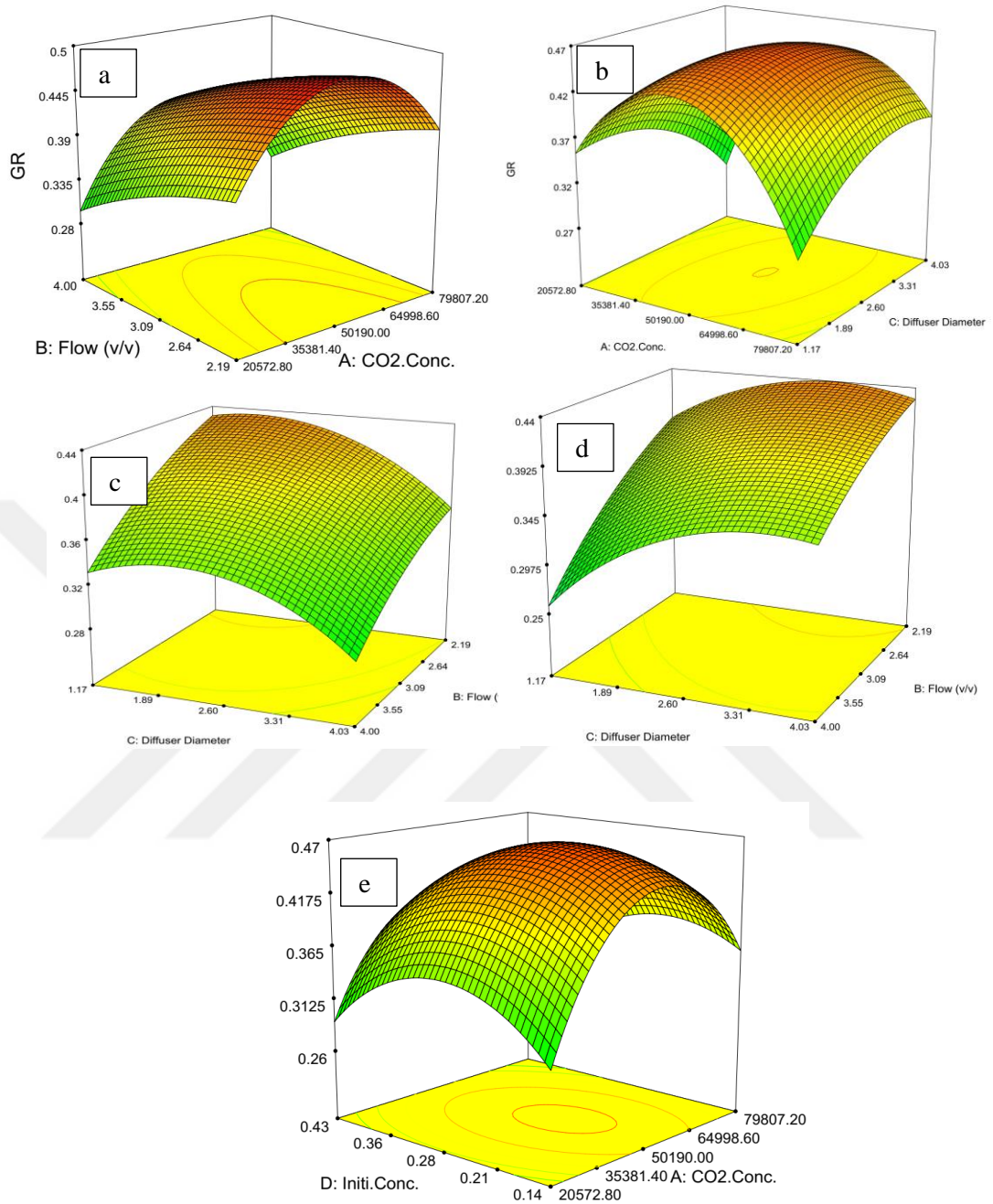


Figure 4.5. The 3D plot output of the quadratic model, a) GR vs CO₂C&FR at DD:2.6 mm, IC:0.280 gr/l, b) GR vs CO₂C&DD at FR:3.16 vvm, IC:0.280 gr/l, c) GR vs DD&FR at CO₂C: 26648 ppm, IC:0.280 gr/l, d) GR vs DD&FR at CO₂C: 75250 ppm, IC:0.280, e) GR vs CO₂C&IC at DD:2.6 mm, FR:3.16 gr/l

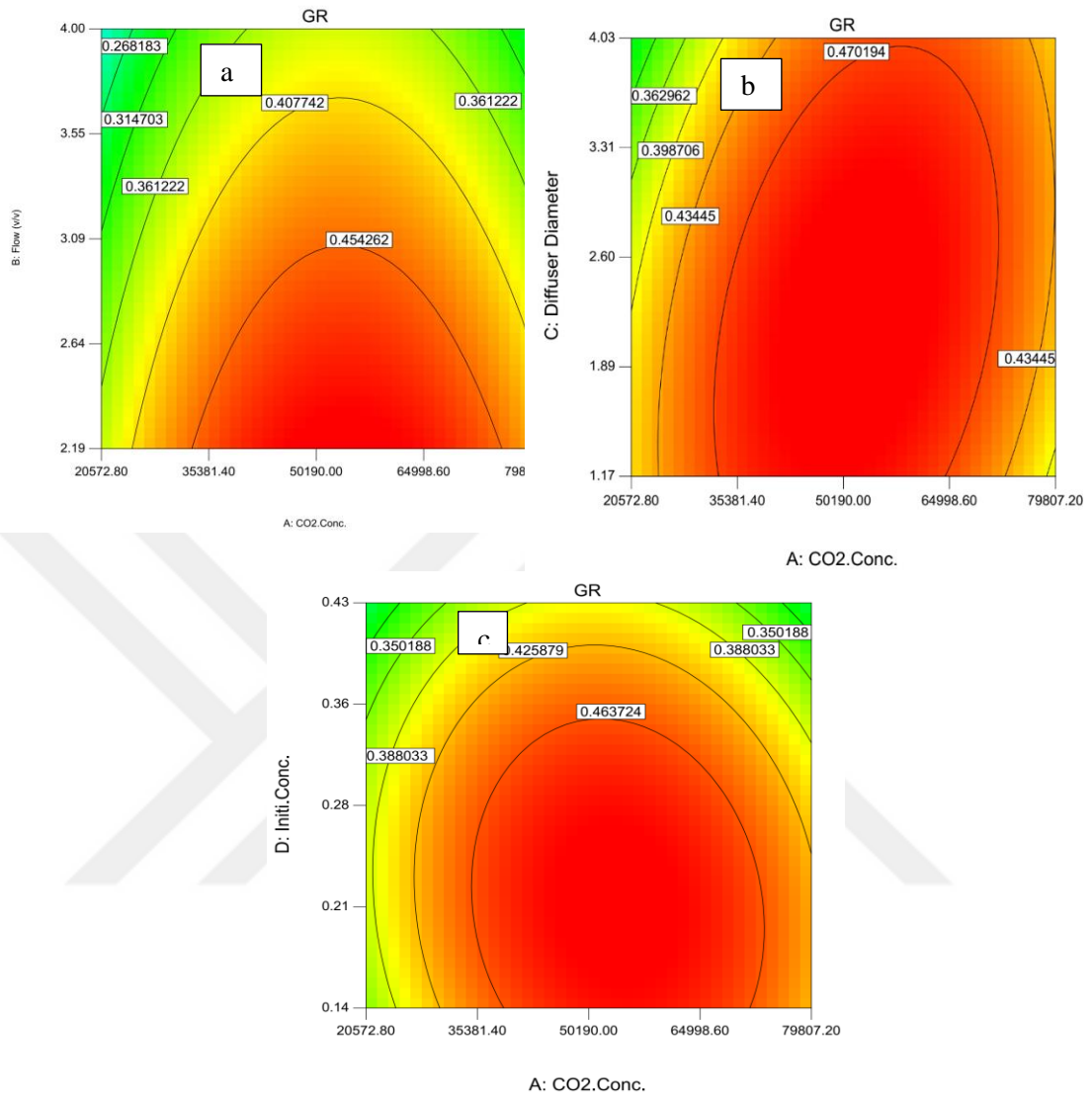


Figure 4.6. The contour plot output of the software solution for the optimized values a) GR vs CO₂C&FR at DD:2.86 mm, IC:0.190 gr/l, b) GR vs CO₂C&DD at FR:2.19 vvm, IC:0.190 gr/l, c) GR vs CO₂C&IC at FR: 2.19 vvm, DD:2.86 mm

4.2.5. The effect of gas flow rate

It was realized that for 1.17 to 4.03 mm range of diffuser size, lower flow rate resulted in higher growth rate (Figure 4.5c&d). But the correlation value for all experiments result vs diffuser size showed a weak 0.06 positive value. It was revealed that the effect of flow rate may change with other factors where in the plotted range of

model was not observable. Therefore experimental data for different flow rates at the same CO₂ percentage and diffuser diameter was plotted at categorized series as is shown in figure 4.7. It was clear that for smaller diffuser diameters (DD < 4 mm), the higher flow rate enhanced the growth rate but for larger diffusers the opposite was true. Higher flow rates provides better mixing and at the same time larger bubbles. Larger bubbles comparing to smaller bubbles provide less surface area which hinders mass transfer rate. The 3D plot in figure 4.5c&d shows that in the 2.0% to 8.0% CO₂ range, lower gas flow rate was more favorable.

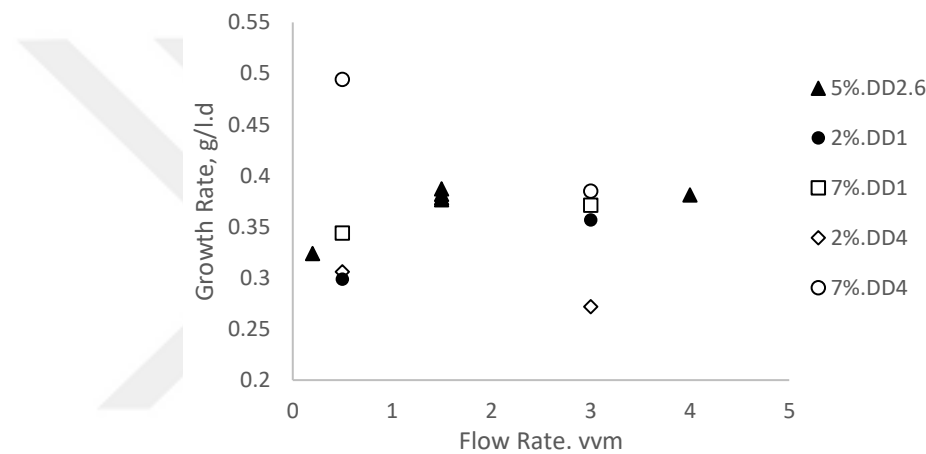


Figure 4.7. The experimental result for growth rate vs flow rate at different DD and CO₂C

4.2.6. The effect of gas diffuser diameter

The number of researches reporting on the operational effect diffuser diameter in a photobioreactor was very low [87]. From a mass transport phenomena prospective, it is an important factor since it has effect on the size of produced bubbles. Akita and Yoshida [88] in their study on the bubble size and liquid phase mass transfer in a bubble column reported that two main factors affect the size of initial bubbles (i. e. the bubbles immediately leaving diffuser), are gas flow rate and the diffuser diameter. The effect of diffuser diameter was more significant when small gas velocity are applied which means at higher gas velocities the volumetric liquid phase mass transfer coefficient k_{LA} is independent from orifice diameter because at higher flow rates larger bubbles coalesce and break to smaller bubbles [89, 90].

The output of the statistical evaluation showed that 1.47 mm diffuser diameter was the optimum value (Figure 4.6b). The estimations for GR at different diffusers diameter revealed that diffusers size was a very important factor (Figure 4.6c&d). Interestingly, the effect of diffuser diameter varied with the range of CO₂ concentration. For lower concentrations (~ 2.0% CO₂) a smaller diffuser size was more effective whereas for higher CO₂ concentrations (~ 7.0% CO₂) larger diffuser was more effective. The smaller diffuser size provides smaller bubbles and more surface area for mass transfer. The higher mass transfer rate in general is favorable but when intolerable high concentrations of CO₂ is applied, less mass transfer rate from gas phase to liquid would be beneficial to avoid low pH in the cultivation broth.

4.2.7. The effect of initial inoculum concentration

The presumption was that higher initial inoculum size would exhibit higher linear phase growth rate. There are not many previous papers reporting on this factor [91]. Since the availability of the light is a very important growth factor, self-shading may inhibit growth when higher initial inoculum densities were used [91]. As can be seen from figure 4.6e, initial inoculum size had very strong influence on the GR where neither a very high nor a very low densities were favorable. There was an optimum value for the initial inoculum density in the range of 0.14 to 0.43 g/l. This value was found to be 0.230 g/l for the first solution but in fact the software provides many solutions with maximum desirability of “one” where for majority of them the initial inoculum density falls in the range of 0.18 to 0.28 g/l. On the contrary, Starting with higher inoculum size gave the chance of avoiding lag phase (Figure 4.3). In lag phase the cells are getting adopted to the environment and no significant growth happens. This is practically a disadvantage since providing light and aeration for some days without considerable growth impose extra operational cost.

4.2.8. Microalgae potential as biofuel feedstock in large scale

Microalgae technology is hopefully being vastly studied as a future energy resource. Potentially, it can be also used to reduce the carbon dioxide emissions of existing plants like power plants or other large factories like in cement industries or petrochemical complexes. It is helpful to have a sensible size overview of such microalgae plants when applied for these two sets of application which possibly can be

integrated as well. Here the aim is to simply estimate the size of a microalgae cultivation plant when applied for:

1- Capturing CO₂ emissions of a power plant

An existing coal burning plant was taken as example. ICDAS Biga facility (Çanakkale, Turkey) is a medium sized coal burning power plant which produces 405 MWe electric power. With an approximate emission factor of 762 kg CO₂/MWh of electric energy [72] for such plant, approximately 7406640 kg/day CO₂ is being released to the atmosphere. The following equation can be used to estimate the microalgae plant size (MAPS);

$$MAPS(m^3) = \frac{6.55 \times P \times E_f}{GR \times C_e} \quad (4.3)$$

where P is the power plant electric production capacity(MWe), E_f is carbon dioxide emission factor for that plant (kg CO₂/kWh), GR is the microalgae growth rate (g/l.d), C_e is the elemental carbon fraction in dried biomass.

Using the below equation the occupied land area for building such microalgae can be estimated;

$$Area(ha) = MAPS \times 10^{-4} / \eta_r \quad (4.4)$$

Where η_r (m³/m²) is the ratio of reactor volume per unit area specific for a special design of photobioreactor. For example if the bubble column reactor units can be designed so that in every square meter of land one cubic meter reactor volume could be available, then η_r value equals one. It must be considered that reactors might be vertically enlarged but providing enough light (natural sunlight) could be an issue. More ever, taller columns will impose more compression cost for aeration.

With the obtained data in the present study, microalgae plant size for capturing the above mentioned power plant using Eq. 3, is 8.04×10⁶ m³. Assuming a η_r value of “one”, the occupied area calculated from (4) equals 804 ha. This is roughly the area of a 2.83 km by 2.83 km square shaped land.

The above estimations for occupied land area shows that microalgae biotechnology when overall process efficiency is modified and photobioreactor facility could be designed efficiently, can be applied for large scale carbon dioxide fixation. The produced biomass of such a gigantic facility might be evaluated as energy source to compensate part of consumed energy.

2- Producing biofuel as much as a real fossil fuel refinery factory

Microalgae was used as a biofuel feed stock in many studies. The biodiesel has gained more notice since the process is considerably less complex and more efficient comparing to other biofuels like bioethanol or pyrolytic bio-oil. The need of biomass for a biodiesel production facility as large as an existing fossil based diesel is estimated. Then, the MAPS was calculated from below equation:

$$MAPS(m^3) = \frac{D_{pr} \times \rho_d \times 0.159}{GR \times L \times C_f} \quad (4.5)$$

where D_{pr} is diesel production rate of a fossil diesel producing factory (bpd), ρ_d is biodiesel density (kg/l), GR is the growth rate of microalgae (gr/l.d), L is the lipid fraction in biomass and C_f is the conversion factor of lipid to FAME.

Ras Tanura Refinery (Aramco, Saudi Arabiya), is a petroleum refinery complex with a diesel production capacity of 181000 bpd was taken as a reference for comparison. According to a previous study [74], the microalgae oil was converted to FAME with an efficiency of almost 77.0 percent for some green microalgae. Assuming an average density equal to 0.880 kg/l (EN 14214) for biodiesel, optimized GR of 0.514 gr/l.d, lipid fraction of 47% (Table 4.1) the size of photobioreactor facility to produce the same amount of diesel as in Ras Tanura, would roughly be 136,400 m³. The use of microalgae for biodiesel production is not far beyond reality and can be achieved after improving the efficiencies of different steps of the process. Similar to the previous discussion, assuming a η_r value of “one”, the occupied area calculated from Eq. 3 equals 13.64 ha. This is roughly the area of a 370 m side length square.

5. RENEWABLE BIOFUEL FROM FAST PYROLYSIS OF *SYNECHOSYSTIS* AND *SCENEDESMUS* WILD-TYPE MICROALGAE SPECIES

In this study, biomasses of microalgae *Scenedesmus* and *Synechosystis* species were thermochemically converted to biofuel in a fast pyrolysis process. The microalgae species were wild-type and isolated from local habitats. The effect of pyrolysis temperature (400, 500 and 600 °C) on the products yields were investigated. The obtained biooil and biochar were characterized using Fourier transform infrared (FTIR) spectroscopy, CHN/O analysis, Gas chromatography–mass spectrometry (GC-MS), Scanning Electron Microscopy (SEM), Brunauer–Emmett–Teller (BET) analysis. It was observed that both microalgae produced a biomass with high volatile content which converted mainly to liquid biooil product. The best pyrolysis temperature for *Scenedesmus* and *Synechosystis* biomass was respectively 500 °C and 600 °C resulted in higher biooil yield of 80.0 wt % and 71.0 wt %. The produced biooil had higher calorific value than that of wood source biooil where lower O/C ratio was observed. The produced biochar had low surface area but with considerable nitrogen, phosphorus and other minerals content was suggested as fertilizer. The biooil samples were mainly composed of nitrogenous phenolic compounds, carboxylic acids, amines compounds and heavy hydrocarbons. It was concluded that microalgae biomass was more suitable for biooil production compared to lignocellulosic feed stock especially with higher production rate of microalgae.

5.1. Materials and method

5.1.1. Chemicals

The chemicals NaNO_3 , K_2HPO_4 , $\text{MgSO}_4 \cdot 7\text{H}_2\text{O}$, $\text{CaCl}_2 \cdot 2\text{H}_2\text{O}$, Citric acid, Ammonium ferric citrate, EDTANa_2 , Na_2CO_3 , H_3BO_3 , $\text{MnCl}_2 \cdot 4\text{H}_2\text{O}$, $\text{ZnSO}_4 \cdot 7\text{H}_2\text{O}$, $\text{Na}_2\text{MoO}_4 \cdot 2\text{H}_2\text{O}$, $\text{CuSO}_4 \cdot 5\text{H}_2\text{O}$, $\text{Co}(\text{NO}_3)_2 \cdot 6\text{H}_2\text{O}$ were used during microalgae culturing and large volume cultivation, purchased from Sigma-Aldrich, USA. Acetone, chloroform, methanol, phenol, sulfuric acid, KCl, and propanol were provided by Tekkim, Turkey. All the chemicals were of reagent grade. Reagent water was utilized in laboratory using a water purification unit (Thermo Scientific, Germany). Dichloromethane (DCM) was used as solvent for pyrolysis liquid product provided by Sigma-Aldrich, USA. Sodium sulfate anhydrous was used to dehydrate the pyrolysis liquid product, also purchased from Sigma.

5.1.2. Microalgae strain and cultivation

The wild-type strains of *Scenedesmus* (SCE) and *Synechosystis* (SYN) microalgae and were isolated from porsuk river (Eskisehir, Turkey, 39°46'12.0"N 30°29'54.6"E) as was described in our previous work [86]. The medium for cultivation was BG11 according to [67]. The isolated microalgae were then batch cultured by transferring to 250 ml flasks. After almost 3 weeks and clear growth, cultures were transferred to 1liter volume flasks used as photobioreactors. At this stage, the culture solution was bubbled with a continuous 2 vvm gas stream of 5% CO₂ mixture with air (MKS instruments, USA) and kept under 3500 lux (T-10MA Konica Minolta; Japan) white fluorescent light (15 w, ORSAM, Turkey). To produce enough biomass, larger photobioreactors were implemented. Based on previous experiences, for SCE sp. a bubble column type (Figure 5.1) and for SYN a rectangular cross section configuration (Figure 5.1) was used. SCE sp. had a large cell size and could settle easily when mixing was stopped, therefore the bubble column was a good choice. On the other hand, the SYN sp. which was floating in the solution was very stable so that even with no mixing for long time they still could stay floated. The mass production rate of SYN was low. Therefore a rectangular type photobioreactor with 50 liter volume was implemented. The growth condition was adjusted as described for 1 liter flask step unless that the light was provided by white light LED strips twisted around the reactors so that 3500 lux light intensity was maintained. The well-grown cultures in 1 liter flasks were transferred to the large photobioreactors and the adequate amount of BG11 solution was added. Samples were taken regularly to monitor the growth by reading the optical density (OD) at 680 nm (Shimadzu UV-1800 UV-Vis Spectrophotometer). The OD was converted to gr/l in dried mass basis using conversion factors withdrawn for each species after calibration of OD vs biomass concentration in dry basis (db). When the growth curve appeared to reach the stationary phase, the harvest was started by taking half of the solution. The reactors were then replenished with fresh BG11 medium and cultivation continued.

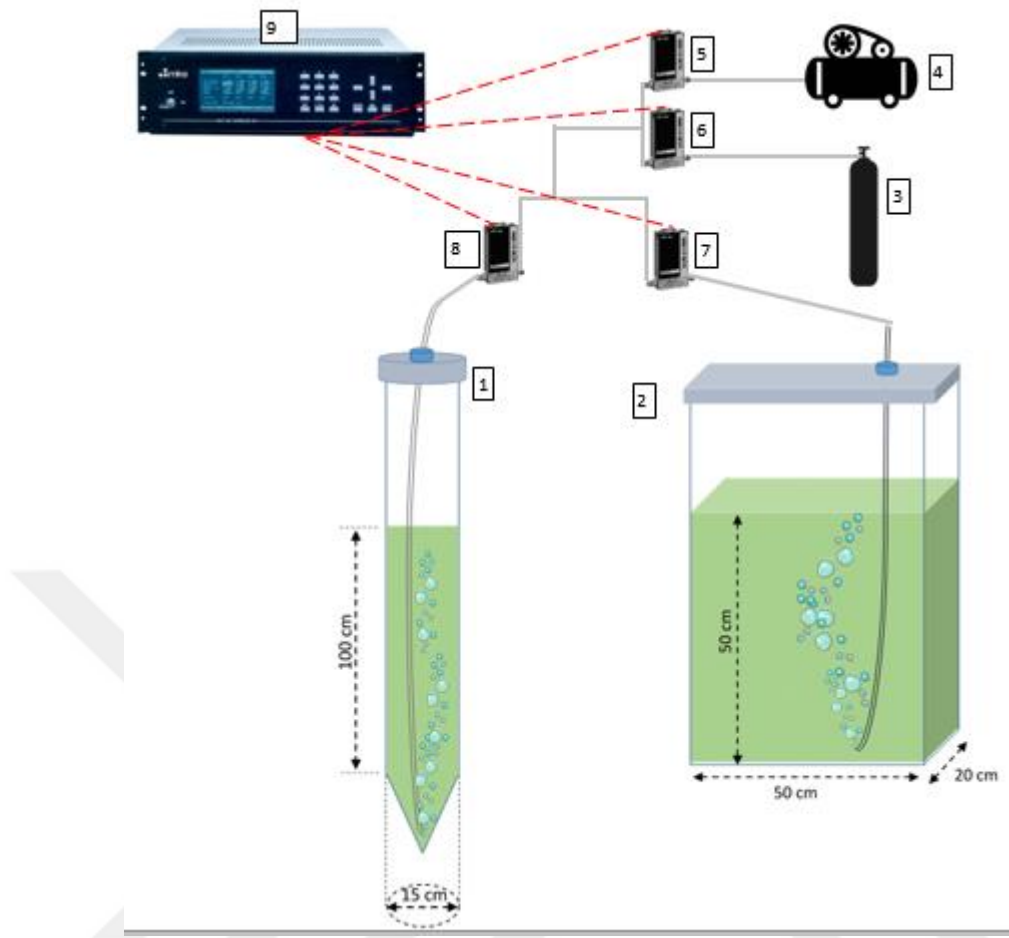


Figure 5.1. *Photobioreactors setup. 1: Bubble column type. 2: Rectangular type photobioreactors. 3: CO₂ cylinder. 4: Air compressor. 5&6&7&8: Mass flow controllers. 9: Control Unit*

5.1.3. Biomass harvest

Because of different settling characteristics of two species, two approaches were implemented for harvesting. Harvesting is actually a bottle neck confronting microalgae technology. The SCE species could settle down easily so that the obtained sample was left for 24 hours and the top clear layer was siphoned gently. Then 2 liter of deionized distilled water (DDW) was added to the residue and left overnight for settling. This was done to wash out the minerals in the medium left in biomass. Again the top clear layer was siphoned and the residue were dried at 110 °C.

For the SYN, natural settling was not efficient therefore a chemical coagulation approach was implemented. Aluminum sulfate as coagulant was added to the biomass solution so that the final concentration of aluminum sulfate was 0.4 gr/l. The solution was mixed vigorously for 2 minutes and then with the clear appearance of the flocs mixer

speed was lowered and gentle mixing continued for 30 minutes. Then, the mixing was stopped and left overnight. The clear top layer was siphoned and the residue was washed with DDW as described before. The washing was repeated 2 or 3 times to ensure the abatement of residual aluminum sulfate. Finally the biomass residue was dried at 110 °C.

5.1.4. Analyses of biomass

The elemental analysis was done using a CHN analyzer (FlashSmart, Thermo Fisher). A scanning electron microscope (SEM, TM3030, HITACHI) device in combination with an Energy Dispersive X-Ray Spectrometer (EDX) equipped with Silicon Drift Detector (SDD) was used to quantify O, Al, S, Cl, K and P elements. For liquid products O was estimated by difference.

The lipid content was gravimetrically determined according to Bligh&Dyer [69] using methanol/chloroform as solvents. The carbohydrate part was colorimetrically estimated at 490 nm (Shimadzu UV-1800 UV-Vis Spectrophotometer) using sulfuric acid/phenol approach according to Dubois et al. [70] with dextran as standard carbohydrate. The protein content was estimated from elemental nitrogen and a conversion factor of 4.78 ± 0.62 as was suggested in a previous study [71] for microalgae. Moisture, ash, volatile material and fixed carbon were determined according to ASTM D7582. High heating value (HHV) was estimated using following formula proposed by Meraz and friends [92]:

$$HHV \left(\frac{Mj}{kg} \right) = (1 - H_2O/100) \times -0.3708[C] - 1.1124[H] + 0.1391[O] - 0.3178[N] - 0.1391[S] \quad (5.1)$$

5.1.5. Pyrolysis

The pyrolysis unit was a 1 meter height vertical straight pipe with 1 cm² internal cross sectional area. Per each run, 3.0 gram of biomass was taken. Biomass was formerly grinded to have < 1 mm particles. A small amount, ~ 0.65 gr of crimped steel fiber was used to maintain a fixed bed and inserted into the reactor column by means of a long steel rod. Then the biomass was purred from the top and with the same rod pushed toward the bed without pressing hard. The set points for pyrolysis temperature, heating rate and time of pyrolysis were adjusted. When all the joints and connections were fixed, N₂ as carrying inert gas was flown for almost 3 minutes to ensure abatement of oxygen in the reactor before applying electricity. A control unit automatically operated the process upon start.

A heating rate of 500 °C/min with pyrolysis temperatures of 400, 500 and 600 °C and reaction time of 3 minutes was followed.

The pyrolysis unit upon completion of run was left to cool down to 50 °C and then after stopping N₂ current, the joints opened and the liquid product which was a highly viscose sticky paste, was washed with DCM and collected. The obtained product in this way was dehydrated by dripping the solution over a funnel filled with anhydrous sodium sulfate. The dehydrated solution was collected in a pre-weighed evaporating flask. Excess fresh DCM was dripped over the funnel to ensure complete gain of product. The collected solution at the bottom was again concentrated by evaporation of DCM using rotary evaporator at 45 °C and 750 mm Hg vaccume. (Heidolph, Germany). Evaporation continued until no dripping was observed in condenser side. Then the evaporating flask was detached and left under hood and regularly weighted till constant weight. The final weight was recorded for liquid product yield calculation. The obtained liquid product was then transferred with the help of some droplets of DCM to glass containers and the containers cap were left half closed to let the excess DCM evaporate. After some days the cap was tightened and the product stored in 4 °C. The solid part of the product along with the steel fiber bed was taken out of the column with the help of a long steel rod and weighted. This value was used for produced char yield calculation. The char was stored in a tight cap falcon for later analysis.

5.1.6. Analyses of product

The liquid and solid products were analyzed for elemental CHN and Oxygen content was calculated by difference. Then FT-IR analysis (Nicolet iS10, Thermo Scientific) was performed to determine the functional groups. Liquid products were subjected to GS-MS analyze to find out the constituents.

Surface area of the biochar was estimated using Brunauer–Emmet–Teller analyze (BET, NOVAtouch, Quantachrome, UK). Degasification was performed before analysis at 450 °C under 38 tor vacuum for 16 h. Topography of the biochar surface were evaluated using scanning electron microscopy (SEM, TM3030, HITACHI)

5.2. Results and Discussion

5.2.1. Microalgae cultivation

The oil-immersion microscopic view of the *Scenedesmus* and *Synechocystis* species provided in figure 5.2. SCE sp. had a green color while SYN sp. looks blue-green which is the characteristics of their belonging microalgae family chlorophyte and cyanophyte respectively. The obvious larger size of the SCE sp. is an advantage during harvest because they settle easily when mixing is stopped but is also a disadvantage during cultivation because continuous mixing is required to maintain homogeneous growth condition. The reverse applies for SYN. The growth curves are presented in figure 5.3. The SCE growth in bubble column reactor had better performance than the SYN in rectangular cross section reactor perhaps because of more efficient mixing. At the linear region SCE growth rate was 80 mg/l/d whereas this value for SYN was 17 mg/l/d.

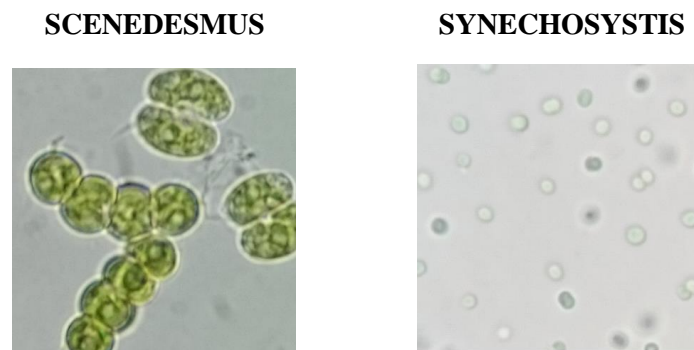


Figure 5.2. Oil immersion microscopy of microalgae living cells

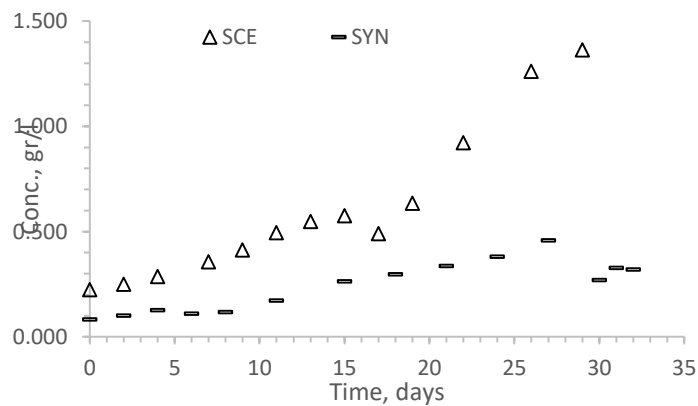


Figure 5.3. Growth curve for microalgae living cells in photobioreactors

5.2.2. Biomass characteristics

SYN *sp.* compared to SCE *sp.* had much smaller cell size being approximately 3-4 μm against 20-30 μm for SCE (Figure 5.2). The smaller cell size in practice could result in a denser dried biomass, something that was revealed in SEM image of dried biomass (Figure 5.4). There are other factors which also affect the mechanical property of biomass like method of harvest. In the SEM images of dried biomass, the cells are not distinguishable because of the deformations and mild sintering of the cells and liquid extracts during drying step. It seems that very small pores are also formed during drying, perhaps because of moist evaporation. The structure of SCE biomass seems to be more porous than SYN biomass which was related to the application of coagulant during harvest of SYN and also cell morphology as well. Porous structure helps more uniform an efficient heat transfer by convectional circulation of hot gases. The organic nature of biomass hinders efficient heat transfer. The proximate analysis, ultimate analysis of CHN/O in dried basis wt % (db) and dried ash free basis wt % (daf), and elemental and biochemical composition of the biomasses are summarized in Table 5.1. For comparison, the data for wood is also included in Table 5.1 which is taken from the published work of Trinh and friends [1]. The volatiles for SCE and SYN was 91.6 and 81.4 wt % db. This value for wood was 84.3 wt % db [1]. Analyze of biochemical composition showed that biomass was mainly composed of Lipid, Protein and Carbohydrate which for SCE were 43.2, 47.6 and 41.0 wt % whereas for SYN were 4.2, 52.8 and 26.6 wt % respectively. Lipid and carbohydrate content of SCE was higher than for SYN where on contrary, the protein content of SYN was higher. The Ash residue of SYN (15.1 wt %) was much higher than SCN (2.7 wt %) due to the different way of harvest since SCN was left to settle without addition of coagulant but for SYN was used. The elemental aluminium in the biomass for SYN represented 4.41 wt % db of the biomass. Aluminum sulfate used during coagulation, precipitated as $\text{Al}(\text{OH})_3$ and caused floc formation. Low ash is advantageous from an application point of view especially when the energy of the biomass are going to be directly extracted through combustion. Accumulation of high ash in burners especially with obstacles confronting conveying solid material shall be avoided.

This was observed that the oxygen content of SYN biomass was 38.8 wt % daf while for SCN composed only 24.1 wt % daf but still lower than lignocellulosic resources [1]. The presented value for elemental CHN/O shows significant higher carbon content

of SCN which was 62.1 wt % daf compared to 39.7 wt % daf for SYN. Higher carbon content results in higher HHV of SCN (34.29 MJ/kg) compared to SYN (19.49 Mj/kg). The high N content equal to 9.97 wt % daf for SCN and 10.34 wt % daf for SYN was a disadvantage of both microalgae biomass. In contrast, S content was insignificant. The N and S oxidizes to NO_x and SO_x gases upon combustion.

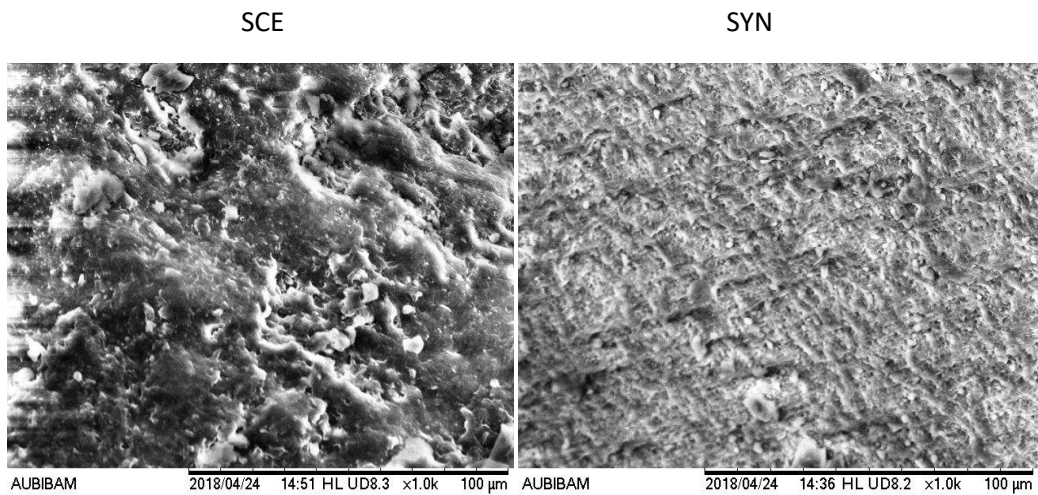


Figure 5.4. SEM image of SCE and SYN dried biomasses

Table 5.1. Proximate, ultimate, elemental and biochemical analysis of microalgae biomass

	SCE	SYN	Wood ^b
Proximate analysis (% wt)			
Moisture	7.0	9.7	9.1
Ash (% wt db)	2.7	15.2	2.7
Volatile Material (% wt db)	85.3	73.7	84.3
Fixed carbon (% wt db)	5.0	1.5	13
Ultimate analysis (% wt db)			
C	61.9	39.7	51.3
H	7.4	7.3	5.7
N	9.0	10.3	0.21
O ^a	24.1	36.3	40.5
Ultimate analysis (% wt daf)			
C	62.1	42.4	52.7
H	7.4	7.8	5.9
N	9.0	11.0	0.22
O ^a	24.1	38.8	41.0
Elemental analysis^a (% wt db)			
Al	0.34	4.41	0.05
S	0.65	0.35	0.03
Cl	na	0.1	<0.01
K	1.14	0.84	0.14
P	0.42	1.66	0.01
Biochemical composition (not normalized)			
Lipid	47.32	4.23	
Protein	43.2	52.8	
Carbohydrate	41.0	26.62	
HHV (Mj/kg)	30.90	22.6	

^a estimated by EDX

^b Data for wood are taken from reference [1]

5.2.3. Pyrolysis product yield

The pyrolysis converted the biomass into solid, liquid and gas products with different yields based on type of the microalgae and the temperature as is presented in figure 5.5. The highest liquid product for SCN was 21.1% obtained when the SCN biomass pyrolyzed at 500 °C whereas for SYN the largest yield (71.0 %) obtained at 600 °C. For both biomasses the lowest amount was produced at 400 °C with yields of 27.1 and 14.6 % respectively for SCN and SYN. Greenhalf and friends [58] reported a biooil yield of 34.97 % and 63.17% respectively from wheat straw and beech wood when subjected to fast pyrolysis at 520 °C . In another research [62], a Bio-Oil yield of 57.9% was reported for *Chlorella* microalgae biomass at an operating temperature equal to 500 °C. Generally, a higher yield was achieved from lipid rich microalgae biomass than lignocellulosic biomass like [62]. Microalgae being a prokaryote microorganism owes a much simpler structure than eukaryotic plants with rigid cell walls that are interconnected firmly with long chains of polymerized lignin and cellulose. The main components of microalgae are lipid, carbohydrate and proteins whereas for higher plants, cellulose (~39%), lignin (~24%) and hemicellulose (~22%) compose almost more than 80% of the mass. Microalgae biochemical constituent is an important factor affecting biooil yield where higher lipid content is believed to enhance the biooil yield. Vardon et al. [93] showed that pyrolysis of a defatted *Scenedesmus* biomass resulted in 7 wt % percent decrease in yield compared to normal *Scenedesmus* biomass. This was also observed in this study where SYN biomass with 4.3 wt % lipid at the best case converted to 21.1 wt % biooil, and SCE biomass with 47.3 wt % lipid gave 35.3 wt % biooil yield.

At the pyrolysis temperature where maximum liquid was produced, the biochar was minimized comparing to the other temperatures. For SCN at 500 °C biochar yield was 18.8 wt % where for SYN at 600 °C biochar yield was 39.4 wt %. In general, biochar composed higher proportion of products for SYN comparing to SCE. Low pyrolysis temperature favors biochar production because of uncompleted decomposition of biomass. Therefore, lower pyrolytic conversion at reduced temperatures resulted in high char yield and low oil product yield.

Bio-gas was calculated by difference. The highest bio-gas proportion was observed at 600 °C for SYN and SCE respectively being 39.5 and 52.45 % respectively. The difference in the yield between SYN and SCE was related to higher ash content of SYN biomass and also higher lipid content of SCE biomass which increases the share of char

in the product. The other reason could be the higher lipid content of SCE where small chain fatty acid may evaporate or decompose to gas products more readily.

In general, the results in figure 5.5 showed that the pyrolysis yield was strongly dependent on the temperature which indicates, for a large scale application, careful control of the temperature and maintaining homogeneous temperature profile in the reactor has crucial importance.

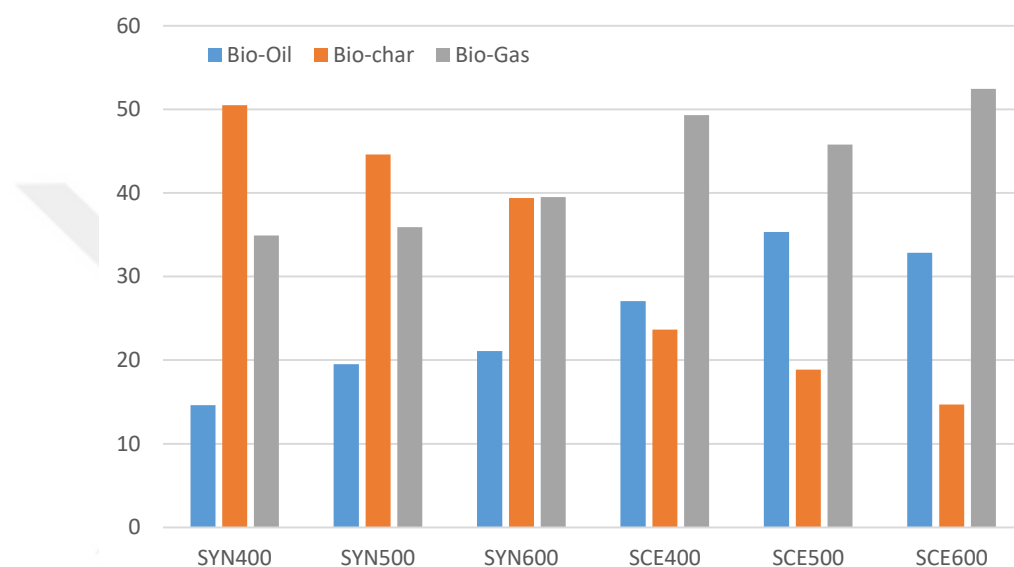


Figure 5.5. The production yield of biooil, biochar and biogas for SCE and SYN biomasses at 400, 500 and 600 °C

5.2.4. Bio-oil characteristics

Bio-oil produced from microalgae in appearance was a dark brownish sticky paste with low mobility in room temperature (~ 20 °C). It was important to be addressed because the liquid nature of the bio-oil is always magnified for transportation capability through pipelines. For such a goal, bio-oil in this form may need heating or addition of solvents at dispatch and re-evaporating at receiving point or application of cracking techniques for conversion of bio-oil to even lighter compounds to make the pumping task economically feasible.

The CHN/O analyses of the products are presented in Table 5.2. These data reveals that comparing to original biomass, the liquid product had less nitrogen content. For SCE

it was 8.0, 6.9 and 7.62 wt % respectively for pyrolysis temperatures of 400, 500 and 600 °C . This value for SYN biooil was 9.95, 9.46 and 9.50 wt % accordingly with no considerable variation at different temperatures. For both species, the lowest nitrogen belonged to the temperature where highest biooil efficiency was achieved. For biooil quality, low nitrogen and sulfur are welcomed for reduced pollution upon combustion. Trinh et al. has reported 0.5 % and 1.62% nitrogen in bio-oil of wood and straw respectively. Clearly, nitrogen content of microalgae biooil as in the present study was much higher which was related to the fact that microalgae has high protein content in compare to wood.

Table 5.2. *Elemental analysis and HHV values for biooils*

	N	C	H	O	O/C	HHV
SYN400	9.95	72.06	8.76	9.23	0.13	38.45
SYN500	9.46	71.33	10.1	9.11	0.13	39.54
SYN600	9.5	65.59	8.94	15.97	0.24	35.17
SCE400	8	71.1	10.12	10.78	0.15	38.78
SCE500	6.9	67.17	9.48	16.45	0.24	35.47
SCE600	7.62	70.08	9.44	12.86	0.18	37.23

The oxygen content for SCE biooil was 10.87, 16.45 and 12.86 wt % whereas for SYN biooil was 9.23, 9.11 and 15.97 wt % respectively at 400, 500 and 600 °C. In previous studies, oxygen content of biooil was reported 19.43 wt % for chlorella microalgae [61], 35.3 wt % for wood oil and 31.3 wt % for straw oil [1]. It was observed that the oxygen was less in microalgae biooil comparing to lignocellulosic biooil, something that was also emphasized by Wang and friends [63]. Lower oxygen is beneficial for stability of the product and also higher calorific value.

The calculated HHV value (Table 5.2) for produced biooil samples was in the range 35-40 MJ/kg which was higher than HHV of SCE biomass (34.29 MJ/kg) and significantly higher than SYN biomass (19.49 MJ/kg). For lignocellulosic origin biooil, HHV in the range 23-35 MJ/kg was previously reported [1, 94].

5.2.5. FTIR spectroscopy

The FTIR chromatogram of the biooil are presented in supplementary figure (Figure S.1-6) in the appendix. The wide peaks on the spectrum along with the high absorbance for most of wavenumbers revealed that a very complex mixture with variety of functional groups were present in samples. The similar spectrum of all six biooil samples revealed their similar chemical composition with some concentration variations. The peaks on the spectrum mainly correspond to aromatics, carboxylic acids, hydrocarbons and amine compounds. Unless for the range of 1900-2500 cm^{-1} and $> 3500 \text{ cm}^{-1}$ there was strong absorbance on the rest of spectrum. Very low absorbance at 2000-2500 cm^{-1} range reveals the absence of nitrile compounds. The spectra was interpreted with refer to previous similar studies [93, 95, 96]. The spectra high absorption in the range 3200 and 3550 cm^{-1} are assigned to either O-H (H-bonded) as in phenolic compounds or N-H stretching bonds representing hydroxyl or amine group compounds in the bio crude. Very strong absorption corresponding to CH_3 , CH_2 & CH stretch (2840-3000 cm^{-1}) and their medium intensity bending vibrations (Respectively ,1350-1470 cm^{-1} , 1370-1390 cm^{-1} and 720-725 cm^{-1}) were observed. Additionally, peaks corresponding to heteroatom-containing functional groups appeared in all samples (1800–600 cm^{-1}). Peaks at $\sim 1709 \text{ cm}^{-1}$ were possibly due to H-bonded C=O group in carboxylic acids. Peak at around $\sim 737 \text{ cm}^{-1}$ and $\sim 702 \text{ cm}^{-1}$ could be due to =C-H or C-H out of plane bending. Peak at $\sim 1266 \text{ cm}^{-1}$ was related to The C-N absorptions are as in aromatic amines which appears in 1200 to 1350 cm^{-1} range.

5.2.6. GC-MS analysis

The GC/MS techniques was used to identify the components of the biooil samples and also quantify it by calculating chromatogram peaks area as are presented in Table 5.3. The chromatograms are presented in figure S.7-12 in the appendix. As can be seen, the number of peaks are low which shows that the biooil from microalgae are less complex than the other lignocellulosic biooil. For example, in the work of Ateş and Işıkdağ [94], chromatogram of biooil from wheat straw showed almost 56 significant peaks. The less complex nature of microalgae biooil was related to the lack of lignocellulosic material in microalgae biomass [63]. The share of aromatics was low because they are mainly lignin originated compounds [97]. Variety of organic groups including phenols, furfurals, terpene, carboxylic acids, nitriles and aromatics were detected. Heptadecane,

Neophytadiene, 2-Hexadecene, 3,7,11,15-tetramethyl, (E)-6,6-Dimethylcyclooct-4-en-1-on, Pentadecanenitrile, 2-Hydroxy-3,5,5-trimethyl-2-cyclohexenone, n-Hexadecanoic acid, Phytol, 9-Octadecenoic acid and Hexadecanamide were the most common compounds ranging from 1.5-35.06 wt % of the biooil composition. Interestingly, nitrogen containing compounds were found more frequently in SYN biomass which was related to higher protein content of SYN species. Nitrogen mass percent calculated from GC/MS data (Table 5.3) also revealed the higher nitrogen content of SYN biomass. Comparing to the CHN/O elemental analysis as in Table 5.2, GC based nitrogen mass percent was much lower (0.2-1.7 wt % comparing to 6.9-9.9 wt %). This was attributed to undetectable high molecular weight compounds by GC [60]. It was concluded that the SCE biomass which had higher lipid content provided higher quality products as biofuel. This was also suggested elsewhere [62]. Phytol, an acyclic diterpene alcohol which originates from lipid were more abundant in SCE biooil. Phytol is also a valuable chemical used as precursor for commercial synthesis of vitamins [98]. Neophytadiene which is a terpenoid, along with n-Hexadecanoic acid and 9-Octadecenoic acid were other abundant lipid derived compounds. Significant amount of Heptadecane, an alkane hydrocarbon was detected in SYNE biooil which was advantageous for biofuel quality. In general, more volatile and light organics were contained in SYN biooil compared to SCEN biooil. It could be related to the catalytic role of Al present in the biomass. The catalytic role of Al was investigated elsewhere [99].

Table 5.3. GC-MS analyze of biooil samples

Retention Time	Components	Formula	SYN	SYN	SYN	SCN	SCN	SCN
			400	500	600	400	500	600
			Biooil	Biooil	Biooil	biooil	Biooil	Biooil
			Peak Area (%)					
12.082	Phenol, 4-methyl-	C7H8O				0.51		
13.65	Benzeneacetonitrile	C8H7N				1.6		
16.562	Benzenepropanenitrile	C9H9N		2.28	1.69			
17.151	4-(trimethylsilyl)dibenzofuran	C12H8O	4.73	3.83	3.74			
18.153	1H-Indole	C8H7N	3.82	3.59	4.82			
19.572	alpha-Ionene	C13H18			1.19			
20.55	7-Methylindole	C9H9N			1.19			
27.714	Heptadecane	C17H36	8.38	8.29	6.52	2.25	2.69	
30.667	NEOPHYTADIENE	C20H38	12.48	12.01	11.27	10.35	13.76	12.71
30.793	2-Hexadecene, 3,7,11,15-tetramethy	C20H40		2.21	2.31	4.65	4.8	4.1
31.525	(E)-6,6-Dimethylcyclooct-4-en-1-on	C10H16O	6.55	6.61	7.33	8.06	8.12	8.37
31.92	Pentadecanenitrile	C15H29N	2.99	2.79	3.16	5.11		
33.059	2-Hydroxy-3,5,5-trimethyl-2-cyclohexenone	C9H14O2		6.08	4.86	9.38	10.91	10.52
33.551	n-Hexadecanoic acid	C16H32O2	35.06	29.97	28.11	17.09	20.94	17.54
35.942	Phytol	C20H40O	2.16	2.01	1.7	21.51	20.93	24.15
36.652	9-Octadecenoic acid	C18H34O2	12.24	10.35	9.98	9.16	13.92	18.39
37.333	Hexadecanamide	C16H33NO	8.79	8.99	7.38	7.16	3.93	4.23
40.239	7-Pentadecyne	C15H30			1.05			
40.274	Oleamide	C18H35NO				2.94		
43.124	Phthalic Acid	C8H6O4	2.81		1.58			
<u>Elemental concentration wt % based on peak area</u>								
	C		78.34	77.96	78.78	76.94	78.64	78.48
	H		11.88	11.80	11.50	12.24	12.45	12.38
	N		1.13	1.34	1.68	0.71	0.22	0.23
	O		8.66	7.92	8.02	7.76	8.70	8.92

5.2.7. Biochar characteristics

The SEM images of the biochar products as well as feed biomass at different temperatures are presented in figure 5.6. The SEM images of products reveals that higher temperatures produces a more porous structure but still very less porous when compared to lignocellulosic feed stocks [100].

The results for surface area determination using BET analysis (Table 5.4) reveals very low porosity of the microalgae biochar. While for some of the samples the value was not in detectable range of the device, the obtained highest value was 4.85 m²/gr for SYN biomass at 500 °C and 6.1 m²/gr for SCE at 600 °C. In a previous study, 175.4 m²/gr was reported for biochar obtained from pitch pine [59].

CHN/O Elemental analysis of biochar and also inorganic mineral contents are summarized in Table 5.4. Carbon element proportion decreases with the increase of temperature for both species. Carbon composed about 70.2 wt % of the SCE biochar and 53.8 wt % of the SYN biochar produced at 400 °C. Lower carbon of the SYN biochar was because of high amount of inorganic element and especially Al which was added during harvest as coagulant something that was not detected in SCE biochar.

Nitrogen has decreased in biochars for both biomasses compared to initial feed stocks but still nitrogen composed a considerable proportion in the range of 3.06-8.42 wt % for SYN and 3.4-7.5 wt % for SCE. Nitrogen along with other soil nutrients like P, K and Mg suggests potential use of biochar as fertilizer.

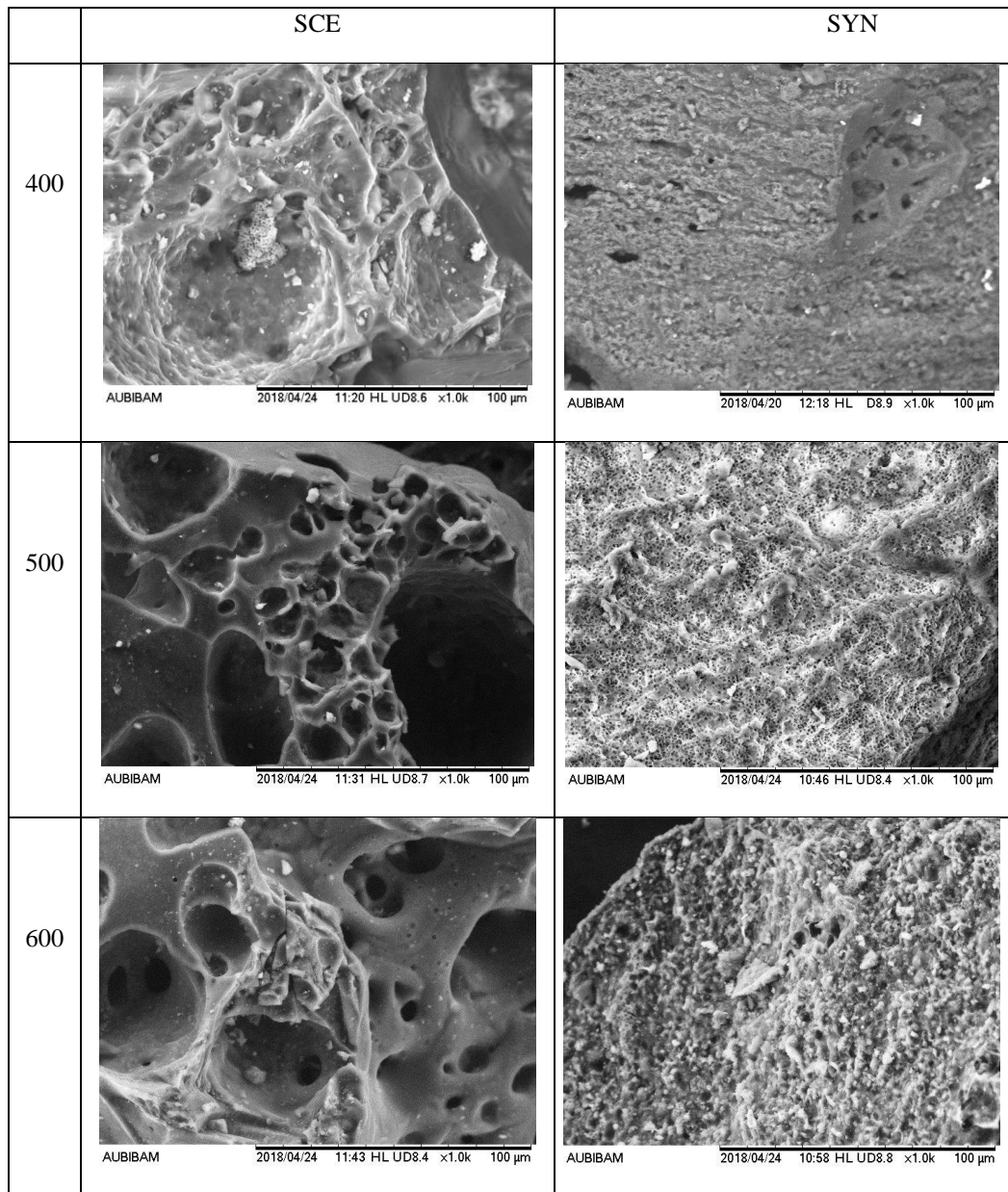


Figure 5.6. SEM image of SCE and SYN biochar at 400, 500 and 600 °C

Table 5.4. Elemental analyze of SYN and SCE biochars at 400, 500 and 600 °C

	N	C	H	O	Al	P	K	Na	Mg	BET
	CHN analyze (wt %)			EDX analyze (wt %)						
SYN400	8.42	53.82	3.21	34.55	7.19	2.8	1.75	2.36	0.77	1.84
SYN500	7.17	46.45	3.97	27.59	8.24	3.31	2.12	1.55	0.46	6.1
SYN600	6.21	48.58	2.93	21.36	10.2	3.61	1.28	2.77	0.81	n.d ^a
SCE400	7.495	70.29	6.315	10.82	0.59	2.39	1.56	0.55	0.69	n.d
SCE500	4.725	45.385	2.44	8.92	0	1.55	2.24	0.38	0.39	0.01
SCE600	3.0645	43.195	1.7665	9.5	0	1.27	2.67	0	0.55	4.85

^{n.d} Not detected

5.2.8. Large Scale Biooil production

The results as was discussed above, showed that pyrolysis of microalgae biomass provides a bio crude oil with high energy density. The HHV of the produced bio crude was almost 35 MJ/kg of biomass. It was comparable to that of fossil crude oil with HHV of 42-44 MJ/kg [101]. The applicability of such technology for large scale bio crude oil production can be evaluated with some assumptions when compared to a fossil crude oil refinery facility. In this study, for SCE *sp.* the highest growth rate was 80 mg/d in db per liter of cultivation. It corresponded to 64 mg of bio crude oil per day per liter of cultivation when an 35.3 wt % yield for pyrolysis was assumed. A large capacity fossil crude oil refinery facility like Ras Tanura Refinery (Aramco, Saudi Arabiya) can receive 550,000 bpd which roughly equals to 77000 tons per day [102]. A photobioreactor facility which supposedly can produce enough biomass for bio crude oil feed of such refinery should have a volume of 1.2 billion m³. Assuming that with the help of vertical photobioreactors, 1 m³ volume would occupy just 1 m² of area, then the assumed photobioreactor facility would be mounted in 1200 km². This equals to the area of a 35 km length square. As for now, this may seems far beyond practice but remembering that this estimation was based on non-optimized growth condition. With efficient designs of vertical photobioreactors so that less area would be occupied (assuming 2 m³/m²) and also with optimization of microalgae growth rate for 10 folds increase, the estimated required land area would reduce by 20 times.

Altogether, fast growing nature of microalgae, high yield of biooil production and the quality of such fuels makes microalgae technology a promising solution for future energy demands.



6. CONCLUSION

The findings of the present research on the isolated microalgae species from central Anatolia region showed that there are promising species with potential use as biofuel feed stock. Some of them, especially from green microalgae, had considerable lipid content which makes them a potential biomass producer for oil based biofuel applications. Interestingly, their quiet high growth rate, which was actually achieved without optimization of the growth conditions, creates even more hope for commercial scale biofuel projects. But this technology, does not seems to be a reliable approach for instance to capture/fixate CO₂ emissions of a fossil fuel burning power plant. Green microalgae species were also observed to have high carbohydrate content being suitable for bioalcohol biofuels. On the other hand, blue-green species had higher protein content which makes them suitable for animal or even human feed source.

Amongst the isolated species, there were species which naturally settle down in the solution almost completely when mixing were stopped. This is important because the harvesting costs is a bottle neck in microalgae biotechnology.

The application of microalgae biotechnology confronts bottle necks which till now hindered their propagation. One of this bottle necks is to find a method for cell disruption to increase the yield of valuable materials extraction from the cell. The available methods consumes lots of energy for example in mechanical bead beating or thermal extraction approaches. In the present work, the idea was, instead of applying lots of energy in various form of compression or shear to collapse the cell, glass microparticle with sharp edges would scrape and cut the cell wall with much less energy. This idea was examined with a general factorial design statistical approach in this study. The application of glass microparticles in solvent based methods for lipid extraction was an effective method to enhance the efficiency. In this study, the efficiency increased by almost 45% for *Chlorella* when 40 µm glass particles were added without applying high mixing rates. Because of the different characteristics of microalgae cell wall and their resistance to solvents, there may be a significant underestimation of their lipid content using common methods. This is important to be considered especially in screening studies.

The results of this study clearly showed the significant effect of operational factors like carbon dioxide concentration, aeration rate, initial inoculum size of microalgae *Scenedesmus sp.* and the diffuser size on the growth rate and the maximum concentration of microalgae in the solution. There are many other factors like light intensity, light-dark

period, light color, temperature and pH, which based on similar previous researches can be modified. The maximum estimated growth rate was 0.513 g/l.d while just four factors was modified. Taking these findings into account, our estimations for large scales application of microalgae technology as carbon dioxide sink as well as a renewable source for biodiesel production in compare to the capacity of existing fossil fuel production facility revealed that such microalgal facility could be constructed in a reasonable sized land. The remaining issues could be mainly the operational cost of such facilities which can be the subject of future research.

Microalgae, a promising biomass feed stock, are known for their high biomass production rate and photosynthetic efficiency which are composed of mainly lipid, protein and carbohydrate that can easily be converted thermochemically to liquid and solid biofuels are believed to be advantageous over other lignocellulosic plant biomasses. As was observed in the present study, biomass could be efficiently converted to biooil with significant yield as high as 35.3 wt %. The high lipid content *Scenedesmus* species resulted in higher efficiency compared to *Synechosystis* species. The higher nitrogen content of the final products compared to that of wood sourced biomasses was a disadvantage but in contrary, their lower O/C ratio provides a more stable fuel with higher calorific value. Future attempts for increasing the rate of mass production and design of more efficient photobioreactors will make the microalgae technology feasible for large scale application and especially biofuel plans.

REFERENCES

- [1] Trinh, T.N., P.A. Jensen, K. Dam-Johansen, N.O. Knudsen, et al., (2013). Comparison of lignin, macroalgae, wood, and straw fast pyrolysis, *Energ. Fuel.*, 273, 1399-1409.
- [2] Sydney, E.B., W. Sturm, J.C. de Carvalho, V. Thomaz-Soccol, et al., (2010). Potential carbon dioxide fixation by industrially important microalgae, *Bioresource. Technol.*, 10115, 5892-5896.
- [3] Wang, B., Y. Li, N. Wu, and C.Q. Lan, (2008). CO₂ bio-mitigation using microalgae, *Appl. Microbiol. Biot.*, 795, 707-718.
- [4] Gouveia, L., Microalgae as a Feedstock for Biofuels, in *Microalgae as a Feedstock for Biofuels 2011*, Springer. 1-69.
- [5] Lee, R.A. and J.-M. Lavoie, (2013). From first- to third-generation biofuels: Challenges of producing a commodity from a biomass of increasing complexity, *Animal Frontiers*, 32, 6-11.
- [6] Singh, A., P.S. Nigam, and J.D. Murphy, (2011). Renewable fuels from algae: an answer to debatable land based fuels, *Bioresource. Technol.*, 1021, 10-16.
- [7] Muylaert, K., L. Bastiaens, D. Vandamme, and L. Gouveia, 5 - Harvesting of microalgae: Overview of process options and their strengths and drawbacks A2 - Gonzalez-Fernandez, Cristina, in *Microalgae-Based Biofuels and Bioproducts*, Muñoz, R., Editor 2017, Woodhead Publishing. 113-132.
- [8] Arenas, E., R. Palacio, A. Juantorena, S. Fernando, et al., (2017). Microalgae as a potential source for biodiesel production: techniques, methods, and other challenges, *Int. J. Energ. Res.*, 416, 761-789.
- [9] Duran, S.K., P. Kumar, and S.S. Sandhu, (2018). A review on microalgae strains, cultivation, harvesting, biodiesel conversion and engine implementation, *Biofuels*, 1-12.
- [10] Velazquez-Lucio, J., R.M. Rodríguez-Jasso, L.M. Colla, A. Sáenz-Galindo, et al., (2018). Microalgal biomass pretreatment for bioethanol production: a review, *BioFuel. Res. J.*, 51, 780-791.
- [11] Harman-Ware, A.E., T. Morgan, M. Wilson, M. Crocker, et al., (2013). Microalgae as a renewable fuel source: Fast pyrolysis of *Scenedesmus* sp, *Renew. Energ.*, 60, 625-632.
- [12] Christaki, E., P. Florou-Paneri, and E. Bonos, (2011). Microalgae: a novel ingredient in nutrition, *Int. J. Food. Sci. Nutr.*, 628, 794-799.
- [13] Jorquera, O., A. Kiperstok, E.A. Sales, M. Embiruçu, et al., (2010). Comparative energy life-cycle analyses of microalgal biomass production in open ponds and photobioreactors, *Bioresource. Technol.*, 1014, 1406-1413.
- [14] Brooks, A.N., S. Turkarslan, K.D. Beer, F. Yin Lo, et al., (2011). Adaptation of cells to new environments, *Wires. Syst. Biol. Med.*, 35, 544-561.
- [15] Sriswasdi, S., C.-c. Yang, and W. Iwasaki, (2017). Generalist species drive microbial dispersion and evolution, *Nat. Commun.*, 81, 1162.
- [16] Pandit, S.N., J. Kolasa, and K. Cottenie, (2009). Contrasts between habitat generalists and specialists: an empirical extension to the basic metacommunity framework, *Ecology*, 908, 2253-2262.
- [17] Ghadiryanfar, M., K.A. Rosentrater, A. Keyhani, and M. Omid, (2016). A review of macroalgae production, with potential applications in biofuels and bioenergy, *Renew. Sust. Energ. Rev.*, 54, 473-481.

- [18] Mata, T.M., A.A. Martins, and N.S. Caetano, (2010). Microalgae for biodiesel production and other applications: a review, *Renew. Sust. Energ. Rev.*, 141, 217-232.
- [19] Jose, S. and S. Archanaa, Environmental and Economic Sustainability of Algal Lipid Extractions: An Essential Approach for the Commercialization of Algal Biofuels, in *Algal Biofuels: Recent Advances and Future Prospects*, Gupta, S. K., A. Malik, and F. Bux, Editors. 2017, Springer International Publishing: Cham. 281-313.
- [20] Kim, D.-Y., D. Vijayan, R. Praveenkumar, J.-I. Han, et al., (2016). Cell-wall disruption and lipid/astaxanthin extraction from microalgae: *Chlorella* and *Haematococcus*, *Bioresource. Technol.*, 199, 300-310.
- [21] Aguirre, A.-M. and A. Bassi, (2014). Investigation of high pressure steaming (HPS) as a thermal treatment for lipid extraction from *Chlorella vulgaris*, *Bioresource. Technol.*, 164, 136-142.
- [22] Kurokawa, M., P.M. King, X. Wu, E.M. Joyce, et al., (2016). Effect of sonication frequency on the disruption of algae, *Ultrason. Sonochem.*, 31, 157-162.
- [23] Sharma, A.K., P.K. Sahoo, S. Singhal, and G. Joshi, (2016). Exploration of upstream and downstream process for microwave assisted sustainable biodiesel production from microalgae *Chlorella vulgaris*, *Bioresource. Technol.*, 216, 793-800.
- [24] Yoo, G., W.-K. Park, C.W. Kim, Y.-E. Choi, et al., (2012). Direct lipid extraction from wet *Chlamydomonas reinhardtii* biomass using osmotic shock, *Bioresource. Technol.*, 123, 717-722.
- [25] Postma, P., T. Miron, G. Olivieri, M. Barbosa, et al., (2015). Mild disintegration of the green microalgae *Chlorella vulgaris* using bead milling, *Bioresource. Technol.*, 184, 297-304.
- [26] Keris-Sen, U.D. and M.D. Gurol, (2017). Using ozone for microalgal cell disruption to improve enzymatic saccharification of cellular carbohydrates, *BioMass. BioEnerg.*, 105, 59-65.
- [27] Shankar, M., P.K. Chhotaray, A. Agrawal, R.L. Gardas, et al., (2017). Protic ionic liquid-assisted cell disruption and lipid extraction from fresh water *Chlorella* and *Chlorococcum* microalgae, *Algal Res.*, 25, 228-236.
- [28] Choi, S.-A., Y.-K. Oh, M.-J. Jeong, S.W. Kim, et al., (2014). Effects of ionic liquid mixtures on lipid extraction from *Chlorella vulgaris*, *Renew. Energ.*, 65, 169-174.
- [29] Lee, O.K., Y.H. Kim, J.-G. Na, Y.-K. Oh, et al., (2013). Highly efficient extraction and lipase-catalyzed transesterification of triglycerides from *Chlorella* sp. KR-1 for production of biodiesel, *Bioresource. Technol.*, 147, 240-245.
- [30] Demuez, M., C. González-Fernández, and M. Ballesteros, (2015). Algicidal microorganisms and secreted algicides: New tools to induce microalgal cell disruption, *Biotechnol. Adv.*, 338, 1615-1625.
- [31] Wu, C., Y. Xiao, W. Lin, J. Li, et al., (2017). Aqueous enzymatic process for cell wall degradation and lipid extraction from *Nannochloropsis* sp, *Bioresource. Technol.*, 223, 312-316.
- [32] Halim, R., R. Harun, M.K. Danquah, and P.A. Webley, (2012). Microalgal cell disruption for biofuel development, *Appl. Energ.*, 911, 116-121.
- [33] Pragma, N., K.K. Pandey, and P.K. Sahoo, (2013). A review on harvesting, oil extraction and biofuels production technologies from microalgae, *Renew. Sust. Energ. Rev.*, 24, 159-171.

- [34] Balasundaram, B. and A. Pandit, (2001). Selective release of invertase by hydrodynamic cavitation, *BioChem. Eng. J.*, 83, 251-256.
- [35] Lee, A.K., D.M. Lewis, and P.J. Ashman, (2012). Disruption of microalgal cells for the extraction of lipids for biofuels: Processes and specific energy requirements, *BioMass. BioEnerg.*, 46, 89-101.
- [36] Wijffels, R.H. and M.J. Barbosa, (2010). An outlook on microalgal biofuels, *Science*, 3295993, 796-799.
- [37] Pulz, O. and W. Gross, (2004). Valuable products from biotechnology of microalgae, *Appl. Microbiol. Biot.*, 656, 635-648.
- [38] Han, F., H. Pei, W. Hu, M. Song, et al., (2015). Optimization and lipid production enhancement of microalgae culture by efficiently changing the conditions along with the growth-state, *Energ. Convers. Manage.*, 90, 315-322.
- [39] Cheah, W.Y., P.L. Show, J.C. Juan, J.-S. Chang, et al., (2018). Enhancing biomass and lipid productions of microalgae in palm oil mill effluent using carbon and nutrient supplementation, *Energ. Convers. Manage.*, 164, 188-197.
- [40] Christenson, L. and R. Sims, (2011). Production and harvesting of microalgae for wastewater treatment, biofuels, and bioproducts, *Biotechnol. Adv.*, 296, 686-702.
- [41] Welter, C., J. Schwenk, B. Kanani, J. Van Blargan, et al., (2013). Minimal medium for optimal growth and lipid production of the microalgae *Scenedesmus dimorphus*, *Environ. Prog. Sustain. Energy*, 324, 937-945.
- [42] Sakai, N., Y. Sakamoto, N. Kishimoto, M. Chihara, et al., (1995). *Chlorella* strains from hot springs tolerant to high temperature and high CO₂, *Energ. Convers. Manage.*, 366, 693-696.
- [43] Wang, C.-Y., C.-C. Fu, and Y.-C. Liu, (2007). Effects of using light-emitting diodes on the cultivation of *Spirulina platensis*, *BioChem. Eng. J.*, 371, 21-25.
- [44] Zhao, B. and Y. Su, (2014). Process effect of microalgal-carbon dioxide fixation and biomass production: A review, *Renew. Sust. Energ. Rev.*, 31, 121-132.
- [45] Kumar, A., S. Ergas, X. Yuan, A. Sahu, et al., (2010). Enhanced CO₂ fixation and biofuel production via microalgae: recent developments and future directions, *Trends Biotechnol.*, 287, 371-380.
- [46] Yun, Y.S., S.B. Lee, J.M. Park, C.I. Lee, et al., (1997). Carbon dioxide fixation by algal cultivation using wastewater nutrients, *J. Chem. Technol. Biot.*, 694, 451-455.
- [47] Jacob-Lopes, E., L.M. Cacia Ferreira Lacerda, and T.T. Franco, (2008). Biomass production and carbon dioxide fixation by *Aphanothece microscopica* Nägeli in a bubble column photobioreactor, *BioChem. Eng. J.*, 401, 27-34.
- [48] Chae, S.R., E.J. Hwang, and H.S. Shin, (2006). Single cell protein production of *Euglena gracilis* and carbon dioxide fixation in an innovative photo-bioreactor, *Bioresource. Technol.*, 972, 322-329.
- [49] Anjos, M., B.D. Fernandes, A.A. Vicente, J.A. Teixeira, et al., (2013). Optimization of CO₂ bio-mitigation by *Chlorella vulgaris*, *Bioresource. Technol.*, 139, 149-154.
- [50] Silva, H.J. and S.J. Pirt, (1984). Carbon Dioxide Inhibition of Photosynthetic Growth of *Chlorella*, *Microbiology*, 13011, 2833-2838.
- [51] Fidalgo, J., A. Cid, E. Torres, A. Sukenik, et al., (1998). Effects of nitrogen source and growth phase on proximate biochemical composition, lipid classes and fatty acid profile of the marine microalga *Isochrysis galbana*, *Aquaculture*, 1661-2, 105-116.

- [52] Kuei-Ling, Y., C. Jo-Shu, and c. Wen-ming, (2010). Effect of light supply and carbon source on cell growth and cellular composition of a newly isolated microalga *Chlorella vulgaris* ESP-31, *Emg. Life. Sci.*, 103, 201-208.
- [53] Wahal, S. and S. Viamajala, (2010). Maximizing algal growth in batch reactors using sequential change in light intensity, *Appl. Biochem. Biotechnol.*, 1611-8, 511-522.
- [54] Moon, M., C.W. Kim, W.-K. Park, G. Yoo, et al., (2013). Mixotrophic growth with acetate or volatile fatty acids maximizes growth and lipid production in *Chlamydomonas reinhardtii*, *Algar Res.*, 24, 352-357.
- [55] Chiranjeevi, P. and S.V. Mohan, (2016). Critical parametric influence on microalgae cultivation towards maximizing biomass growth with simultaneous lipid productivity, *Renew. Energ.*, 98, 64-71.
- [56] Brennan, L. and P. Owende, (2010). Biofuels from microalgae—A review of technologies for production, processing, and extractions of biofuels and co-products, *Renew. Sust. Energ. Rev.*, 142, 557-577.
- [57] Mettler, M.S., D.G. Vlachos, and P.J. Dauenhauer, (2012). Top ten fundamental challenges of biomass pyrolysis for biofuels, *Energy Environ. Sci.*, 57, 7797-7809.
- [58] Greenhalf, C.E., D.J. Nowakowski, A.B. Harms, J.O. Titiloye, et al., (2013). A comparative study of straw, perennial grasses and hardwoods in terms of fast pyrolysis products, *Fuel*, 108, 216-230.
- [59] Kim, K.H., J.-Y. Kim, T.-S. Cho, and J.W. Choi, (2012). Influence of pyrolysis temperature on physicochemical properties of biochar obtained from the fast pyrolysis of pitch pine (*Pinus rigida*), *Bioresource. Technol.*, 118, 158-162.
- [60] Mohan, D., C.U. Pittman, and P.H. Steele, (2006). Pyrolysis of wood/biomass for bio-oil: a critical review, *Energ. Fuel.*, 203, 848-889.
- [61] Miao, X., Q. Wu, and C. Yang, (2004). Fast pyrolysis of microalgae to produce renewable fuels, *J. Anal. Appl. Pyrol.*, 712, 855-863.
- [62] Miao, X. and Q. Wu, (2004). High yield bio-oil production from fast pyrolysis by metabolic controlling of *Chlorella protothecoides*, *J. Biotechnol.*, 1101, 85-93.
- [63] Wang, K., R.C. Brown, S. Homsy, L. Martinez, et al., (2013). Fast pyrolysis of microalgae remnants in a fluidized bed reactor for bio-oil and biochar production, *Bioresource. Technol.*, 127, 494-499.
- [64] Shuping, Z., W. Yulong, Y. Mingde, L. Chun, et al., (2010). Pyrolysis characteristics and kinetics of the marine microalgae *Dunaliella tertiolecta* using thermogravimetric analyzer, *Bioresource. Technol.*, 1011, 359-365.
- [65] Xie, Q., M. Addy, S. Liu, B. Zhang, et al., (2015). Fast microwave-assisted catalytic co-pyrolysis of microalgae and scum for bio-oil production, *Fuel*, 160, 577-582.
- [66] Anand, V., V. Sunjeev, and R. Vinu, (2016). Catalytic fast pyrolysis of *Arthrospira platensis* (spirulina) algae using zeolites, *J. Anal. Appl. Pyrol.*, 118, 298-307.
- [67] Rippka, R., J. Deruelles, J.B. Waterbury, M. Herdman, et al., (1979). Generic assignments, strain histories and properties of pure cultures of cyanobacteria, *Microbiology*, 1111, 1-61.
- [68] Elsey, D., D. Jameson, B. Raleigh, and M.J. Cooney, (2007). Fluorescent measurement of microalgal neutral lipids, *J. Microbiol. Methods*, 683, 639-642.
- [69] Bligh, E.G. and W.J. Dyer, (1959). A rapid method of total lipid extraction and purification, *Can. J. Biochem. Physiol.*, 378, 911-917.

- [70] Dubois, M., K.A. Gilles, J.K. Hamilton, P.t. Rebers, et al., (1956). Colorimetric method for determination of sugars and related substances, *Anal. Chem.*, 283, 350-356.
- [71] Lourenço, S.O., E. Barbarino, P.L. Lavín, U.M. Lanfer Marquez, et al., (2004). Distribution of intracellular nitrogen in marine microalgae: calculation of new nitrogen-to-protein conversion factors, *Eur. J. Phycol.*, 391, 17-32.
- [72] Rubin, E.S., C. Chen, and A.B. Rao, (2007). Cost and performance of fossil fuel power plants with CO₂ capture and storage, *Energ. Policy*, 359, 4444-4454.
- [73] Yun, H.-S., H. Lee, Y.-T. Park, M.-K. Ji, et al., (2014). Isolation of Novel Microalgae from Acid Mine Drainage and Its Potential Application for Biodiesel Production, *Appl. Biochem. Biotechnol.*, 1738, 2054-2064.
- [74] Wahlen, B.D., R.M. Willis, and L.C. Seefeldt, (2011). Biodiesel production by simultaneous extraction and conversion of total lipids from microalgae, cyanobacteria, and wild mixed-cultures, *Bioresource. Technol.*, 1023, 2724-2730.
- [75] Gonçalves, A.L., C.M. Rodrigues, J.C.M. Pires, and M. Simões, (2016). The effect of increasing CO₂ concentrations on its capture, biomass production and wastewater bioremediation by microalgae and cyanobacteria, *Algar Res.*, 14, 127-136.
- [76] Abo-Shady, A., Y. Mohamed, and T. Lasheen, (1993). Chemical composition of the cell wall in some green algae species, *Biologia plantarum*, 354, 629-632.
- [77] Yaakob, Z., E. Ali, A. Zainal, M. Mohamad, et al., (2014). An overview: biomolecules from microalgae for animal feed and aquaculture, *J. Biol. Res.-THESSALON*, 211, 6.
- [78] Becker, E.W., (2007). Micro-algae as a source of protein, *Biotechnol. Adv.*, 252, 207-210.
- [79] Folch, J., M. Lees, and G. Sloane-Stanley, (1957). A simple method for the isolation and purification of total lipids from animal tissues, *J Biol Chem*, 2261, 497-509.
- [80] Safi, C., S. Camy, C. Frances, M.M. Varela, et al., (2014). Extraction of lipids and pigments of *Chlorella vulgaris* by supercritical carbon dioxide: influence of bead milling on extraction performance, *J. Appl. Phycol.*, 264, 1711-1718.
- [81] Lee, J.-Y., C. Yoo, S.-Y. Jun, C.-Y. Ahn, et al., (2010). Comparison of several methods for effective lipid extraction from microalgae, *Bioresource. Technol.*, 1011, S75-S77.
- [82] Park, J.-Y., K. Lee, S.-A. Choi, M.-J. Jeong, et al., (2015). Sonication-assisted homogenization system for improved lipid extraction from *Chlorella vulgaris*, *Renew. Energ.*, 79, 3-8.
- [83] Araujo, G.S., L.J.B.L. Matos, J.O. Fernandes, S.J.M. Cartaxo, et al., (2013). Extraction of lipids from microalgae by ultrasound application: Prospection of the optimal extraction method, *Ultrason. Sonochem.*, 201, 95-98.
- [84] Concas, A., M. Pisu, and G. Cao, (2015). Disruption of microalgal cells for lipid extraction through Fenton reaction: Modeling of experiments and remarks on its effect on lipids composition, *Chem. Eng. J.*, 263Supplement C, 392-401.
- [85] Park, J.-Y., Y.-K. Oh, J.-S. Lee, K. Lee, et al., (2014). Acid-catalyzed hot-water extraction of lipids from *Chlorella vulgaris*, *Bioresource. Technol.*, 153Supplement C, 408-412.
- [86] Derakhshandeh, K.M., T. Aı̇ıç, and Ü. Tezcan Ün, (2018). The screening of microalgae species isolated from central anatolia region for lipid, carbohydrate and protein content, *Submitted for publication*.

- [87] Ryu, H.J., K.K. Oh, and Y.S. Kim, (2009). Optimization of the influential factors for the improvement of CO₂ utilization efficiency and CO₂ mass transfer rate, *J. Ind. Eng. Chem.*, 154, 471-475.
- [88] Akita, K. and F. Yoshida, (1974). Bubble size, interfacial area, and liquid-phase mass transfer coefficient in bubble columns, *Ind. Eng. Chem. Proc. DD.*, 131, 84-91.
- [89] Akita, K. and F. Yoshida, (1973). Gas holdup and volumetric mass transfer coefficient in bubble columns. Effects of liquid properties, *Ind. Eng. Chem. Proc. DD.*, 121, 76-80.
- [90] Sideman, S., Ö. Hortaçsu, and J.W. Fulton, (1966). Mass transfer in gas-liquid contacting systems, *Ind. Eng. Chem.*, 587, 32-47.
- [91] Lau, P.S., N.F.Y. Tam, and Y.S. Wong, (1995). Effect of algal density on nutrient removal from primary settled wastewater, *Environ. Pollut.*, 891, 59-66.
- [92] Meraz, L., A. Domínguez, I. Kornhauser, and F. Rojas, (2003). A thermochemical concept-based equation to estimate waste combustion enthalpy from elemental composition☆, *Fuel*, 8212, 1499-1507.
- [93] Vardon, D.R., B.K. Sharma, G.V. Blazina, K. Rajagopalan, et al., (2012). Thermochemical conversion of raw and defatted algal biomass via hydrothermal liquefaction and slow pyrolysis, *Bioresource. Technol.*, 109, 178-187.
- [94] Ates, F. and M.j.A. Işıkdag, (2008). Evaluation of the role of the pyrolysis temperature in straw biomass samples and characterization of the oils by GC/MS, *Energ. Fuel.*, 223, 1936-1943.
- [95] Jena, U., K.C. Das, and J.R. Kastner, (2011). Effect of operating conditions of thermochemical liquefaction on biocrude production from *Spirulina platensis*, *Bioresource. Technol.*, 10210, 6221-6229.
- [96] Grierson, S., V. Strezov, and P. Shah, (2011). Properties of oil and char derived from slow pyrolysis of *Tetraselmis chui*, *Bioresource. Technol.*, 10217, 8232-8240.
- [97] Zhao, C., Y. Kou, A.A. Lemonidou, X. Li, et al., (2009). Highly Selective Catalytic Conversion of Phenolic Bio-Oil to Alkanes, *Angew. Chem.*, 12122, 4047-4050.
- [98] Netscher, T., (2007). Synthesis of vitamin E, *Vitam. Horm.*, 76, 155-202.
- [99] Torri, C., I.G. Lesci, and D. Fabbri, (2009). Analytical study on the production of a hydroxylactone from catalytic pyrolysis of carbohydrates with nanopowder aluminium titanate, *J. Anal. Appl. Pyrol.*, 841, 25-30.
- [100] Onay, O., (2007). Influence of pyrolysis temperature and heating rate on the production of bio-oil and char from safflower seed by pyrolysis, using a well-swept fixed-bed reactor, *Fuel. Process. Technol.*, 885, 523-531.
- [101] Jena, U., K.C. Das, and J.R. Kastner, (2012). Comparison of the effects of Na₂CO₃, Ca₃(PO₄)₂, and NiO catalysts on the thermochemical liquefaction of microalga *Spirulina platensis*, *Appl. Energ.*, 98, 368-375.
- [102] (2016). Saudi Aramco Annual Review 2016, *Aramco Company*.

APPENDIX

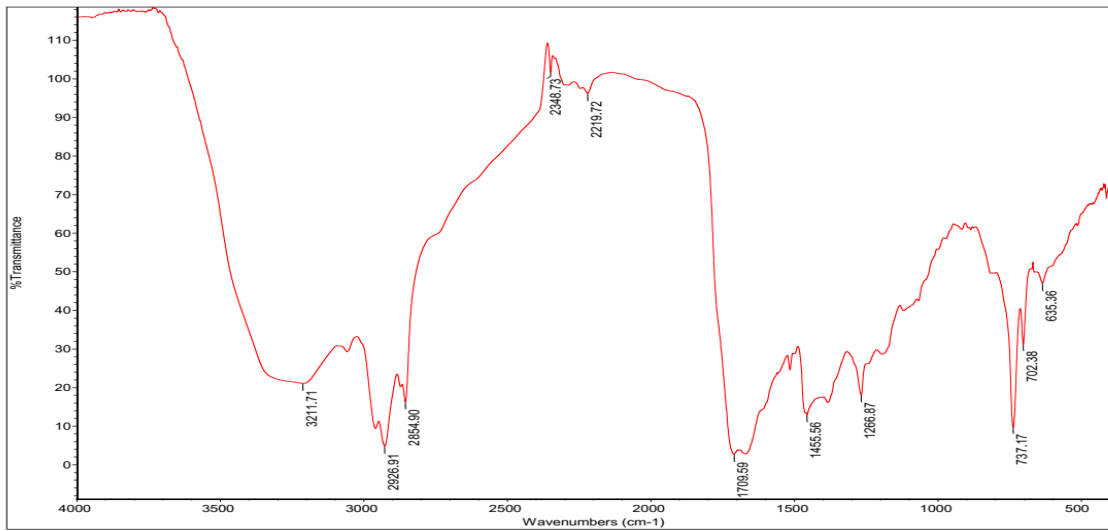


Figure A.1. FTIR Spectrum for SYN at 400 °C

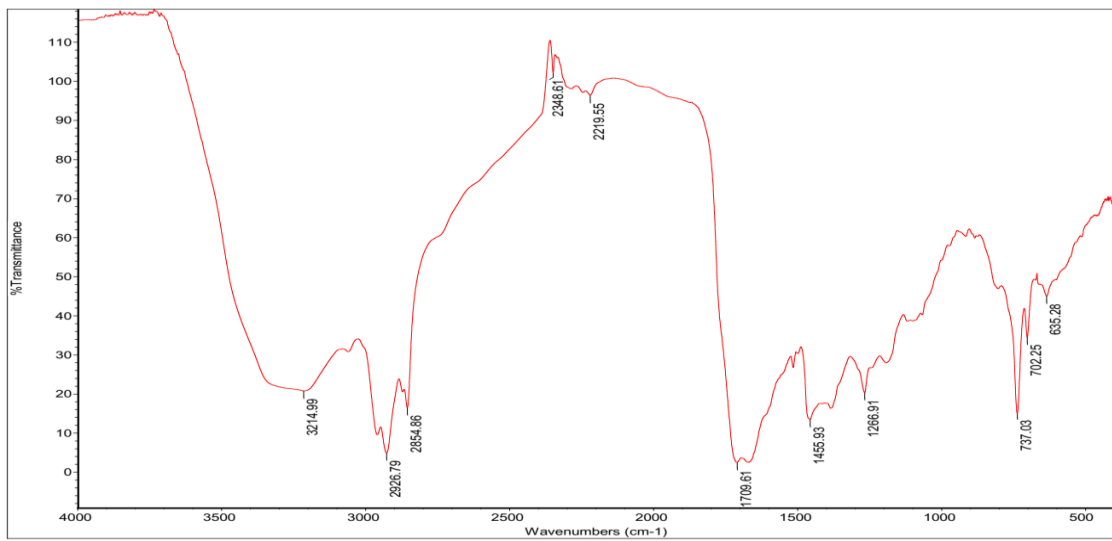


Figure A.2. FTIR Spectrum for SYN at 500 °C

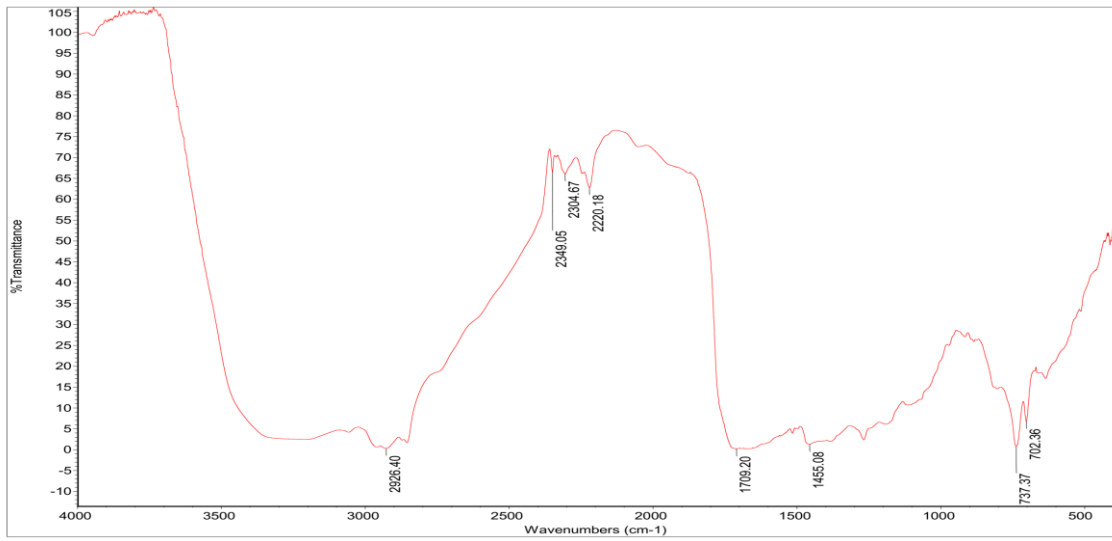


Figure A.3. *FTIR Spectrum for SYN at 600 °C*

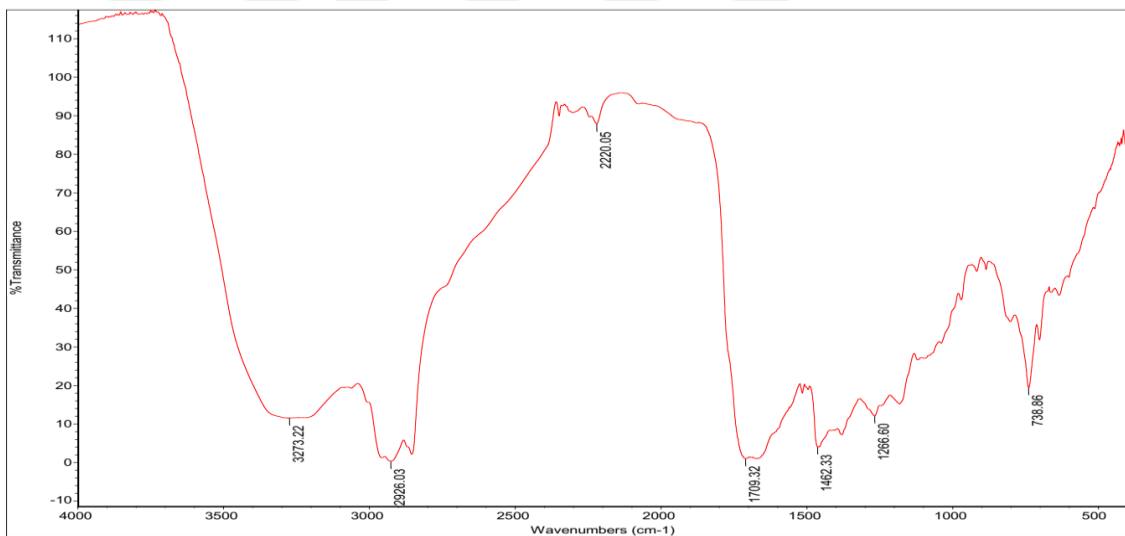


Figure A.4. *FTIR Spectrum for SCE at 400 °C*

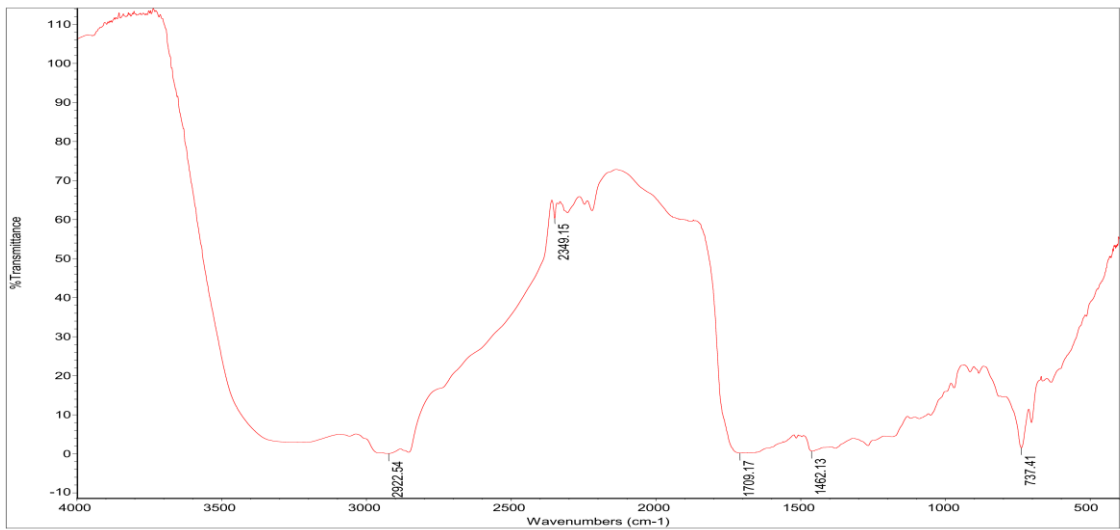


Figure A.5. *FTIR Spectrum for SCE at 500 °C*

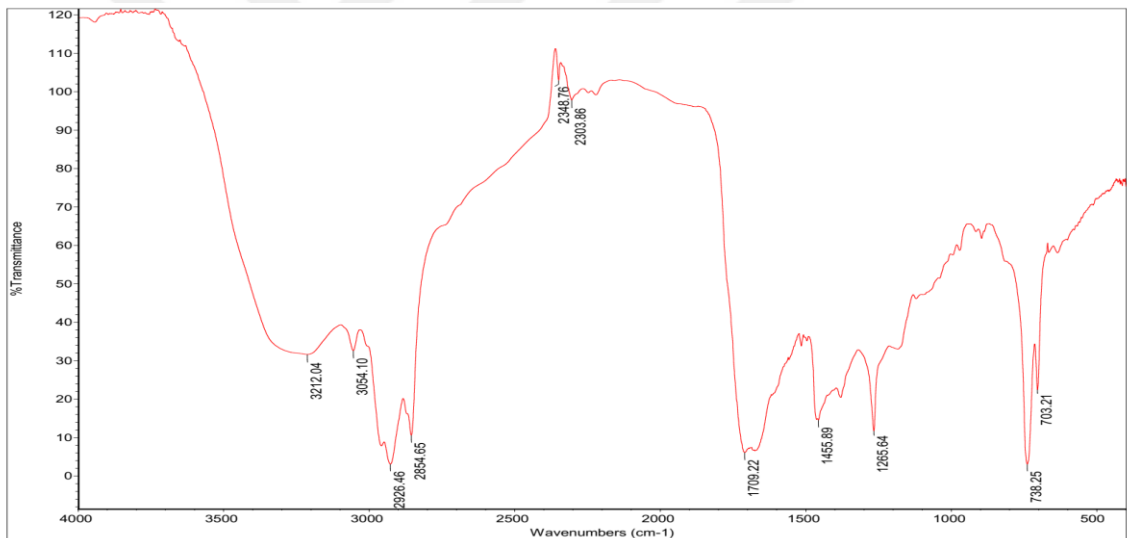


Figure A.6. *FTIR Spectrum for SCE at 600 °C*

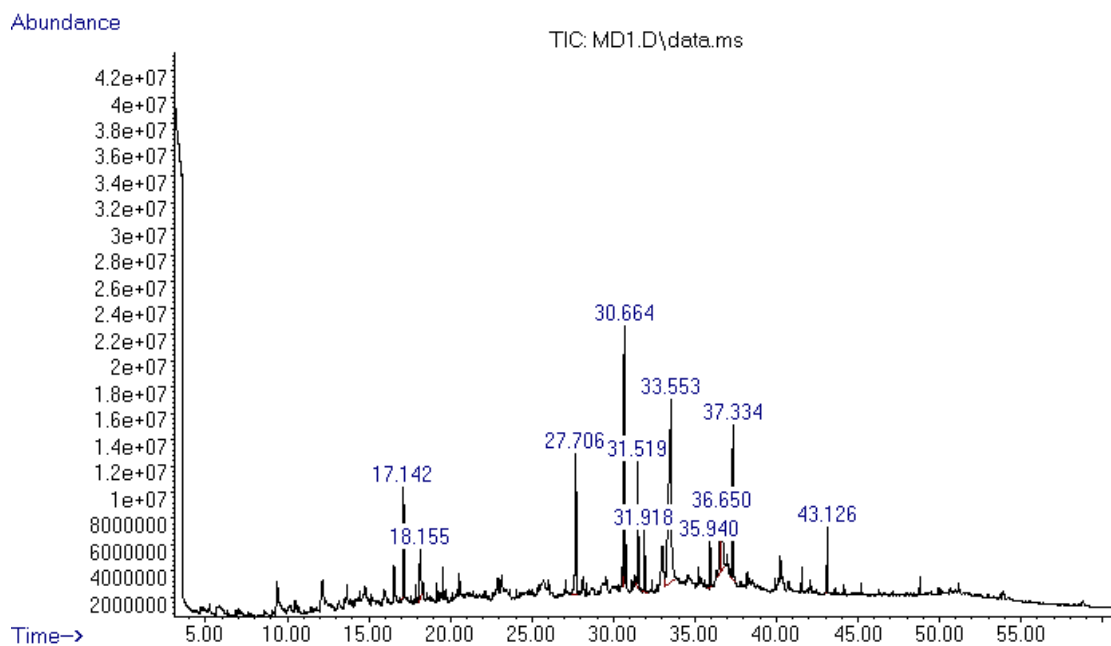


Figure A.7. GC chromatograms for Biooil sample for SYN at 400 °C

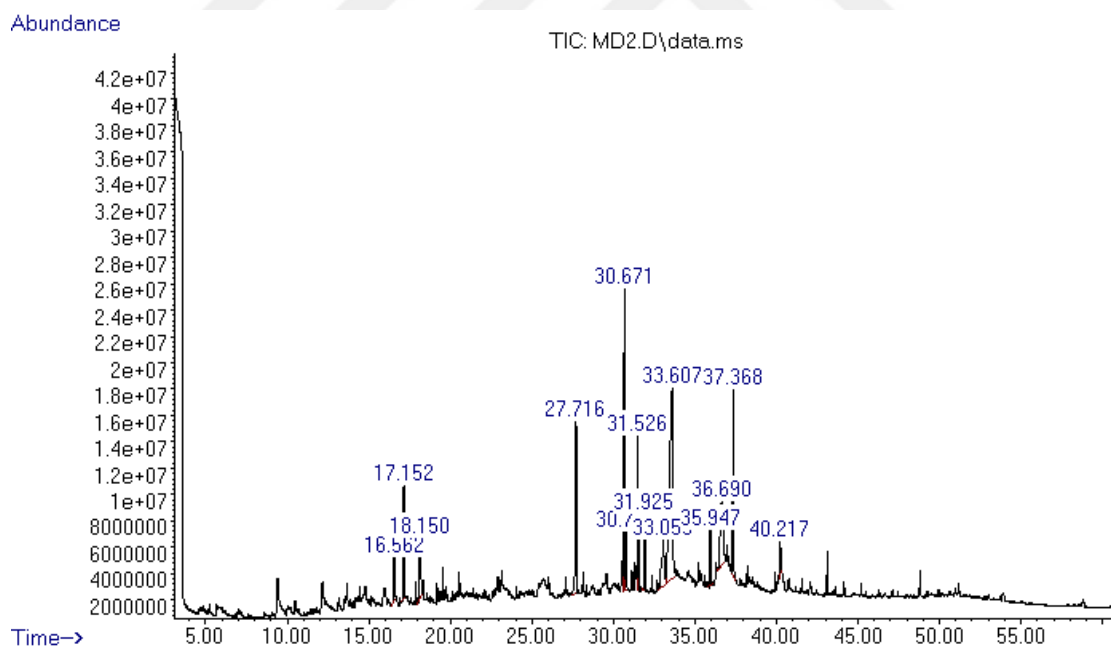


Figure A.8. GC chromatograms for Biooil sample for SYN at 500 °C

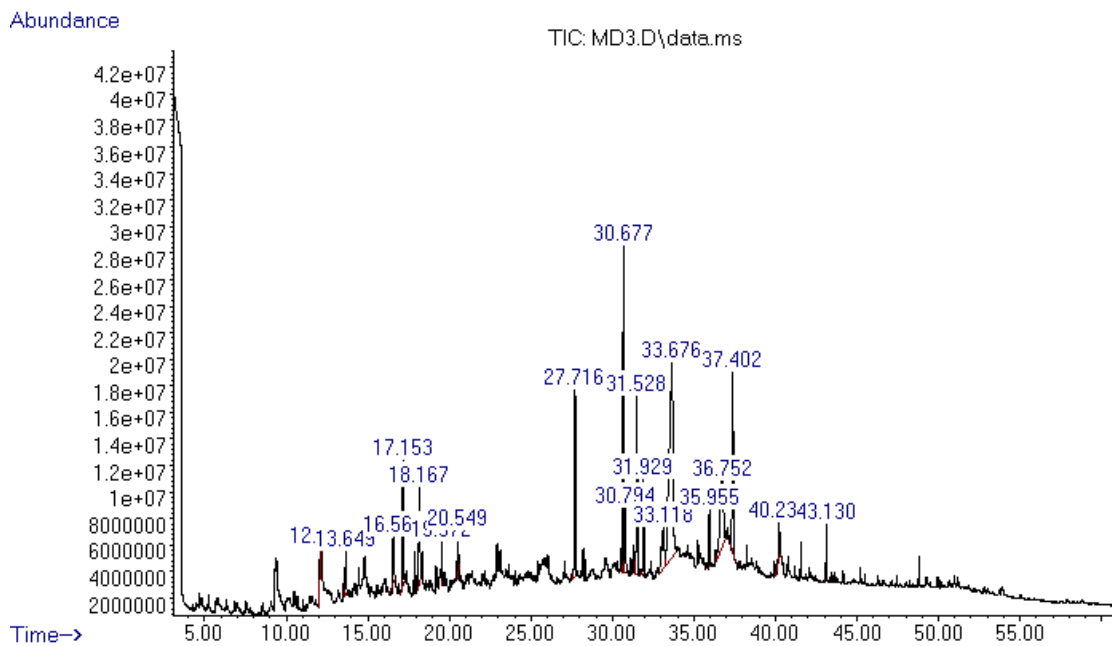


Figure A.9. GC chromatograms for Biooil sample for SYN at 600 °C

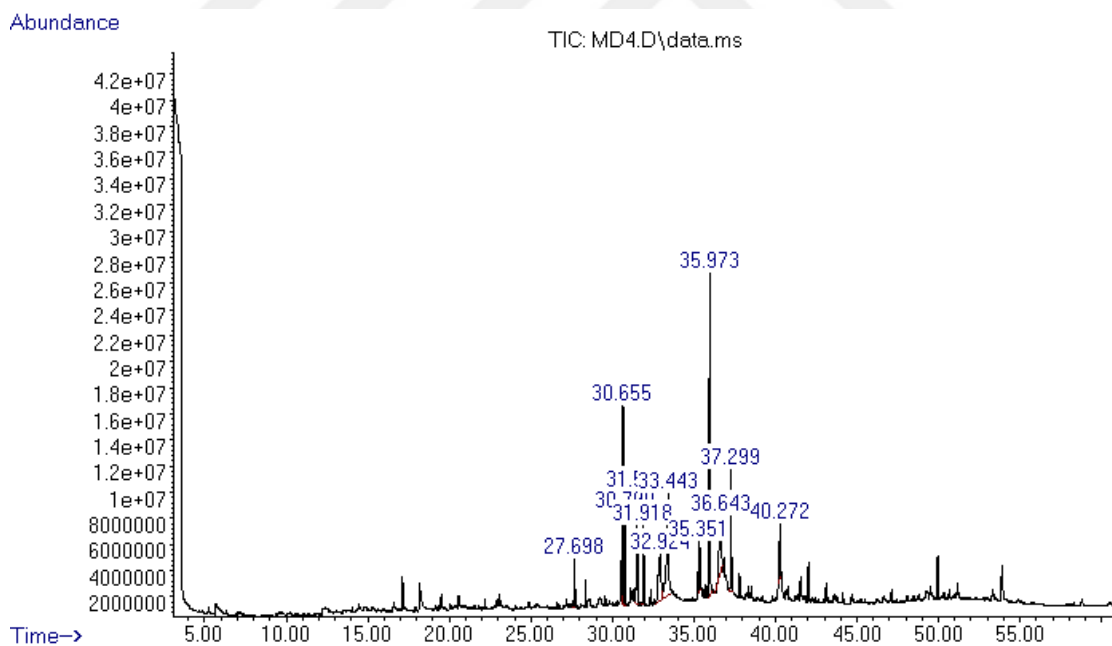


Figure A.10. GC chromatograms for Biooil sample for SCE at 400 °C

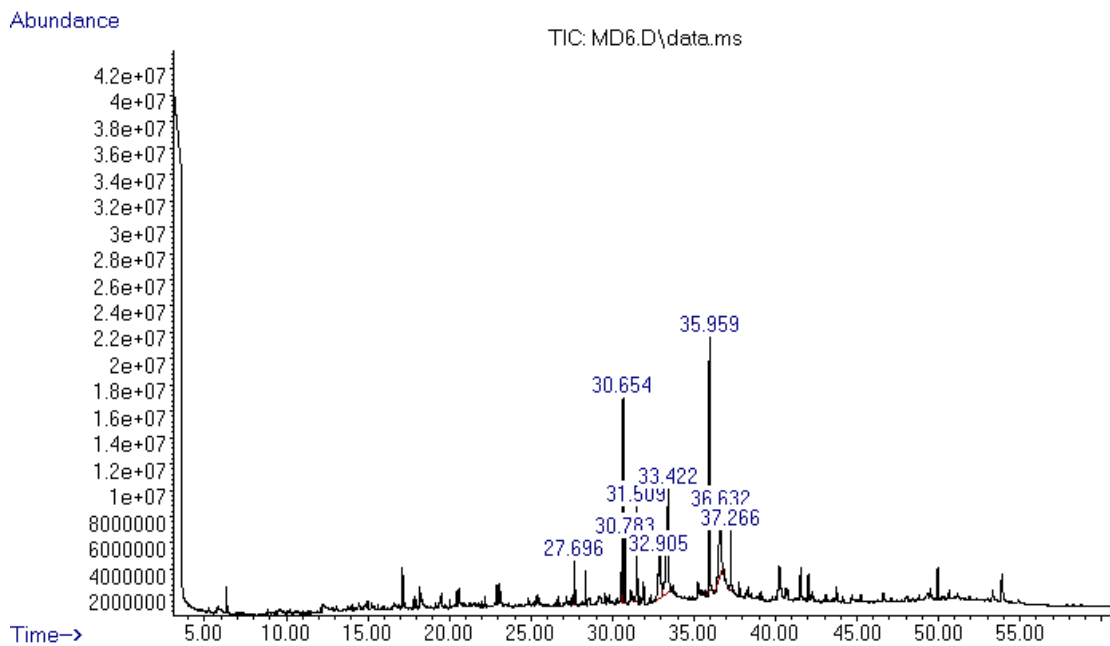


Figure A.11. GC chromatograms for Biooil sample for SCE at 500 °C

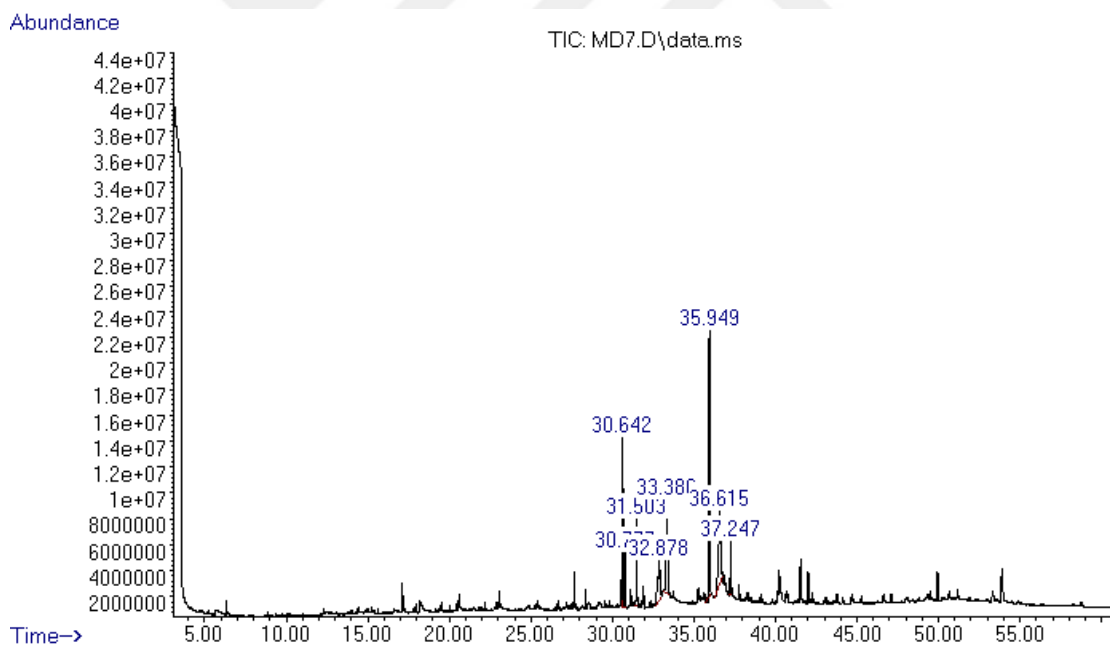


Figure A.12. GC chromatograms for Biooil sample for SCE at 600 °C



Figure A.13. *Sampling Points in Eskişehir, 1: Botanic park, 2: Razif Özgür park*



Figure A.14. *Batch cultivation of mixed samples and pure stocks*

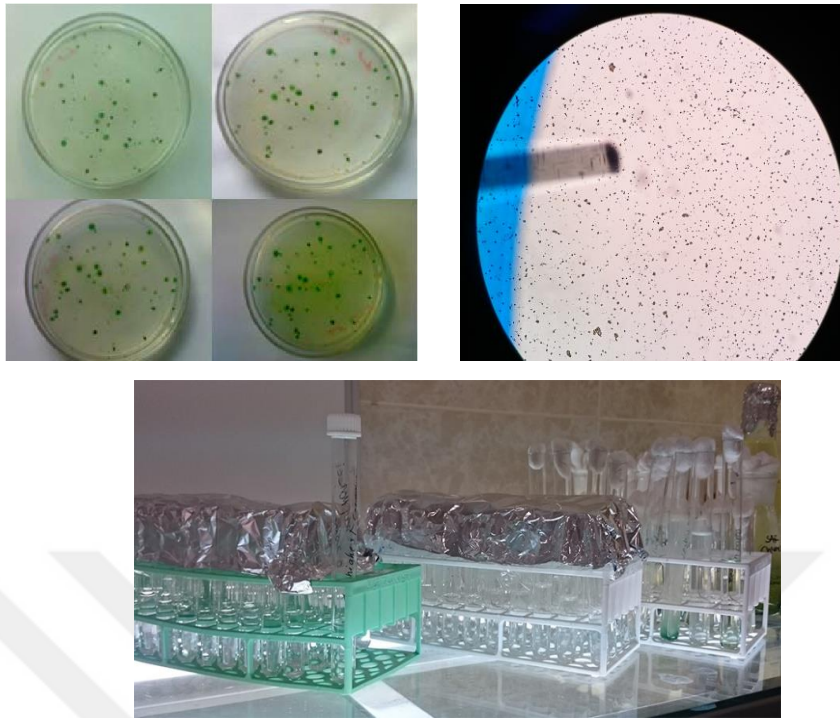


Figure A.15. *Three different cell isolation techniques, Top left: striking on agar media, Top right: single cell catch method, Down: serial dilution*



Figure A.16. *Left: fluorometric method for lipid determination, Right: Separated two phase during lipid extraction*

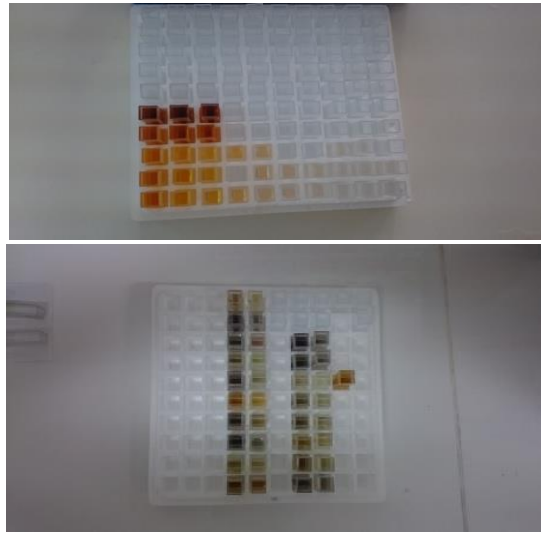


Figure A.17. *Top: Standard reference for colorimetric carbohydrate determination, Down: Samples prepared for carbohydrate determination*

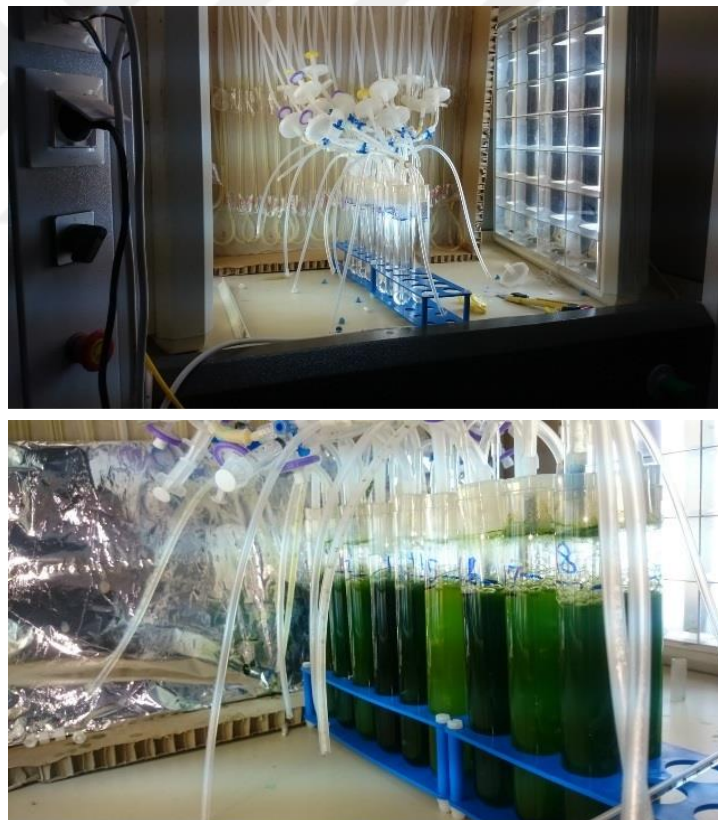


Figure A.18. *Photobioreactor set up for growth rate determination, Top: First day of inoculation, Down: Well grown microalgae samples*

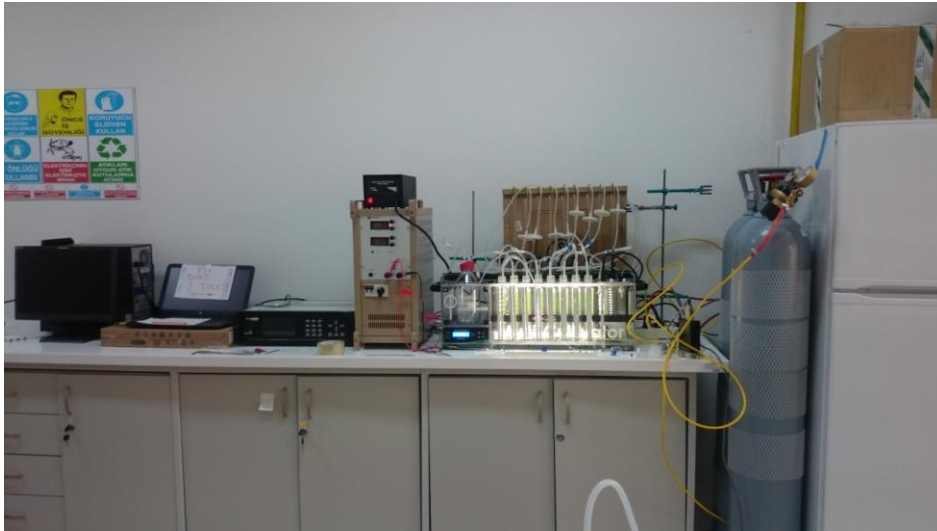


Figure A.19. *Photobioreactor set up for growth rate optimization study*

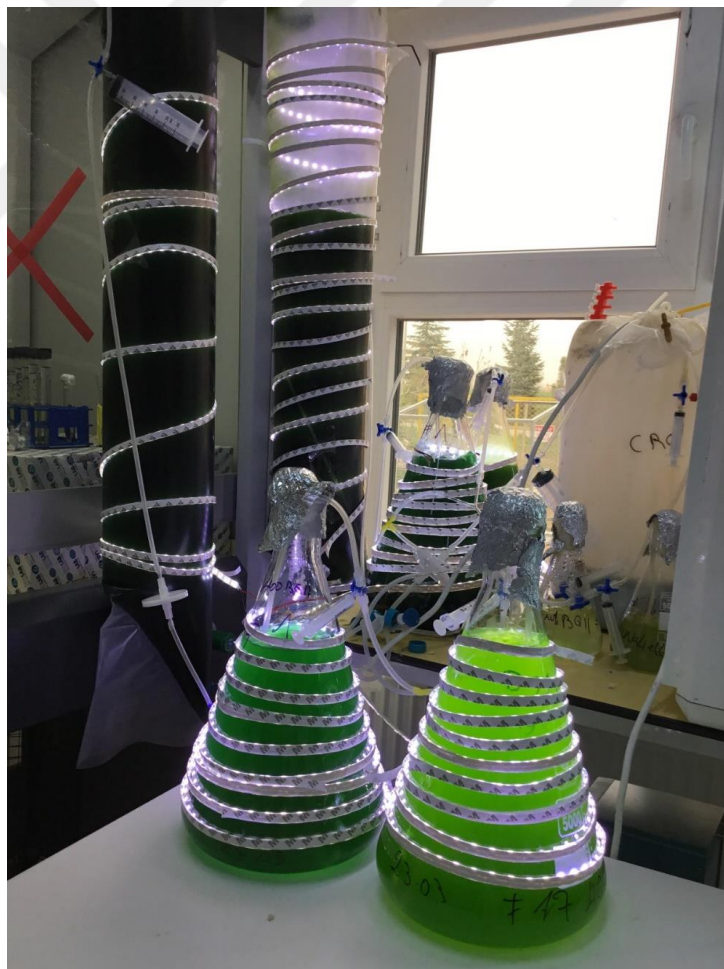


Figure A.20. *Large volume photobioreactor for biomass production to be used in pyrolysis study*

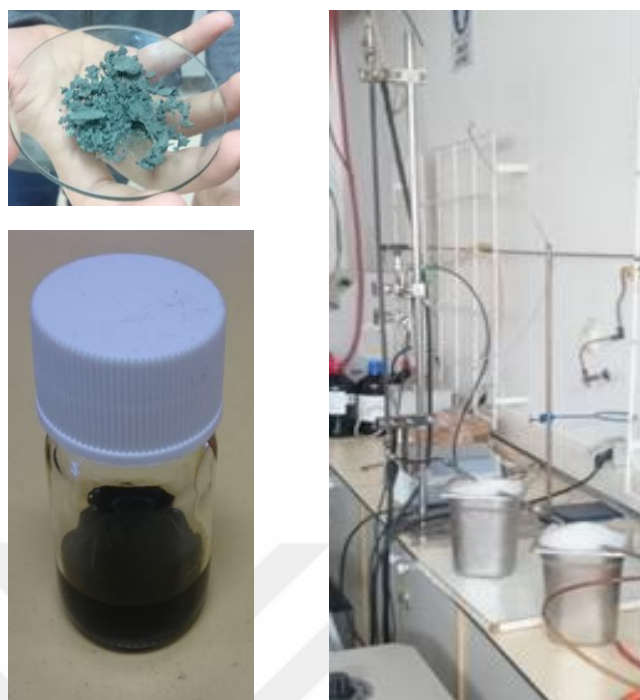


Figure A.21. *Dried biomass (left top), produced bio-oil (left down) and fast pyrolysis set up (right)*

CV

Name : Masoud DERAKHSHANDEH

Foreign Language : Persian, English, Arabic

Place of Birth and Date : Lamerd, Iran/1984

E-Mail : kadmasood@gmail.com; masoudderakhshandeh@anadolu.edu.tr

Education and work Experiences:

- 2002-2006, Shiraz University, Engineering Faculty, Chemical Eng. Department, B. Sc.
- 2010-2012, Amirkabir University, Engineering Faculty, Environmental Chemical Eng. Department, M. Sc.
- 2014-2018, Anadolu University, Engineering Faculty, Environmental Eng. Department, PhD.

Publication and/or scientific, art activities:

- Publications during M.Sc. Program:
 - 1) Azari, A. Kalbasi, M. Derakhshandeh, M. (2012). An experimental comparison of water based alumina and silica nanofluids heat transfer in laminar flow regime. J of Central South University. <http://link.springer.com/article/10.1007/s11771-013-1884-1>
 - 2) Azari, A., Kalbasi, M. Derakhshandeh, M. Rahimi, M. (2013). An Experimental Study on Nanofluids Convective Heat Transfer through a Straight Tube under Constant Heat Flux Chinese Journal of Chemical Engineering, <http://www.sciencedirect.com/science/article/pii/S1004954113606187>
 - 3) Derakhshandeh, M. Rostami, H. Goudarzi, G. Rostami, M. Z. (2014). Evaluation of the Tendency to migration in the case of Ahvaz dust storm occurrence: A public survey, J of Advances in Civil and Environmental Engineering, <http://jacee.us/archive/viewmore.php?pid=16>
 - 4) Azari, A. Derakhshandeh, M. (2015) An experimental comparison of convective heat transfer and friction factor of Al₂O₃ nanofluids in a tube with and without butterfly tube inserts, J of the Taiwan Institute of Chemical Engineers, <http://www.sciencedirect.com/science/article/pii/S1876107015000528>
 - 5) Halladj, R. Derakhshandeh, M., Azari, A. (INCNN 2012) Experimental Stability Analysis of Different Water-based Nanofluids: pH Adjustment Approach, first International Conference on Nanostructures and Nanomaterials: Science and Application, Iran Masjed Soleyman, Islamic Azad University

- PhD Program Publications:

- 1) DERAKHSHANDEH, M. ATICI, T. TEZCAN UN, Ü (2018) Lipid Extraction from Microalgae *Chlorella* and *Synechocystis* sp. Using Glass Microparticles, *Biochemical Engineering Journal*, Submitted
- 2) DERAKHSHANDEH, M. TEZCAN UN, Ü (2018) Investigation of Electro and Chemical Coagulation for Microalgae Biomass Harvest, Data acquired.
- 3) DERAKHSHANDEH, M. ATICI, T. TEZCAN UN, Ü (2018) The Screening of Microalgae Species Isolated from Central Anatolia Region for Lipid, Carbohydrate and Protein Content, *BioEnergy Research*, Submitted.
- 4) DERAKHSHANDEH, M. TEZCAN UN, Ü (2018) Carbon fixation by high lipid content Microalgae *Scenedesmus quadricauda*: Optimization for maximum growth rate, Ready for submission.
- 5) DERAKHSHANDEH, M. TEZCAN UN, Ü. ATEŞ, F (2018) Renewable Biofuel from Fast Pyrolysis of *Synechocystis* and *Scenedesmus* Wild-Type Microalgae Species, Ready for submission.

- Conferences:

- 1) DERAKHSHANDEH, M. UNVER, Z. M. ATICI, T. TEZCAN UN, Ü (2017) Enhanced Lipid Extraction from Microalgae *Synechocystis* and *Chlorella* Sp. Using Micro and Nano Particles of Glass 7th Int. CeBiTec Research Conference on Prospects and challenges for the development of algal biotechnology, Bielefeld Germany, 24-27 September 2017.
- 2) DERAKHSHANDEH, M. TEZCAN UN, Ü. (2018) The effect of bubble size on the performance of photobioreactors for producing microalgae biomass 2nd international students SCIENCE congress, İzmir Turkey 04-05 May 2018.